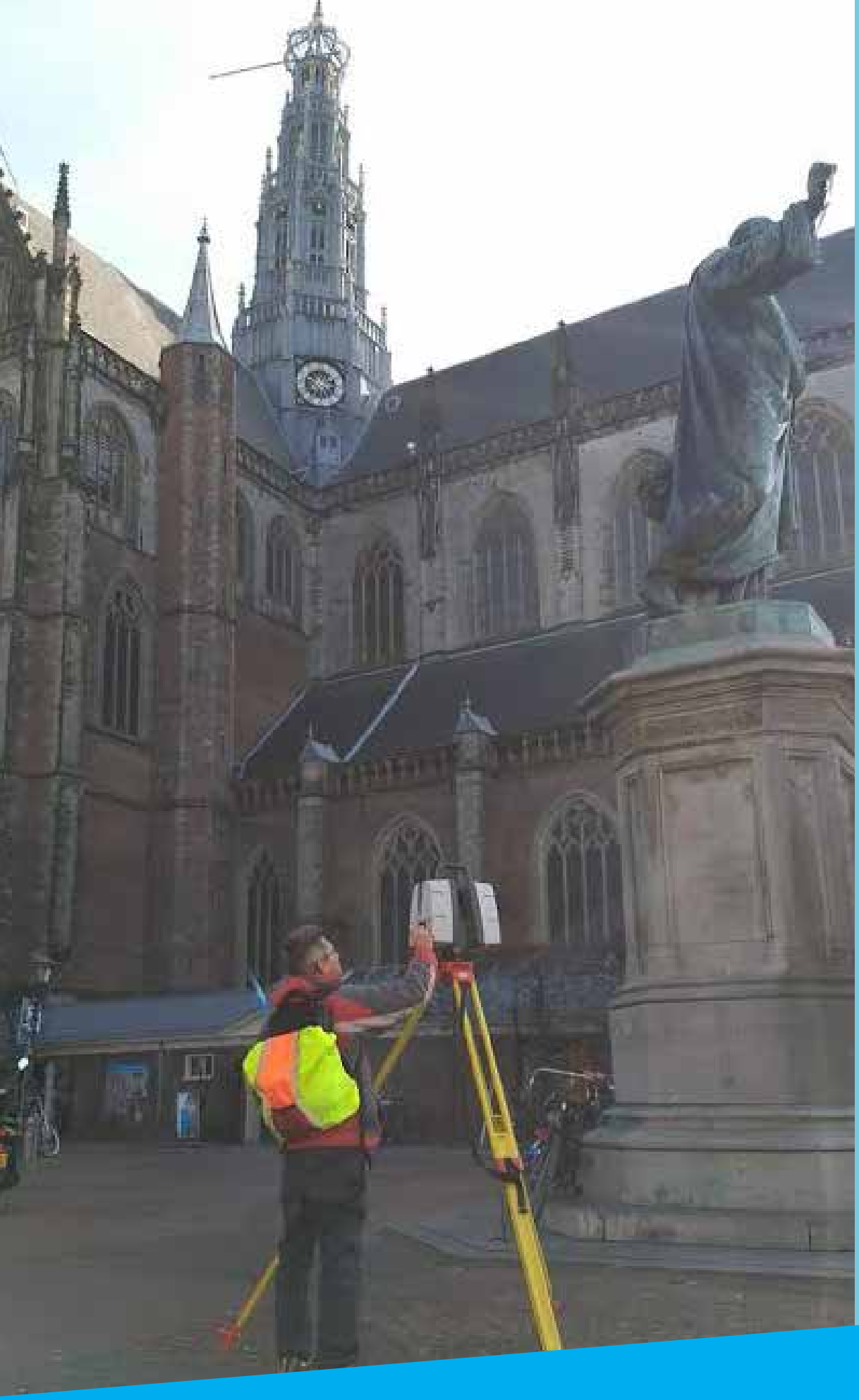

The Current State of the St. Bavo Church Tower

An Structural Analysis and Verification Study of the wooden tower of the Grote of St. Bavokerk in Haarlem, The Netherlands

TU Delft Delft University of Technology

Author
Pieter Woudenberg

The Current State of the St. Bavo Church Tower

A Verification Study and Structural Analysis of the Wooden Tower of the St. Bavo Church in Haarlem, The Netherlands

Master Thesis
by
Pieter Woudenberg

Msc Structural engineering, specialization: Steel, Timber and composite structures.
Date - June 2019

Supervisors:
Prof. Dr. Ir. J. W. G. van de Kuilen (Delft University of Technology)
Drs. W. F. Gard (Delft University of Technology)
Dr. R. C. Lindenbergh (Delft University of Technology)
Dr. Ir. H. F. Kaan (St. Bavo Church council)

An electronic version of this project report is available at
http://repository.tudelft.nl/

TU Delft Delft University of Technology

Preface

This master thesis is written to conclude my master study in Structural Engineering at the University of Technology in Delft. The master thesis is a part of the requirements to obtain a Master of Science Degree in Civil Engineering. Within my master Structural Engineering, I followed the specific track Steel, Timber and Composite Structures.

I want to give special thanks to the members of the "Vrienden van de Grote of St. Bavokerk" and in special to Henk Kaan, who gave me the opportunity to do my master thesis about the tower of the Grote of St. Bavokerk. He taught me a lot about the history of the church and supervised the entire process. During the entire process, I did a lot of practical work inside the tower and visited lots of places in the 500 years old church, which are closed for regular visitors. Due to the practical work in the tower, the process of creating this master thesis was versatile. In order to understand the complicated structure of the tower, I was able to use a scale model of the tower created by Theo van Paradijs, which saved me a lot of time and I want to thank him very much for his generosity to share the scale model with me.

Furthermore, I want to thank my graduation committee members of the TU Delft, Prof. Dr.Ir. J.W.G. van de Kuilen, Drs. W.F. Gard and Dr. R.C. Lindenbergh, for the supervising the entire process and providing feedback on the decisions I made.

Moreover, I want to thank two other persons from the TU Delft. Namely, Dr. L. Troung Hong for assisting me with the laser scanning and Dr.Ir G.J.P. Ravenshorst for the assistance with the longitudinal vibration tests.

Also, I want to thank Drs. K.C.M. Beijer for her assistance with the writing of the report and Thomas Harrewijn and Wouter Gerittsen with some practical help in the tower, which could not be done alone. Lastly, I want to thank my family and friends, who supported me through the entire process.

Pieter Woudenberg

Delft, May 2019

Acknowledgements

During this project I had a lot of support from different people and I want to express my gratitude towards these people who have contributed to my master thesis.

Vrienden van de Grote of Sint Bavo kerk.	
Henk Kaan	Supervisor from the church
Koen Vermeij	Supervisor from the church

TU Delft	
Jan-Willem van der Kuilen	Supervisor from the TU Delft
Wolfgang Gard	Supervisor from the TU Delft
Roderik Lindenbergh	Supervisor from the TU Delft
Lihn Truong Hong	Contributed to the 3D Lidar laser scanning of the tower
Geert Ravenshorst	Contributed to the longitudinal vibration tests

Other	
Theo van Paradijs	Creator of the Scale model of the tower
Wouter Gerritsen	Helped with the longitudinal vibration tests
Thomas Harrewijn	Helped with some heavy labour in the tower

Abstract

The Grote of St. Bavochurch is located in Haarlem, the Netherlands. In order to get more knowledge about the structural reliability of the tower, the church council proposed to do a verification study, which will form a part of "Het Grote Bavo boek". Het Grote Bavo boek is a book, which will be published in honour of the 500th anniversary of the finished construction of the tower of the Grote of St. Bavochurch in Haarlem in 2020 and the 650th anniversary of the first laid stone of the church in 2020. Back in the 16th century, the constructions were based on intuition and no extensive calculations were made. Hence, no precise knowledge about the structural reliability of the tower is known. Consequently, the main research question is formulated as:

What is the structural reliability of the timber tower of the St. Bavochurch, based on an assessment with modern technologies?

In order to find the force distribution through the tower and search critical locations in the tower, a Finite Element Model is created. With the Finite Element Model, one is able to draw conclusions regarding the structural reliability. The following approach is used to create the Finite Element Model. Firstly, rough sketches are created to clarify the structure. Afterwards, the geometry is mapped by using the rough sketches and measuring the dimensions by hand from within the tower and from a precise scale model created by Theo van Paradijs. Furthermore, in order to calculate the force distribution, the mechanical properties of the timber in use should be obtained. The modulus of elasticity is determined by using longitudinal vibration tests on dismantled timber beams, which have been renovated in the past. The strength class D18 from the Eurocode is then chosen, based on the average modulus of elasticity. This strength class is used for most timber elements in the tower. However, by visual grading all the timber elements, elements with large defects according to the NEN-EN 384 have been halved in strength properties. With this information, an accurate representation of the tower is created in the Finite Element Model. Moreover, the loads on the tower have been determined according to the NEN-EN 1990 and take wind loads, self-weight and imposed floor loads into consideration. Lastly, the tower is clearly inclined in the North-West direction. By using 3D Lidar Laser Scanning technology a point cloud of the entire tower is obtained. The total inclination has been measured by hand from the point cloud of the tower and is roughly estimated around 2 m. This inclination is taken into consideration in the Finite Element Model with a non-linear combination. The impact of the inclination will be compared to combinations, which do not take any inclination into consideration.

After extensively investigating the force distribution, several critical connections and locations have been determined. After analyzing the resistance of the critical connections and locations and comparing this to the maximum forces, one is able to conclude that the entire structure suffices all modern structural demands according to the NEN-EN 1995 and is structural reliable. Furthermore, the dynamic behaviour of the tower has also been investigated by determining the natural frequencies of the tower with the Finite Element Model. One is able to conclude that the tower is not sensitive to wind loads and no dynamic problems are present. Hence, the structural reliability of the tower is remarkably high and one is able to conclude the construction has been over-dimensioned.

In addition to the conclusions above, some simplifications have been made in the process and all the results are indications of reality. By mapping the dimensions more accurately, using more samples to represent the mechanical properties and programming the entire Finite Element, a more accurate representation of reality could be obtained. However, the indication is precise enough to substantiate the previously mentioned findings.

Deliverables

This master thesis is concluded with the following deliverables:

	Deliverable	Format
1	Technical report	PDF file
2	Final presentation	MS PowerPoint
3	SCIA report of tower of the Grote of St. Bavochurch	PDF-file
4	Hand calculations for the inclination	MS Excel
5	Point cloud from the outside of the tower	BIN-file

The deliverables two, three, four and five can be sent upon request by e-mailing pieter.woudenberg@hotmail.com

Contents

Acronyms and Abbreviations **xi**

List of Symbols **xiii**

1 Introduction **1**
1.1 Problem Definition . . . 2
1.2 Objectives . . . 3
1.3 Approach . . . 3
1.4 Thesis Outline . . . 5

2 Preliminary Study **7**
2.1 Historical Timber in Buildings . . . 7
2.1.1 The Assessment of Old Timber Structures . . . 8
2.1.2 Strength Grading . . . 9
2.2 3D-Lidar Scanning Technology . . . 14
2.2.1 Terrestrial Laser Scanners . . . 14
2.2.2 Hand-held Laser Scanners . . . 15
2.3 The loads on the Tower . . . 15
2.3.1 Wind Loads . . . 15
2.3.2 Snow Loads . . . 15
2.3.3 Variable Loads . . . 15
2.4 The Ongoing Inclination of the Tower . . . 16

3 Methodology **17**
3.1 Structure of the Tower . . . 17
3.2 Mechanical Properties of the Wood in the Tower . . . 17
3.3 The Loads on the Tower . . . 19
3.4 Determination of the Critical Elements in the Tower . . . 20
3.5 The Deflections of the Tower . . . 21
3.6 The Angle of Inclination of the Tower . . . 21
3.7 Overview of the Chosen Methods . . . 22
3.8 Discussion . . . 22

4 The Structure of the Tower **23**
4.1 The Structure of the Tower . . . 23
4.2 Discussion . . . 27

5 Mechanical Properties of the Wood in the Tower **29**
5.1 Longitudinal Vibration Tests . . . 29
5.2 Visual Grading . . . 32
5.3 The Indicated Values for the Mechanical Properties . . . 32
5.4 Discussion . . . 33

6 The Inclination of the Tower **35**
6.1 Determination of the Inclination of the Tower . . . 35
6.2 Possible Causes of the Inclination of the Tower . . . 38
6.3 Discussion . . . 40

7 The Finite Element Model of the Tower **41**
7.1 Results of the Finite Element Model in Straight Conditions . . . 41
7.2 Results of the Finite Element Model with Inclusion of the Inclination . . . 44
7.3 The natural frequencies of the tower . . . 46
7.4 discussion . . . 47

8 Strength and Stability Verifications **49**
8.1 Structural Elements 49
8.2 Connections 50
8.3 discussion 52

9 Discussion **53**

10 Conclusion **55**

11 Recommendation **57**

Bibliography **59**

List of Figures **61**

List of Tables **65**

A Geometry Sketches **67**

B Longitudinal Vibration Tests **85**
B.1 Test Samples 85
B.2 Results of the Longitudinal Vibration Tests 103

C Visual Grading **109**

D SCIA Input **129**

Acronyms and Abbreviations

Acronym / abbreviation	Description
2D	two Dimensional
3D	Three Dimensional
FEA	Finite Element Analysis
GNSS	Global Navigatin Satellite system
Lidar	Light Detection and Ranging
MC	Moisture Content
MOE	Modulus of Elasticity
MOR	Modulus of Rupture
RH	Relative Humidity
St.	Sint

List of Symbols

Parameter	Description	Unit
A	Cross-sectional area	m^2
E_0	Modulus of elasticity parallel bending	N/mm^2
$E_{0.05}$	5% modulus of Elasticity parallel bending	N/mm^2
E_{90}	Modulus of Elasticity perpendicular bending	N/mm^2
E_{din}	Dynamic modulus of elasticity	N/mm^2
E_f	Dynamic modulus of elasticity from transverse vibration tests	N/mm^2
E_l	Dynamic modulus of elasticity from longitudinal vibration tests	N/mm^2
E_{sta}	Static modulus of elasticity	N/mm^2
f	Frequency	Hz
$f_{c,0,k}$	Compression stress resistance parallel to the grain	N/mm^2
$f_{c,90,k}$	Compression stress resistance perpendicular to the grain	N/mm^2
$f_{t,0,k}$	Tension stress resistance parallel to the grain	N/mm^2
$f_{t,90,k}$	Tension stress resistance perpendicular to the grain	N/mm^2
$f_{m,k}$	Bending stress resistance	N/mm^2
F_v	Shear force	kN
$f_{v,k}$	Shear stress resistance	N/mm^2
$G_{k,j}$	The load due to selfweight	kN/m^2
J	Moment of inertia	mm^4
k	Constant of the fundamental mode in free-free flexural vibration	-
k_{def}	Deformation factors	-
k_{mod}	Modification factor for load duration and moisture content	-
l	Length	mm
m	Mass	kg
q_k	Distributed load	kN/m^2
Q_k	Point load	kN
$Q_{k,wind}$	Distributed load due to the wind	kN/m^2
$Q_{k,imp}$	Distributed load due to the wind	kN/m^2
R	Load force required to penetrate the timber for hardness tests	kN
V	Velocity of the longitudinal stress wave	m/s
w_{final}	Final deformations	mm
$w_{instantaneous}$	Instantaneous deformations	mm

*continues on next page

Parameter	Description	Unit
α	Angle of inclination	°
α_1	Constant depending on the material	-
β_1	Constant depending on the material	-
$\gamma_{G,j}$	Partial safety factor for the permanent loads	-
γ_m	Partial material factor	-
$\gamma_{Q,imp}$	Partial safety factor for the imposed floor loads	-
$\gamma_{Q,wind}$	Partial Safety factor for the wind loads	-
Δ	Reduction factor for the defectiveness of an element	-
Δ_{xy}	Change in the horizontal plane between two points	mm
Δ_z	Change in the vertical plane between two points	mm
ϵ_j	Reduction factor for unfavorable permanent loads	-
ρ	Density	kg/m^3
σ_c	Compression Stress	N/mm^2
σ_{max}	Tensions stress	N/mm^2
$\sum$	Sum	-
ψ_0	Factor for combination value of a variable action	-
ψ_1	Factor for frequent value of a variable action	-
ψ_2	Factor for quasi-permanent value of a variable action	-

1 Introduction

In honour of the 500th anniversary of the finished construction of the tower of the Grote of St. Bavo Kerk in Haarlem in 2020 and the 650th anniversary of the first laid stone of the church also in 2020, the church council proposed a verification study of the timber tower, aiming to acquire more knowledge of the current structural reliability of the timber tower and its future prospective.

The St. Bavo church in Haarlem is one of the biggest churches in the Netherlands. With a total height of 78 meters the church rises far from outside the city and is a characteristic monument in Haarlem. The tower is approximately 49 meters high. The construction of the church roughly started in 1370 (Kamphuis, 2001) and with the inclusion of the wooden tower, the church was finished in 1520. In 1500, the construction of the tower on top of the church started. The initial idea was to make a stone tower. In 1505, two of the four main pillars tilted inwards and cracks occurred in the walls next to the pillars, due to the heavy weight of the stone tower and another solution was required (Kamphuis, 2001). These phenomena happened while the tower was still under construction. It is not clear what happened in the years after 1505. The demolition of the stone tower on top of the church started in 1514 and lasted until 1519. In order to finish the tower, a lighter material was required. Timber performs better in a strength/weight ratio in comparison to stone. In order to mimic the idea of a stone tower, a lead cladding is laid over the timber on the outside of the tower. In 1519, the construction of the timber tower started, presumably under supervision of Jacob Symonsz from Edam (Kamphuis, 2001). The construction of the tower took approximately 2 years and was finished in 1520. The total weight of the timber tower was approximately 200 tons and the stone tower approximately 700 tons (Von der Dunk, 2016). Due to the difference in weight, timber is a more suitable material in this specific scenario.

During the lifetime of the St. Bavo church, no major renovations of the tower have been done. (De Boer et al., 1985). The main load bearing construction in the tower still consists of the timber from the 16th century. The timber used in the St. Bavo tower is European Oakwood. Besides mimicking a stone look of the tower, the lead cladding also protects the timber on the outside from the outdoor environment (Emmens et al., 2002). The main problem through the ages is a chemical reaction between the lead cladding and the acetic acids in Oakwood. The reaction causes the lead to corrode and leave behind white lead (Emmens et al., 2002). In places of white lead, the lead might crack and this might cause leakage towards the timber, which will severely damage the timber (Emmens et al., 2002). Another reason for leakages is poor workmanship with insufficient overlap between the lead parts (Emmens et al., 2002). In some spots, the timber has rotten away underneath the lead. During restorations, these timber parts have been renewed (Emmens et al., 2002). However, a lot of the timber in the tower is still the original timber from the 16th century.

1.1. Problem Definition

Back in the 16th century, during the construction of the tower, everything was built on intuition. The architects did not precisely calculate the strength of the construction, but based their decisions on personal knowledge. Due to this, most buildings in this time were over-dimensioned. Nowadays, knowledge about the strength of the tower back in the 16th century but also the current strength of the tower is still unknown. The tower is built up from a lot of different elements. However, it is not clear whether all elements are necessary in order to provide sufficient strength to the tower.The complex structure is shown in a scale model of the tower in figure 1.1. Whether Jacob Symonsz from Edam was a genius builder with a lot of constructive knowledge or just over-dimensioned the tower is still a mystery these days.

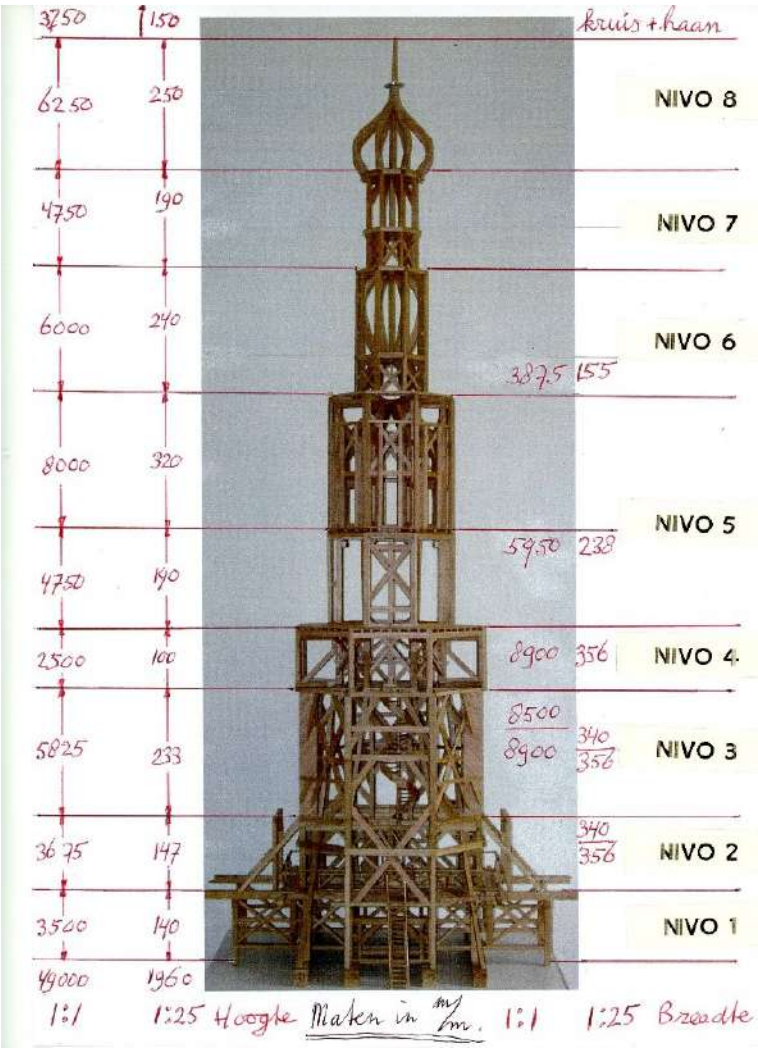

Figure 1.1: The scale model of the St. Bavochurch (1:25), made by Theo van Paradijs, 2017

The degradation of the 500 year old timber, due to insects and other organic processes, is clearly visible these days. Due to a natural drying process, the wood might have cracked on the inside, which is not visible for the naked eye. The degradation of the timber and the cracks in the timber influence the strength of the timber elements. Nowadays, the current mechanical properties of the wood are not known.

The tower has some mysteries. The tower is clearly inclined in the north-west direction, but the cause of the deflection of the tower is unknown. Local volunteers in the church suggest this might be done

on purpose, in order to withstand the north-western wind. However, several other explanations might also be possible.

1.2. Objectives

The objective of this thesis is to give more insight into the strength of the timber tower of the St. Bavochurch. The main research question is formulated below:

What is the structural reliability of the timber tower of the St. Bavochurch, based on an assessment with modern technologies?

In order to answer the main research question, several sub-questions are formulated and divided into two groups: 1) the structural analysis; 2) the verification study. The sub-questions are formulated below.

- structural analysis
  - How is the structural state of timber buildings assessed?
  - What is the structure of the tower?
  - How will the geometry of the tower be mapped?
  - What are the dimensions of the timber tower and the elements within?
  - How will the mechanical properties of the timber in the tower of the St. Bavochurch be determined?
  - What are the mechanical properties of the timber in the tower of the St. Bavochurch?
  - What are the static loads and the variable loads on the tower?
  - Why is the tower inclined in north-west direction?
  - What is the inclination of the tower in north-west direction?
- verification study
  - What are the flow forces in the structural elements in the tower?
  - What is the dynamic behaviour of the timber tower due to wind loads?
  - What structural elements and connections suffer from the highest forces and are critical places in the strength and stability of the timber tower?
  - How are the critical connections built up and what forces can they withstand before failure?
  - What is the strength of the critical structural elements?

1.3. Approach

The approach of the thesis is concisely described below. The detailed methodology can be found in Chapter 3.

In order to clarify the complexity of the tower for the reader, the first requirement is to make an overview of the different elements in the tower. One should understand the structure of the tower, before the structure can be assessed. Clear overview figures are obtained from Kamphuis (2001) and can be found in Chapter 4. The first three floors (see figure 1.1) are clearly described in these overview figures.

The dimensions of the timber tower are the second requirements to obtain. Several options are available to obtain the dimensions of the tower. An accurate scale model of 1:25 has been made by Theo van Paradijs.The scale model is shown in figure 1.1. He measured the dimensions of the timber tower by hand. During his work, he did not map the dimensions accurately, because of the high workload. He made the samples for the scale model directly from the measurements. Therefore, the dimensions of the timber tower are still not clearly mapped. However, it can be assumed the scale model is an

accurate representation of the real tower and parts can be measured from the scale model. Another possibility is measuring the geometry in the real tower by hand. Both of these methods are not very accurate and some critical elements might have to be verified to find an accurate representation. A more accurate way to measure the geometry is 3D-Lidar scanning. This can be done with a terrestrial laser scanner or a hand-held laser scanner. However, including processing the obtained data, the 3D-Lidar scanning gives a higher workload.

In order to properly assess the timber construction, the strength of the timber has to be determined. Some replaced parts, which have been changed during renovation, are still in existence and are made from the same wood as the current structural elements in the tower. The replaced parts can be representative for the mechanical properties of the timber used in the load bearing elements. To find the mechanical properties of the timber and the joints, the timber might be tested in multiple ways. Machine grading, several non-destructive tests and visual grading are the possibilities for grading. After testing the samples with machine grading or non-destructive tests, the results will be confirmed by visual grading in the tower. For more information about the grading of the timber and the required test, the European norms (EN384, EN408, EN14081 and EN14358) and several other reports will be studied in Chapter 2 (Ridley-Ellis et al., 2016).

Furthermore, one can clearly see that the tower is inclined in the North-West direction. In order to make the Finite Element Model as representative as possible, the inclination has to be taken into consideration. Besides using the measurements of the local authorities, a rough estimation of the inclination might be done as well.

The structural analysis will start when the dimensions and the mechanical properties are known. The construction will be modelled and calculated with a Finite Element Analysis (FEA). First, the loads on the structure should be determined. This can be done with the Eurocode (NEN-EN-1991), see Chapter 2. The foundation is assumed to be clamped, since the four main beams are to the utmost extent clamped in between brickwork. The results from the FEA give the flow of forces. These results will be assessed and the strength of the connections and load-bearing elements will be verified. In this way, critical elements and connections in the tower will be determined and verified. These results will clarify whether the construction is structurally reliable.

1.4. Thesis Outline

In this section, the structure of the thesis is described. The outline is given in figure 1.2.

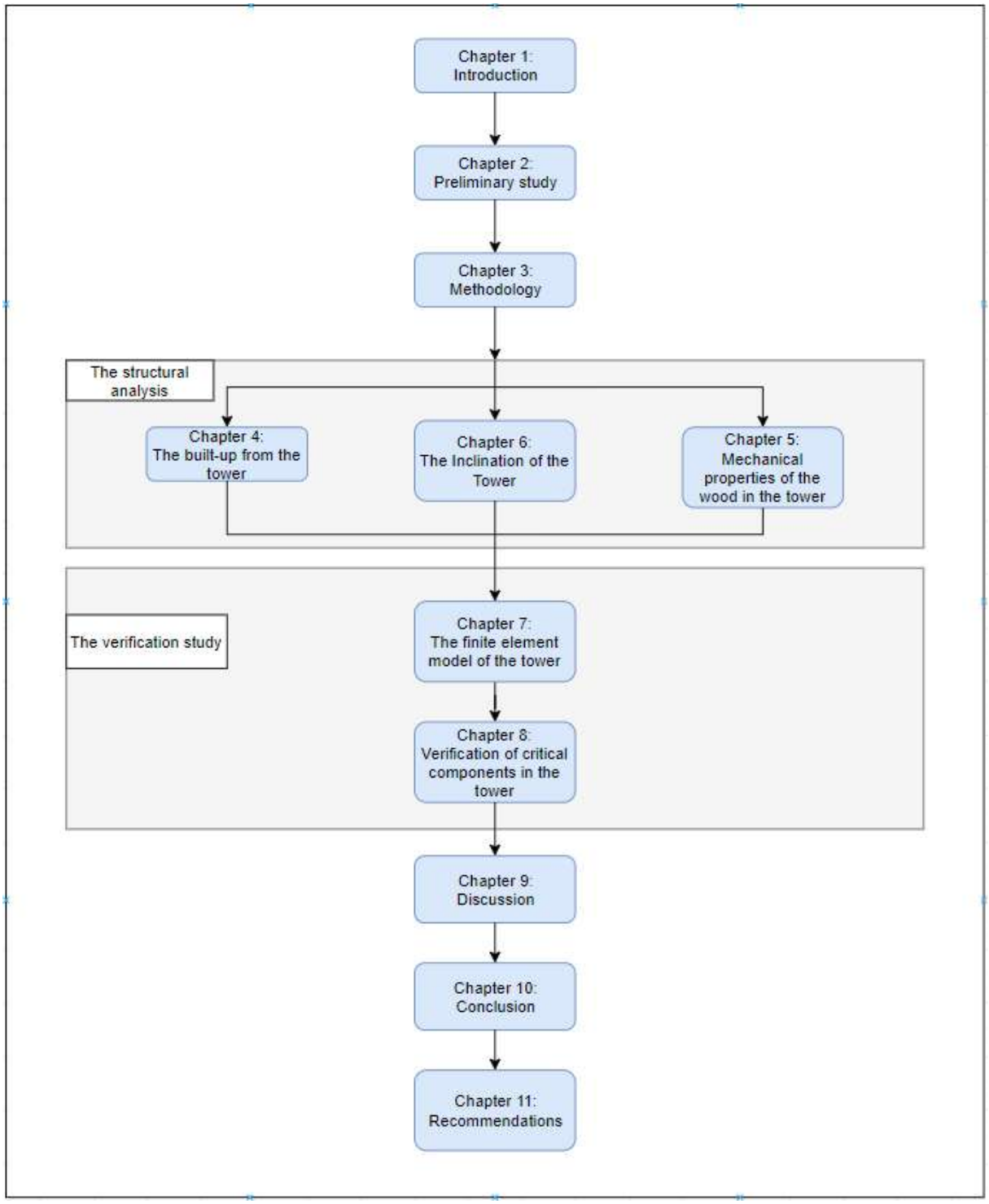

Figure 1.2: The outline of the thesis

2

Preliminary Study

The preliminary study provides a base for this thesis and aims to widen the relevant knowledge in order to answer the research questions.

2.1. Historical Timber in Buildings

According to Nilsson and Rowell (2012) and Niemz and Mannes (2012), timber will undergo little change in mechanical properties and structure over centuries if the timber is stored in dry conditions. According to Sonderegger et al. (2015), the ageing of woods influences the colour and a reduction of the impact bending strength. However, no significant differences were found for the bending and fracture toughness, sorption and swelling. The mechanical properties of timber over time are influenced by a lot of factors such as moisture, pH, temperature, oxygen, ultraviolet energy, contaminates and microorganisms (Nilsson and Rowell, 2012). These factors interact with the timber due to the chemical structure of the timber (Nilsson and Rowell, 2012). The degradation chemistries and causes of the type of degradations are given in table 2.1. Biotic deterioration is only accountable for moisture contents above 20% (Sonderegger et al., 2015). Therefore, timber for indoor usage undergoes little change over time. Furthermore, the indoor usage provides protection against weathering conditions, which covers a lot of the other possible causes of degradation from table 2.1.

Table 2.1: Major degradation pathways and chemistries by Nilsson and Rowell (2012).

Chemistries	possible causes
Biological Degradation	Fungi, bacteria, insects, termites, enzymatic reactions oxidation, hydrolysis, reduction, free radical
Chemical reactions	Oxidation, hydrolysis, reduction, free radical
Mechanical degradation	Chewing, dust, wind, hail, snow, sand, stress, cracks, fracture, abrasion, erosion, compression
Thermal degradation	Lightning, fire, sun
Pyrolysis reactions	Dehydration, hydrolysis, oxidation, free radical
Water degradation	Rain, sea, ice, acid rain, dew
Water interactions	swelling, shrinking, freezing, cracking, erosion
Weather degradation	Ultraviolet radiation, water, heat

Wood is an anisotropic material and has different mechanical properties in all directions. Even in the same direction, the mechanical properties of timber differ. The reason for this is the presence of knots and different slope of grains, which differs per cross-section, and therefore the mechanical properties differ as well. Furthermore, wood is a natural material, which causes a variation of the mechanical and physical properties (Frese, 2008). The size of the elements also influences the mechanical properties, large beams have a higher heterogeneity and variability inside (Ceccittu and Togni, 1996).

2.1.1. The Assessment of Old Timber Structures

The typical way to assess existing timber buildings is described in this paragraph. According to Blass et al. (1995), the objectives for inspecting an existing timber structure are:

- Obtaining information regarding the stiffness and strength in order to verify the structural elements and connections in the structure.
- Identifying parts which require interventions such as specific reinforcement or substitution.
- Evaluating decay factors which might influence or have influenced the structure and stating measures to prevent such decay risks to reoccur.
- Describing the structural behaviour of the construction and in case the structure has historic value evaluating the history and manufacturing techniques.

In order to achieve these objectives one should asses the timber quality and physical and mechanical properties, detecting existing decay or damage, assessment of the risk of decay in the future and to asses the strength and stiffness of effective cross-sections (Blass et al., 1995).

According to Riggio et al. (2017), the assessment of timber structures starts with an assessment of the entire structure. One assesses missing elements or connections and if the construction is suitable as a load-bearing construction for loads which might occur. The next step is to assess different sub-structures, such as roofs, trusses and frames. The effectiveness, efficiency and robustness of the sub-structures should be assessed for the connections and load paths. The third step is to assess the individual elements. The geometry and state of conservation, decay and present damage should be assessed. Lastly, the supports and connections and their current conditions should be taken into consideration. The connections have a critical role in transferring the loads and are often the weakest parts in timber structures. The assessment method is schematically shown in figure 2.2.

hierarchical organization of the structure / operational category	Environmental characterization	Structural identification	Identification of alterations	Mechanical characterization
SYSTEM	✓	✓	✓	
UNIT		✓	✓	
ELEMENT	✓		✓	✓
CONNECTION		✓	✓	

Table 2.2: Operational categories for the assessment of timber structures by Riggio et al. (2017).

According to Blass et al. (1995), the inspection is split up in two categories. First off is a preliminary assessment in order to get a general idea about the conditions of the structure and if a detailed assessment is required. If required, a detailed assessment is performed in order to asses each timber member in the structure. The preliminary assessment should be able to asses whether the wood is softwood or hardwood, generally considering the timber quality by assessing the fissures, decay and damage, knots and fissures. By investigating the environmental conditions, one should place the structure under one of the service classes from the euro code. Based on the results from the preliminary assessment, one should be able to decide if a detailed assessment is required or not and one should determine the priority of future interventions. A detailed assessment aims to provide the strength and stability of all elements and connections in order to asses them. This will be done by the following:

- Measuring the moisture content in some places in order to obtain the average moisture content.

- Assessing the cross-sections by determining the decayed wood zones and or cavities; knots and resin pockets locations and extension; ring shakes and shrinkage fissures development; heartwood and sapwood distribution; pith location.
- The assessment of timber to timber joints by visually inspecting the decayed areas.
- Assessment of previous restorations.

The detailed assessment could be substantiated with several in situ tests such as static loading tests in order to determine the modulus of elasticity; Endoscopy tests in order to inspect the inside of the timber for defects; X-ray, computer tomography, nuclear magnetic resonance or gamma-ray tests in order to scan the inside of timber members, vibration tests to compute the modulus of elasticity, acoustic tests used to locate highly defective areas, stress wave tests to compute the modulus of elasticity, Pilodyn tests are used to measure the degree of surface degradation; Drilling resistance tests are used for the assessment of internal decay; displacement transducers and strain gauges tests are used to evaluate slip in joins and local strains; hardness tests give information about the surface condition and eventually determining strength values; screw withdrawal tests are used to give information of deterioration (Blass et al., 1995). Some of these tests are further explained in the next section of strength grading.

2.1.2. Strength Grading

To assess an old timber building properly the remaining strength of the timber elements is essential. To determine the strength of the timber elements, the mechanical properties are required. According to Blass et al. (1995), no methods exist to accurately asses exactly the strength of an individual member and the methods are based on determining the characteristic strength of newly sawn timber. This might cause problems for existing timber elements because the large old beams have a pith on a central location, it might be impossible to visually inspect all faces and decay and damage are excluded from grading rules for new timber. There are a lot of different methods to determine the mechanical properties. The main grading methods are visual grading, machine grading and several non-destructive tests. Mostly, several measuring methods are combined. A single parameter is insufficient in describing the conditions of the material. Simple sound transmission measurements barely detect cracks or small knots (Niemz and Mannes, 2012). Only visual grading, as well as non-destructive tests methods cannot supply sufficient information individually. Therefore, both methods have to be combined to get reasonable results (Piazza and Riggio, 2008). The different grading methods will be described below.

Machine Grading Strength properties of timber in Europe are based on strength, stiffness and density. The properties for the European standards are based on a relative Humidity (RH) of 65% and a temperature of 20°C (The moisture content (MC) is 12% for most species) (Ridley-Ellis et al., 2016). The main properties are divided into two classes namely:

- Bending strength, bending stiffness and density
- Tension strength, tension stiffness and density

The main aspects will be determined according to the NEN-EN 408, see the brief description of the NEN-EN 408 below:

- The moisture content can be determined with the NEN-EN 13183-1.
- The density is measured after the timber has cracked and it is favourable to measure as close as possible to the crack.
- For the local modulus of elasticity in bending, a sample is required with a minimum length of 19 times the depth of the cross-section. The sample will be symmetrically loaded in bending at two points over a span of the depth times 18. The sample is simply supported and lateral restraints are present in order to improve lateral torsional buckling. By consistently increasing the load, the maximum load will be determined. Besides, the deformations will be measured. The processing of the results is not further explained.

- The global modulus of elasticity in bending is obtained in the same way as the local modulus of elasticity in bending. However, the results are processed differently.
- The shear modulus will be obtained with the torsion method and it requires a sample with a minimum length of 19 times the depth. The sample is clamped at the supports, which are at least 16 times the depth of the cross section from each other. Torque will be applied on the sample and the relative rotations at two cross sections will be measured.
- The modulus of elasticity in tension parallel to the grain requires a sample with a length of at least 9 times the cross-sectional dimensions. The sample will be loaded by using gripping devices, which will apply a tensile load without inducing bending.
- The tension strength parallel to the grain will be done with the same test setup as the modulus of elasticity in tension parallel to the grain, but the results will be processed differently.
- The modulus of elasticity in compression parallel to the grain requires a length of six times the smaller cross-sectional dimensions. The sample shall be loaded in the middle with a spherically seated loading-head or other devices, which are able to apply a compressive load without inducing bending. The load shall be applied at a constant rate.
- The compression strength parallel to the grain is obtained in the same way as the modulus of elasticity in compression parallel to the grain. However, the results are processed differently.

Other properties will be derived with formulas from these main properties. These "secondary" properties are tension perpendicular to the grain, compressive strength perpendicular to the grain, shear strength and shear modulus. The formulas to obtain the "secondary" properties are given in figure 2.3.

Equation valid for		C classes	T classes	D classes
Species		softwood	softwood	hardwood
Based on		edgewise bending	tension	edgewise bending
Strength properties in N/mm²				
Bending	$f_{m,k}$	given	$3{,}66 + 1{,}213 * f_{t,0,k}$	given
Tension parallel to grain	$f_{t,0,k}$	$-3{,}07 + 0{,}73 * f_{m,k}$	given	$0{,}60 * f_{m,k}$
Tension perpendicular to grain	$f_{t,90,k}$	0,4	0,4	0,6
Compression parallel to grain	$f_{c,0,k}$	$4{,}3*(f_{m,k})^{0,5}$	$5{,}5*(f_{t,0,k})^{0,5}$	$4{,}3*(f_{m,k})^{0,5}$
Compression perpendicular to grain	$f_{c,90,k}$	$0{,}007 * \rho_k$	$0{,}007 * \rho_k$	$0{,}010 * \rho_k$ *or* $0{,}015 * \rho_k$ *if* $\rho_k \geq 700\ kg/m^3$
Shear	$f_{v,k}$	$f_{m,k} \leq 24$ MPa: $1{,}6 + 0{,}1*f_{m,k}$ $f_{m,k} > 24$ MPa: 4,0	$f_{t,0,k} \leq 14$ MPa: $1{,}2 + 0{,}2*f_{t,0,k}$ $f_{t,0,k} > 14$ MPa: 4,0	$f_{m,k} \leq 60$ MPa: $3{,}0 + 0{,}03*f_{m,k}$ $f_{m,k} > 60$ MPa: 5,0
Stiffness properties in kN/mm²				
Mean modulus of elasticity parallel to grain	$E_{0,mean}$	given	given	given
Char. modulus of elasticity parallel to grain	$E_{,0,k}$	$0{,}67 * E_{0,mean}$	$0{,}67 * E_{0,mean}$	$0{,}84 * E_{0,mean}$
Mean modulus of elasticity perpendicular to grain	$E_{90,mean}$	$E_{0,mean}/30$	$E_{0,mean}/30$	$E_{0,mean}/15$
Mean shear modulus	G_{mean}	$E_{0,mean}/16$	$E_{0,mean}/16$	$E_{0,mean}/16$
Density in kg/m³				
Char. density	ρ_k	given	given	given
Mean density	ρ_{mean}	$1{,}2 * \rho_k$	$1{,}2 * \rho_k$	$1{,}2 * \rho_k$

Table 2.3: The formulas to derive the other mechanical properties from the NEN-EN 384

Since the number of available samples is limited, the NEN-EN 14358 has to be used to create safe values for the obtained results from the tests. Characteristic values will be calculated according to the 5 percentile demands.

Visual Grading Visual grading focuses on local weak spots of the wood. Failure of structural timber depends on variations in material properties and local defects (Piazza and Riggio, 2008). Knots sizes and location have the biggest influence on the strength of the structural elements (Piazza and Riggio, 2008). For visual grading elements on site, the load cases should also be considered. The position of defects on the timber should be considered with reference to the acting stresses (Piazza and Riggio, 2008). For instance, transverse compression strength, shear strength and hardness increases in the presence of tight knots, which act as pegs. However, knots reduce the modulus of rupture if the knots are present in a tension zone (Piazza and Riggio, 2008).

Visual grading will be done according to the NEN-EN 384. Some guidelines for visual grading have been obtained from NEN-EN 14081-1. The tables from the NEN-EN 14081-1 are shown in figure 2.4 and figure 2.5. The templates in the figures still require expertise in visual grading in order to properly grade the timber (Riggio et al., 2017).

Strength class according to EN 338 [a]		**C18, D18, T11 and below**	**Above C18, D18, T11**
Max. length of fissures [b]	Fissures not going through the thickness	Fissures less than half the thickness may be ignored [f]	
		Not greater than 1,5 m or 1/2 the length of the piece, whichever is the lesser	Not greater than 1 m or 1/4 the length of the piece, whichever is the lesser
	Fissures going through the thickness	Not greater than 1 m or 1/4 the length of the piece, whichever is the lesser. If at the ends, a length not greater than two times the width of the piece	Only permitted at the ends with a length not greater than the width of the piece
Max. warp [c] in mm over 2 m of length	Bow	20 mm	10 mm
	Spring	12 mm	8 mm
	Twist	2 mm/25 mm width	2 mm/25 mm width
	Cup	Unrestricted	Unrestricted
Wane		Wane shall not be greater than one third of the full edge and/or face dimensions of the piece	
Soft rot and dote [d] (see EN 844-10)		Soft rot shall not be permitted Dote is permitted	Soft rot shall not be permitted Dote shall not be permitted
Insect damage		Active infestation shall not be permitted. Insect holes above 2 mm diameter shall not be permitted. Smaller holes shall be assessed as other defects	
Other defects [e]		Where the reduction in strength caused by another defect is obviously less than caused by defects permitted by this table, the piece may be accepted provided the defect is of a type that will not increase after conversion and drying	

[a] For alternative strength classes, visual overrides are checked with corresponding strength value limits

[b] The length of fissures is linked with moisture content and therefore the limits given apply only at the time of grading. Permitted limits for both the depth and length of fissures refer to the sum of fissures in one plane in a piece of timber.

[c] Warp is influenced by moisture content, so the limits apply only at the time of grading. Longitudinal curvature in square section pieces may be assessed using the limits for bow.

[d] Stain is not a structural defect and is acceptable without limitation.

[e] Other defects include for example mechanical damage, top rupture, and included bark.

[f] A 0,2 mm feeler gauge is a suitable device for measuring fissure depth.

Table 2.4: The first part of guidelines for visual grading according to the NEN-EN 14081-1

	Strength class according to EN 338 [a]	
	C18, D18, T11 and below	**Above C18, D18, T11**
Knot diameter on face	up to 1/2 x width of piece	up to 1/4 x width of piece
Knot diameter on edge	up to 3/4 x thickness of piece	up to 1/2 x thickness of piece
Slope of grain	1 in 6	1 in 10

[a] For alternative strength classes, visual overrides are checked with corresponding strength value limits

NOTE 1 These limits are applicable only where the size of knots and slope of grain in the non-fully graded portion exceeds the size of similar characteristics in the fully graded portion of the same piece.

NOTE 2 The knot diameter is measured perpendicular to the longitudinal axis of the piece of timber. For arris knots the above limits apply to the portion of the knot visible on the particular face or edge being considered.

Table 2.5: The second part of guidelines for visual grading according to the NEN-EN 14081-1

A downside to visual grading is the aspect that the density or modulus of elasticity can barely be estimated. Therefore, the strength is generally limited to D40 for hardwoods (Frese, 2008). The density will roughly be estimated with the ring width and with the density the stiffness might be determined (Piazza and Riggio, 2008).

Non Destructive Tests

Non-destructive tests predict the strength of an element. However, in order to determine the "true" strength of an element, destructive tests are required (Piazza and Riggio, 2008). In order to determine the Modulus Of Elasticity (MOE) and Modulus Of Rupture (MOR), hardness tests, vibrations tests or acoustic tests can be used. The elements should be structural members in order to be statistically

robust and reliable (Cavalli et al., 2016). Vibration tests are difficult to do on site because the tests require specific boundary conditions. No loads will be present on the samples and the samples should be free to vibrate (Cavalli et al., 2016). Vibration tests can only be done on dismantled timber members and the density has to be known. In order to perform non-destructive tests, the moisture content should be known (Piazza and Riggio, 2008). The density should be determined with a moisture meter. Another solution is to soak the elements before testing, in this case, the elements have reached the fibre saturation point and the moisture content is known. Furthermore, an estimation of the density can be easily calculated by weighing the elements and determining the volume of the samples. Other ways to measure the density are radiation densitometry, sclerometer testing and drill resistance (Piazza and Riggio, 2008).

Vibration Tests

Vibration tests are inexpensive methods for the assessment of the MOE and despite being inexpensive, the vibrations tests are fast and reliable (Cavalli et al., 2016). The tests are based on the relation between the dynamic MOE and natural vibration frequency of the timber. There are two vibration tests, the transverse vibration test and the longitudinal vibration test (Cavalli et al., 2016) The vibration tests give realistic mean values for the stiffness properties. However, the vibration tests barely take ring shakes, decay or different moisture contents into consideration. The dynamic modulus of elasticity for the transverse vibration tests follows from equation 2.1 (Cavalli et al., 2016).The frequency of the first natural frequency is f, l is the length, k is a constant to the fundamental mode in free-free flexural vibration, J is the moment of inertia and m is the mass. The dynamic modulus of elasticity according to the longitudinal vibration tests follows from equation 2.2. The ρ in this equation is the density.

$$E_f = 4 * \pi^2 * f^2 * l^3/(k^4 * J) * m \tag{2.1}$$

$$E_l = 4 * \rho * l^2 * f^2 \tag{2.2}$$

Hardness Tests

The hardness can be explained as the resistance to indentation (Piazza and Riggio, 2008). The hardness might be estimated by measuring the load required to penetrate 10 mm steel hemispherical bit to 5 mm (Piazza and Riggio, 2008). The wood should be clear without visible defects. The Young modulus can be calculated according to the formula below, obtained from Piazza and Riggio (2008). Where R is the required load, A is a coefficient, which depends on the wood species and where δ is a reduction factor. The hardness test is a good estimation for the modulus of elasticity. However, the modulus of elasticity varies a lot through the cross-section of a beam, due to the different densities of the timber in the beam. The surface properties may be overestimated in comparison to the properties inside.

$$E_0 = \delta * A * R^{0.5} \tag{2.3}$$

Acoustic Tests

The acoustic tests are based on the capacity of a stress wave to travel through the wood (Cavalli et al., 2016). The stress wave is induced by a strike with a hammer. accelerometers are installed on both ends of the beam and the time the waves takes to go from one end to the other is measured. The dynamic modulus of elasticity is easily calculated with equation below, obtained from Piazza and Riggio (2008) ,with ρ = density in kg/m^3 and V = stress wave velocity in km/s.

$$E_{din} = \rho * V^2 \tag{2.4}$$

dynamica modulus of elasticity

The obtained dynamical modulus of elasticity with the acoustic tests and vibrations tests is set to a static value of the modulus of elasticity with a linear relation, this is set to the formula below. Here α_1 and β_1 are constants, which depend on the material. The factors α_1 and β_1 can be found in FLP (1999). The demands are simplified to $E_{din} \geqslant 0.9 * E_{sta}$ (Piazza and Riggio, 2008).

$$E_{sta} = \alpha_1 * E_{din} + \beta_1 \tag{2.5}$$

2.2. 3D-Lidar Scanning Technology

In order to determine the dimensions of the elements several possibilities are available. The most common one is to measure the dimensions by hand. Another solution to measure the dimensions is 3D-Lidar scanning. 3D-Lidar scanning technology uses lasers to measure distances to certain points. By having the same position, different points in a visible field for the laser scanner are mapped and a total point cloud of the area is obtained. This methodology is very accurate to measure areas. The technology is commonly used with airborne laser scanning. The basic principle is an aeroplane crossing an area of interest and the airborne laser scanner measures the area below the plane to create an accurate map of the surface area Vosselman and Haas (2010). The basic principle is given in figure 2.1.

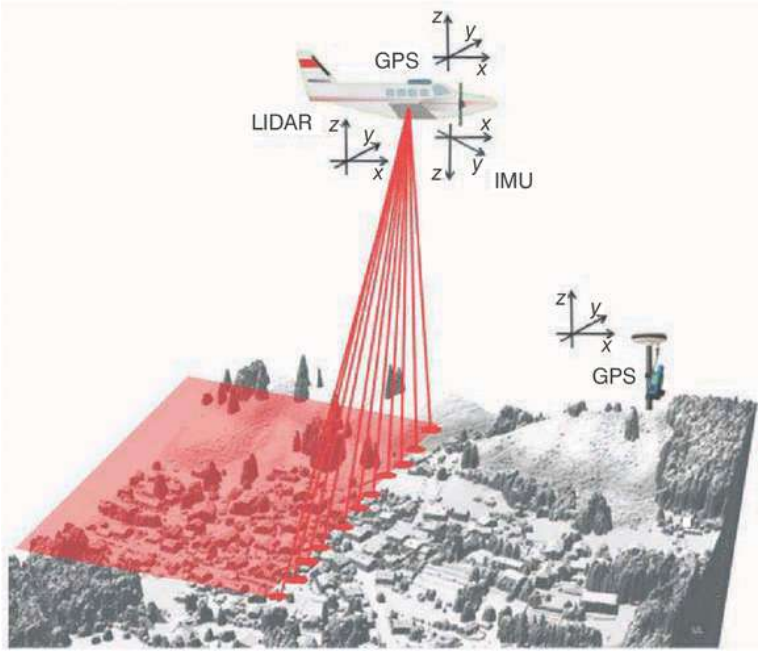

Figure 2.1: Principle of airborne laser scanning by Vosselman and Haas (2010)

2.2.1. Terrestrial Laser Scanners

Terrestrial laser scanners are most of the time used from a tripod (Vosselman and Haas, 2010). On top of the tripod, a 2D scanning device is installed. The available laser scanner is the Leica c10 Scan station. The specifications of the Leica c10 Scanstation state that the scanner is a very high-speed laser scanner, compact, dual-axis compensated and pulsed (Leica-geosystems, Unknown). Every single measurement is accurate up to $6mm$, while the standard deviation of the device is $2mm$, the other $4mm$ accuracy is determined by the distance from the object. The minimum scanning distance is $0.1m$ and the maximum scanning distance is $300m$ (Leica-geosystems, Unknown). The field of view is an angle of 360° in the horizontal plane and 270° in the vertical plane. The total weight of the scan station is $16.2kg$ ($13kg$ (scanner)+ $1.9kg$ (battery external) + $0.4kg$ (battery internal) + $0.9kg$ (AC power supply))(Leica-geosystems, Unknown). The other specifications are of lower importance for this specific application and kept out of consideration, for more information see Leica-geosystems (Unknown). The scan station is shown in figure 2.2.

Figure 2.2: The Leica c10 Scan station on a tripod (Leica-geosystems, Unknown)

Figure 2.3: The Zeb-Revo handheld scanner (OpticalSurveyequipment, 2018)

2.2.2. Hand-held Laser Scanners

The Hand-held laser scanner has advantages in the portable usage of the device. The handheld laser scanner is also based on 3D-Lidar scanning technology. Due to the portable function, it is more suitable for difficult accessible areas and is a faster solution in comparison to the terrestrial laser scanner. However, the accuracy is overall lower than the terrestrial laser scanner.

The suggested hand-held scanner is the ZEB-REVO portable laser scanner. The maximum range of the laser scanner is 30m in optimal conditions, but 15m-20m for normal conditions. The field of view is 270°*360° (*ZEB-REVO-User-Guide*, 2017). The scanner has a total weight of 1kg and with the inclusion of the carry case and contents 4.1kg. The scanner is shown in figure 2.3

2.3. The loads on the Tower

The different loads on the tower will be determined according to the Eurocode. Wind loads and self-weight of the tower will be the major loads on the tower. Other loads on the tower are self-weight of the lead, snow loads on the promenades, the church bells, the church clock and variable floor loads (people, stashed materials). The self-weight of the timber will be implemented in the model and not discussed in this chapter. More information about the loads is described in 3.

2.3.1. Wind Loads

The wind loads will be determined according to the NEN-EN 1991-1-4. The terrain conditions around the tower are terrain category IV (area surrounded by at least 15% buildings, with an average height above of 15 m)(NEN-EN-1991-1-4, ANNEX A). Haarlem is placed in wind area I in the Netherlands (NEN-EN 1991-1-4+A1+C2/NB). The extreme thrust with these conditions, for a height of 79 m is 1.66 $kN/m2$.

2.3.2. Snow Loads

The snow loads will be determined according to the NEN-EN 1991-1-3. The snow load in the Netherlands is $q_k = 0.7kN/m^2$.

2.3.3. Variable Loads

The following assumptions are all based on the knowledge of Henk Verhoef, an expert about the Carilion in the St. Bavo Church. The major clock on the tower is called the Roelant. The total weight of the clock is 4900 kg. The total weight of the carillon (excluding the Roelant) is approximately 4000 kg. The two much clocks smaller within the Damiaatjes, one floor higher up, are approximately 75 kg together and will be neglected. Just below the crown of the tower are three ringing bells present, they weigh approximately 144.86 kg and 61 kg. Since the ringing bells will be in motion, the rule of thumb for these calculations the vertical force is 150% of the weight and the horizontal force is 50% of the

weight. However, both these forces are of a low magnitude and will be neglected for the calculations.

The total weight of the lead cladding is approximately 85000 to 100000 kg. (*De bouw van de Grote Kerk*, n.d.)

The variable floor load is determined according to the NEN-EN-1990-1-1, art. 6.3.1.1. The tower in the church will be seen as a roofing area accessible with occupancy. The next chose is subdividing this category into imposed loads on garages and vehicle traffic areas, imposed loads on floors due to storage and imposed loads on floors, balconies and stairs (imposed loads on floors in areas for domestic and residential activities). The floor loads for domestic and residential areas is most suitable for this case and results in $q_k = 1.5$ to $2kN/m^2$ and $Q_k = 2$ to $3kN$ (NEN-EN-1991-1-1 6.3.1.2 table 6.2).

2.4. The Ongoing Inclination of the Tower

The tower is inclined in the north-west direction, which is clearly visible. Once every few years, the coordinates of the top of the tower are measured by the local authorities in order to see the horizontal movement of the top of the tower. The last measurements are from 2011. According to Selassa (2011), the tower inclined 97 mm towards the south and 19 mm towards the east since 1979. The total displacement vector is 99 mm. The first measurement was in 1898 and the total displacement of the tower from 1898 until 2011 is 320 mm. According to the results from Selassa (2011), the tower moves backwards to an straight condition and the total inclination will only get lower.

3 Methodology

The approach of Chapter 1 will be described in detail in this Chapter. The different methods of Chapter 2 will be considered and the most suitable methods will be determined. Furthermore, the simplifications and assumptions done for the loads will be described.

3.1. Structure of the Tower

A visual representation of the tower is required to get more knowledge about the tower and a better overview of all the elements in the tower. Since the structure is so complicated, it is difficult to describe the structure verbally. Therefore, a visual presentation of the structure is the best way to describe the structure of the tower. A sketch model will be made of all the load bearing elements in the tower to clarify the structure of the tower. The obtained data will be drawn in Autodesk Revit. Autodesk Revit is a suitable program for this specific sketch because one can easily build up a construction per floor layer. The hiding and showing functions per different floor levels are user-friendly. Since this will only be a sketch model, no other programs for the sketch model have been brought into consideration.

The sketch model will be used as a tool for measuring all the real dimensions of the tower. By printing two dimensional and three-dimensional views per floor and adding the correct dimensions, measured in the tower or in the scale model, the correct structure will be obtained. Measuring of the dimensions will be done with several methods. First of all, measurements will be made from the tower itself or from the scale model (see figure 1.1). Furthermore, the dimensions can be measured with a terrestrial laser scanner, a handheld laser scanner or by hand. For visiting floor five and higher (1.1), one requires supervision due to safety reasons. Hence, the structural elements on these floors and several unreachable elements will be measured from the scale model. The lower floors (the first to the fourth floor) will be measured in the real tower, since this will be a more accurate representation. In order to make this master thesis doable in time, the methodology with the lowest workload is preferred. The fastest way to obtain the geometry with cm accuracy is with hand measuring. The handheld laser scanner is more accurate, but more time consuming and the terrestrial laser scanner is even more accurate but even more time-consuming. The lower accuracy of hand measuring is acceptable since the geometry will be used for an indication model to find the flow of forces and critical elements.

With the obtained dimension, the Finite Element Model will be created. The reason for modelling it straight in a Finite Element Program is for regularly checking the construction. By using the self-weight of the beams, the model can be verified and errors can be removed immediately.

3.2. Mechanical Properties of the Wood in the Tower

In order to assess old timber structures, the mechanical properties of the timber are required. A lot of the timber in the tower is still the original timber from the 16th century. Some of the timber parts covered in lead are in worse condition than the other timber parts inside the tower. This is due to the leakage, which is caused by two factors. Firstly, the acetic acids in the oak reacting with the lead

and create white lead. The white lead might crack and leakage towards the covered timber can occur (Emmens et al., 2002). Secondly, due to bad workmanship in earlier renovations in the 20th century, insufficient overlap was applied and leakage could occur between the overlaying parts. The renovated parts, which are stored in the tower, can be used to test the mechanical properties. Since the parts are already renovated, due to damage from moisture, the parts will be on the lower limit of the average mechanical properties of all the timber in the tower. Thus, the parts are weaker and can be representative for the timber in the entire tower, since the timber in the tower will most likely be stronger.

In order to determine the mechanical properties, several methods of machine grading can be used with the addition of visual grading. The most important property for machine grading is the modulus of elasticity. According to the NEN-EN 408, the samples for bending tests require at least a length: thickness proportion of 19:1. Since the timber elements are stored in the tower, the chosen element should be portable in order to get the elements downstairs from the tower. The maximum size for elements to be portable from the tower will be around 1 m, this means the cross section will be 5 by 5 cm. The presences of knots in such a small cross section will drastically decrease the strength of the test sample. Whereas clear wood will overestimate the strength of the sample. Larger samples give more accurate results. In order to get usable values for the mechanical properties from the grading tests, a lot of statistical calculations are required, which takes a lot of time. The statistical calculations should be done according to the NEN-EN 14358. Furthermore, the tests from the NEN-EN 408 are destructive tests. However, the stored elements are monumental heritage and a long procedure to get approval from the authorities is required.

Visual grading is a quick way to roughly determine the mechanical properties. Visual grading should be done according to figure 2.4 and figure 2.5. The visual grading will be done per element and the number of knots on the face and on the edge will be determined. Other demands of the figures are hard to meet since the elements are already in use.

A lot of different non-destructive tests have been developed in order to grade timber elements. The most suitable non-destructive tests to determine the modulus of elasticity are vibrations tests, hardness tests and acoustic tests. Vibration tests are inexpensive methods, which gives fast and reliable results for the modulus of elasticity (Cavalli et al., 2016). The downside of vibrations tests is the lack of consideration for decay and ring shakes (Cavalli et al., 2016). Hardness tests give a good estimation of the density of a beam. However, the density varies a lot across the cross-section of a beam. Therefore, the mechanical properties on the surface may be overestimated Piazza and Riggio (2008). Acoustic tests use a relatively easy method to calculate the modulus of elasticity. The vibration tests require dismantled elements, which is the case for the elements in the tower. The dismantled elements should be placed on two supports, in order to vibrate freely. For this specific case, the longitudinal vibration tests are most suitable. By striking the beam with a hammer, the natural frequencies of the wave can be measured. With the addition of the density and the length of the element, the dynamic modulus of elasticity can be calculated. This will be done according to the formulas from chapter 2. The density will be roughly estimated by weighing the objects and roughly determining the volume of the timber elements.

Furthermore, both longitudinal vibrations tests and visual grading cannot provide sufficient information if it is individually used (Piazza and Riggio, 2008). Therefore, combining both methods gives reliable results for the calculations. By measuring the modulus of elasticity of several dismantled timber elements, a mean modulus of elasticity can be calculated and be used as an accurate representation for the entire structure. The modulus of elasticity will be converted to a modulus of elasticity with a moisture content of 12 %. By taking several samples of the moisture content on randomly chosen elements in the tower, an average moisture content of all elements will be determined and used to determine the average modulus of elasticity with a moisture content of 12 %. The moisture content of the samples will be measured with the FMD6 Moisture Meter. In addition to the longitudinal vibration tests,the load carrying elements will be visually graded. Load carrying elements, which are in worse condition according to the visual grading, will be given lower strength properties in the Finite Element Model. Whereas, most elements will be given properties based on the longitudinal vibration tests. Visual grading and longitudinal vibration tests combined will determine representative mechan-

ical properties, which might be used to create a representative Finite Element Model for reality. The Finite Element Model is still an indication model and the properties might differ from reality. However, this is acceptable for the results. Besides, not every member is able to undergo longitudinal vibration tests and visually grading all the elements will be very time-consuming. For the scope of this master thesis, the method described above will be permitted, despite not being completely accurate.

3.3. The Loads on the Tower

The main loads on the tower will be self-weight, imposed floors loads, snow loads, wind loads and additional weight. The implementation of the load cases will be described below.

- The self-weight is automatically imposed in the Finite Element Model.
- Floors will be laid and all the floors will be loaded by the imposed floor loads.
- The snow loads will only give significant loads on the balustrades. However, when heavy wind loads and high snow loads are both present, the snow will be blown away. Therefore, it is assumed that the snow loads could be neglected.
- The wind loads will be distributed equally over the entire height of the tower. The highest wind load will occur on top of the tower. This force will be applied over the full height of the tower. The wind load will be applied perpendicular to the plane. Since the tower is shaped as an octagon, not only one plane will be loaded perpendicular to the plane, but the two abutting oblique planes will partly be loaded by the wind load. The wind load on the abutting oblique planes will be divided by $\sqrt{2}$, since they are under an angle of approximately 45°. In order to attach the wind loads to the structure, walls will be made for the outer planes. Since the wind loads can come from all directions, eight combinations for the wind will be made. Furthermore, wind loads from a corner direction, perpendicular to the seams of the octagon, will load the two oblique planes to the seam with equal wind forces of $\sin 67.5$ times the wind load and the oblique planes to the two planes will be loaded by forces of $\sin 22.5$ times the wind load. The wind will form a load on 4 planes in this scenario. Wind from this direction gives eight other combinations. Only one combination is present at the time and the sixteen different combinations will all be taken into consideration.
- The lead cladding has a really high self-weight. This self-weight hangs on the outside of the tower. In order to simplify the self-weight of the lead cladding, the self-weight will be attached to the outside walls. By dividing the total weight by the total surface area of all the walls, an equally distributed load for all the walls will be found. The total surface area of all the walls is estimated at 747.6 m^2. The load will be applied vertically and parallel to the walls. Some floor higher up are open and have no walls, the loads due to the lead cladding will be unrealistic for these floors. However, this has not been taken into account.
- The carillon has a significant weight. The Roelant will be attached as a point load to the middle of the ceiling of floor 5b (see chapter 4 for an explanation of the different floors). The other parts of the carillon weigh approximately 4000 kg and will be equally divided in eight point loads attached to the inner octagon beams at the ceiling of floor 5b.

The magnitude of the loads used in the Finite Element model will be given in table 3.1. The gravity constant is assumed to be 9.81 m/s^2.

Table 3.1: The magnitude of the forces used in the Finite Element Model

Load type	magnitude
self weight	ρ_k=655 kg/m^3
wind loads (90 °)	$q_{wind,90}$ = 1.66 kN/m^2
wind loads (67.5 °)	$q_{wind,67.5}$ = 1.53 kN/m^2
wind loads (45 °)	$q_{wind,45}$ = 1.17 kN/m^2
wind loads (22.5 °)	$q_{wind,22.5}$ = 0.64 kN/m^2
Imposed floor load	$q_{imposed,floor}$ = 2.00 kN/m^2
the lead cladding	q_{lead} = (10000 kg *9.81 m/s^2/747.6 m^2) *10^{-3}=1.31 kN/m^2
The Roelant	$F_{Roelant}$ = (5500 kg *9.81 m/s^2) *10^{-3} = 54.00 kN
the carillon	$F_{carillon}$ = (4000 kg *9.81 m/s^2)/8 *10^{-3} = 4.91 kN

The load combinations in Ultimate Limit State (ULS) will be governing for static loads, wind loads and imposed floor loads. The load combinations come from NEN-EN 1990+A1+A1/ C2:2011 in chapter 6.4.3.2. In case the static load is governing, the variable loads will be reduced with a value ψ_0. ψ_0 is 0.7 for every type of usage, except for storage (ψ_0=1) and roofing (ψ_0=0). Since storage usage gives the worst outcome and is closest to the usage of the tower, ψ_0 = 1 will be used for the imposed floor loads. ψ_0 = 0.6 for wind loads. In case the static load is not governing, it will be reduced with a factor ϵ_j, which is 0.89. The load combination for which the static load is governing is given in equation 3.1. The governing combination for wind is given in equation 3.2 and the governing combination for the imposed floor load is given in equation 3.3.

$$\sum(\gamma_{G,j}*G_{k,j})+\gamma_{Q,wind}*\psi_0*Q_{k,wind}+(\gamma_{Q,imp}*\psi_0*Q_{k,imp}) = 1.35*G_{k,j}+0.9*Q_{k,wind}+1.05*Q_{k,imp} \quad (3.1)$$

$$\sum(\epsilon_j*\gamma_{G,j}*G_{k,j})+\gamma_{Q,wind}*Q_{k,wind}+(\gamma_{Q,imp}*\psi_0*Q_{k,imp}) = 1.2*G_{k,j}+1.5*Q_{k,wind}+1.05*Q_{k.imp} \quad (3.2)$$

$$\sum(\epsilon_j*\gamma_{G,j}*G_{k,j})+\gamma_{Q,imp}*Q_{k,imp}+(\gamma_{Q,wind}*\psi_0*Q_{k,wind}) = 1.2*G_{k,j}+1.5*Q_{k,imp}+0.9*Q_{k,wind} \quad (3.3)$$

The Service Limit State (SLS) will be taken into consideration with the frequent load combination. The load combinations come from NEN-EN 1990+A1+A1/ C2:2011 nl in chapter 6.5.3. The frequent combination is applicable for reversible situations. The combinations for the frequent combination are given in equation 3.4, where the wind loads are governing and equation 3.5, where the imposed floor loads are governing. The factors for the wind are ψ_1=0.2 and ψ_2=0. The factors for the imposed loads are ψ_1=0.9 and ψ_2=0.8. The usage for the tower is storage once again, since this has the least favorable factors.

$$\sum(G_{k,j}) + \psi_1 * Q_{k,wind} + \psi_2 * Q_{k,imp}) = G_{k,j} + 0.2 * Q_{k,wind} + 0.8 * Q_{k,imp} \quad (3.4)$$

$$\sum(G_{k,j}) + \psi_1 * Q_{k,imp} + \psi_2 * Q_{k,wind}) = G_{k,j} + 0.9 * Q_{k,imp} \quad (3.5)$$

3.4. Determination of the Critical Elements in the Tower

The flow of forces in the tower will be obtained with the geometry, representative mechanical properties and the loads on the tower. The most important factors to look into are the deflections, the stresses due to bending, the stresses due to compression, the stresses due to tension, the stresses due to combined bending and compression and the shear forces. Based on this, elements with the highest deflections and stresses will be verified if they fulfil the requirements according to the NEN-EN 1995. Furthermore, the critical connections have to be checked. Almost all the connections in the tower are dowel connections. However, the number of dowels and the way the elements are connected differ per connection. In timber structures, the connections are frequently the most critical components.

Since the tower has some symmetry in the structure, several connections will carry almost the same loads. By visual inspection of the identical connections, the weakest one will be determined and be recalculated in order to find out if it fulfils the strength demands of the NEN-EN 1995. In the visual inspection, the cracks and the knots will matter for the connections and also the remaining strength bearing part of the connections. Based on all the obtained results from the calculations of the critical elements, the current strength of the entire tower will be concluded.

3.5. The Deflections of the Tower

The deflection of the tower due to wind forces could be measured by an U-blox ZED-F9P. The U-blox could be installed in the top of the tower and it measures the deflection of the top of the tower for several weeks. In order to measure the deflection of the U-blox, a receiving station is required on a stationary spot. This can be a surrounding building, which does not move during heavy wind forces. The receiver will be a geodetic GNSS receiver with a geodetic zephyr antenna. The U-blox will measure the distances towards the receiver for several weeks and with this information, the maximum deflection of the tower due to wind forces can be determined. After a site investigation, it became clear that this method is not possible. The U-blox requires access to the power net, which is not possible in the top of the tower. It might be possible with the power of a car battery. However, carrying a car battery to the top of the tower might be dangerous. Therefore, this is left out of consideration.

3.6. The Angle of Inclination of the Tower

The inclination of the tower influences the centre of gravity of the entire construction. If the centre of gravity comes outside of the base of the tower, the structure becomes unstable and the tower might be endangered to fall over during unfavourable conditions. In order to take the inclination into consideration in the Finite Element Model, the angle of inclination has to be obtained. The local authorities measure the coordinates of the top of the tower every several years. However, the coordinates give insufficient information about the total inclination of the tower, because the measurements use the measurements of 1898 as zero measurement. However, the tower was most likely already inclined in 1898, which is not taken into consideration. As method to determine the inclination of the tower, the Leica c10 scanstation will be used. By measuring the tower accurately, a Pointcloud model of the tower will be obtained. The point cloud is so accurate, that seams on the tower are easily recognized. The pointcloud will be studied in the software CloudCompare.

In order to find the inclination from the point cloud, two methods can be used. The first method is using segmentation of planes on the seams. The planes have a normal vector and the angle of the vector can be used to determine the angle of inclination of the plane. The other method is taking 2 points per lantern on the seam, the difference in coordinates determines a line parallel to the facade and the angle of inclination might be determined from the line. Since the outer elements on the seam are very complicated shapes, obtaining representative planes for the seam is very difficult. The obtained planes are not reliable in order to determine the angle of inclination. Therefore, the second method is used. The second method is done manually and is therefore sensitive to errors. In order to lower the total error, several measurements per seam will be made and then the average angle of inclination will be used. Every seam will be separately measured. The downside to this method is the received angles of inclination on all 8 seams are all absolute values. However, since the tower is clearly tilted in North West direction (visible for the naked eye), it is assumed that the angles of inclinations are all in North West direction. The results will provide a maximum, minimum and average angle of inclination per seam.
Based on personal knowledge, the Leica c10 scanstation is the best suitable for this, since it has the highest accuracy in comparison to a handheld scanner or methods by hand. Another reason for choosing this method is the availability and the experience with the Leica c10 scanstaion.

3.7. Overview of the Chosen Methods

In order to wrap up the methodology, a clear overview of the chosen methods is given in table 3.2.

Table 3.2: The required results with the chosen methods to obtain the results.

Required results	Chosen method
The built-up of the tower	The scale model and sketches of Kamphuis
Geometry	Measuring by hand from the tower and from the scale model
Mechanical properties	Combining visual grading and longitudinal vibration tests
Moisture content	FMD6 Moisture Meter
Point cloud of the tower	Terrestrial laser scanner
Total inclination of the tower	By hand from the point cloud of the tower
Inclination of the base of the tower	By hand from the point cloud of the tower
Force and stress distribution	Finite Element Model
Determination of critical locations	Finite Element Model
Verification of the critical locations	By hand according to the Eurocode

3.8. Discussion

In this chapter, the methods in order to assess the structural state of the tower are explained. The methods to obtain the mechanical properties of the wood and the geometry of the tower are both chosen based on the workload instead of precision. In order to get more precise results, the geometry should be measured with the laser scan technology. Since the elements are not completely squared and the width or height differs over the length, measuring by hand causes small errors. However, since the geometry is used as an indication this is acceptable.

In order to obtain accurate results for the mechanical properties, machine grading is a more suitable solution. By measuring all mechanical properties instead of picking a strength class based on a modulus of elasticity, more accurate results for all mechanical properties will be obtained. Furthermore, By using the 5% over the obtained results of machine grading, safe values will be obtained. However, besides the lower workload for longitudinal vibration tests, the timber cannot be destructively tested, since it is monumental heritage. Therefore, a combination of longitudinal vibration tests and visual grading seems to be the best solution.

In addition to chapter 2, the static and variable loads on the tower have been determined. Some simplifications have been made to the loads. For instance, the wind load is taken as a static load. More precise results might be obtained by modelling the wind load as a dynamic load. However, due to the high workload this is not done. The model is still an indication and taking the wind as a static load is sufficient.

4

The Structure of the Tower

This chapter is ment to outline the structure of the tower, in order to give the reader a better overview of the complicity of the tower.

4.1. The Structure of the Tower

The structure of the tower of the St. Bavochurch is divided into eight floors, see figure 1.1. However, the fifth, sixth and seventh floor, from figure 1.1 are divided into two floors. From now on, the fifth floor will be divided in floor 5a and 5b, the sixth floor will be divided in floor 6a and 6b and the seventh floor will be divided in floor 7a and 7b. The building method is ”stack building” or ”stapelbouw” for the first four floors of the tower, otherwise known as the base (voet) of the tower. The structure of the base of the tower has a lot of different elements and therefore it is complicated. The structure from the third floor on, see figure 1.1, is made of an outer inequitable octagon and an inner inequitable octagon. After the first promenade, the building method will suddenly switch to a ”sword construction” or ”zwaard constructie”. The structure of the fifth floor consists of an outer equilateral octagon and an inner equilateral octagon, see figure 1.1. From the sixth floor and higher, the structure is carried out as a single equilateral octagon. The clarification of the tower will be done per floor. A consultancy firm (Kamphuis bureau voor bouwhistorie) made a report on the building history of the tower of the St. Bavochurch. Besides the history of the tower, the structure of the first, second, and third have been precisely described and drawn. The first three floors in addition with the fourth floor are the foundation for the three lanterns coming above on top of the first four floors. Each lantern consists out of two floors, the eighth floor is the crown on top of the tower.

The drawings of the structure for the first, second and third floors by Kamphuis (2001), are shown in figures 4.1, 4.2 and 4.3.

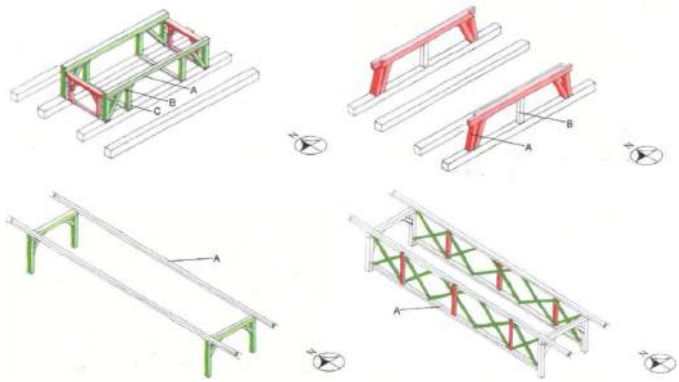

Figure 4.1: The structure of the 1st floor by Kamphuis (2001)

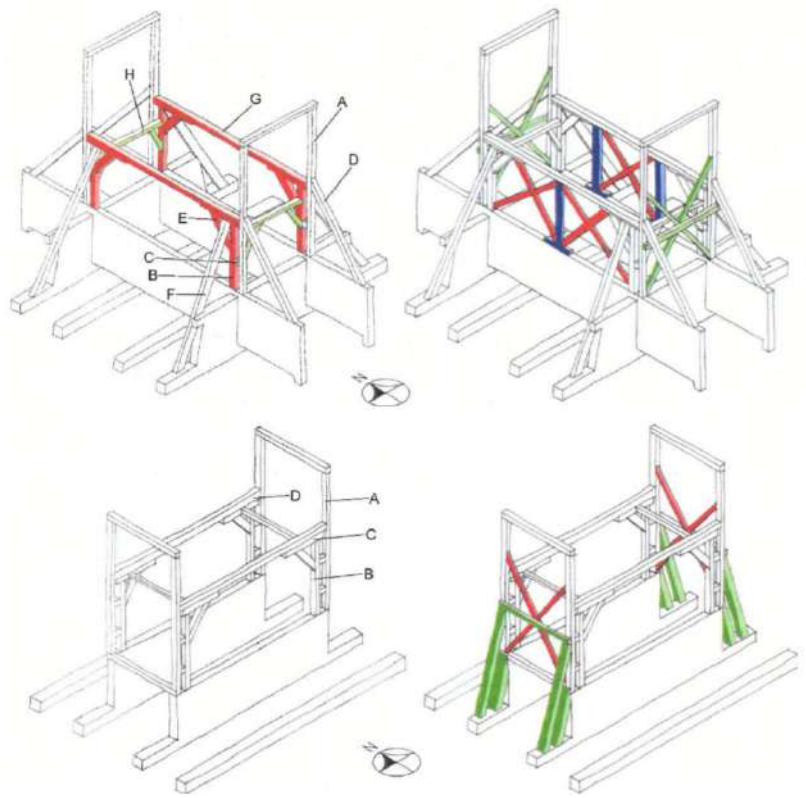

Figure 4.2: The structure of the 2nd floor by Kamphuis (2001)

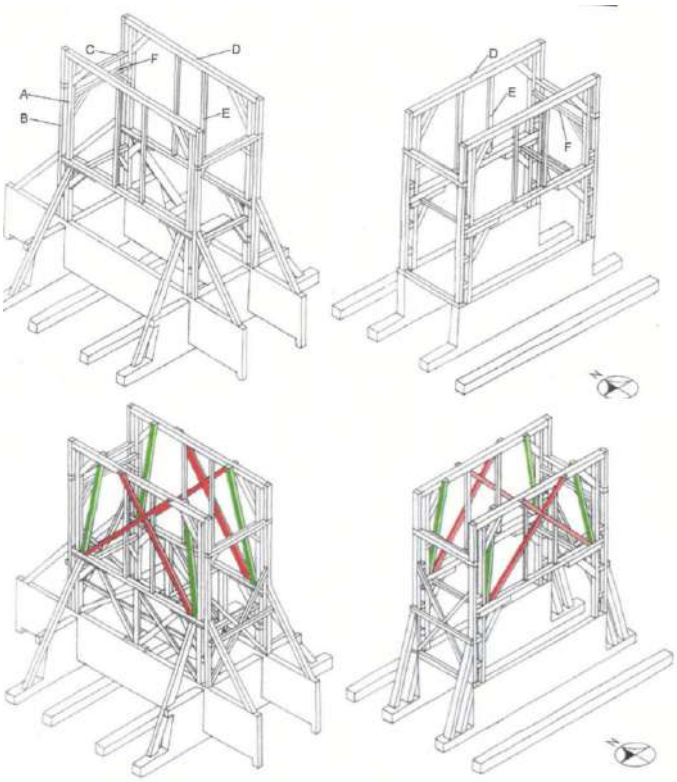

Figure 4.3: The structure of the 3rd and 4th floor by Kamphuis (2001)

The structure of the floors above the first three floors is logical and has been estimated by sketches. Due to the floors in the tower, visualisation of the overlap from one floor to another is difficult to inspect. The connections between floors are based on common sense. For instance, columns have been placed on top of another column. Based on the sketches, a three-dimensional model has been made with Autodesk Revit. The sketch model is shown in figure 4.4. The red, blue and yellow colours are made to clarify the sketch. The red colour symbolizes the load carrying elements, which give strength to the tower. The blue colour symbolizes the elements, which are used as stability elements. The yellow colour symbolizes unnecessary or redundant elements in the tower. The colours have been based on personal knowledge and are not necessarily correct. Whether the elements are in fact load carrying, only for stability or have no impact on the strength and stability of the tower will follow from the results of the Finite Element Model. The dotted lines through the construction are the floor levels used in the Revit model. The sketch model lacks the fourth floor. Due to a mistake during the visual inspection, the fourth floor was assumed to be used in the figures of the structure as made by Kamphuis (2001). However, this mistake has been corrected in the real Finite Element Model.

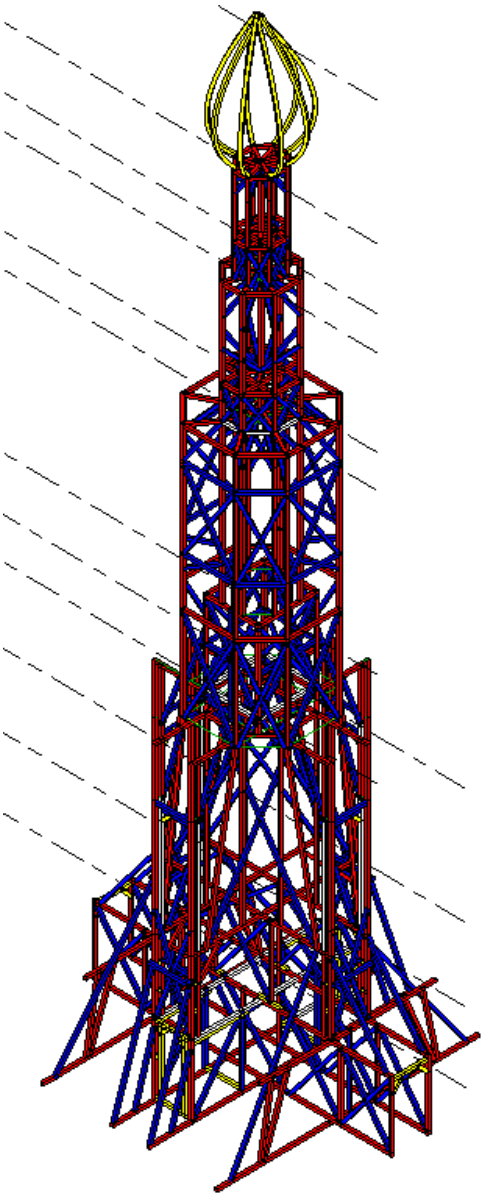

Figure 4.4: The sketch model made in Autodesk Revit

The two-dimensional sketches and three-dimensional sketches created from the entire sketch model are shown in appendix A. The sketches give also more insight into the structure of the tower and all the different elements in the tower. The figures in the appendix have the additional notes and measurements used to create the entire Finite Element Model. The measurements are on centimetre accuracy for the dimensions of the beams. The exact location of beams might differ a bit more since some beams are hard to measure due to the difficult positions. In short, errors might have been added on top of each other and making the total errors larger, further up in the tower. However, the model is an accurate representation for the reality and the flow of forces is sufficient enough to determine the location of critical elements.

With the measured dimensions of the tower, a complete Finite Element Model has been made. The model is visible in figure 4.5. Since SCIA Engineer works with rods, the rod model is also shown in figure 4.5. The rods get a cross-sections and will become visible as beams. However, for the calculations, only the rods are used. therefore, it is of high importance to have the nodes, which connect the rods, properly modelled.

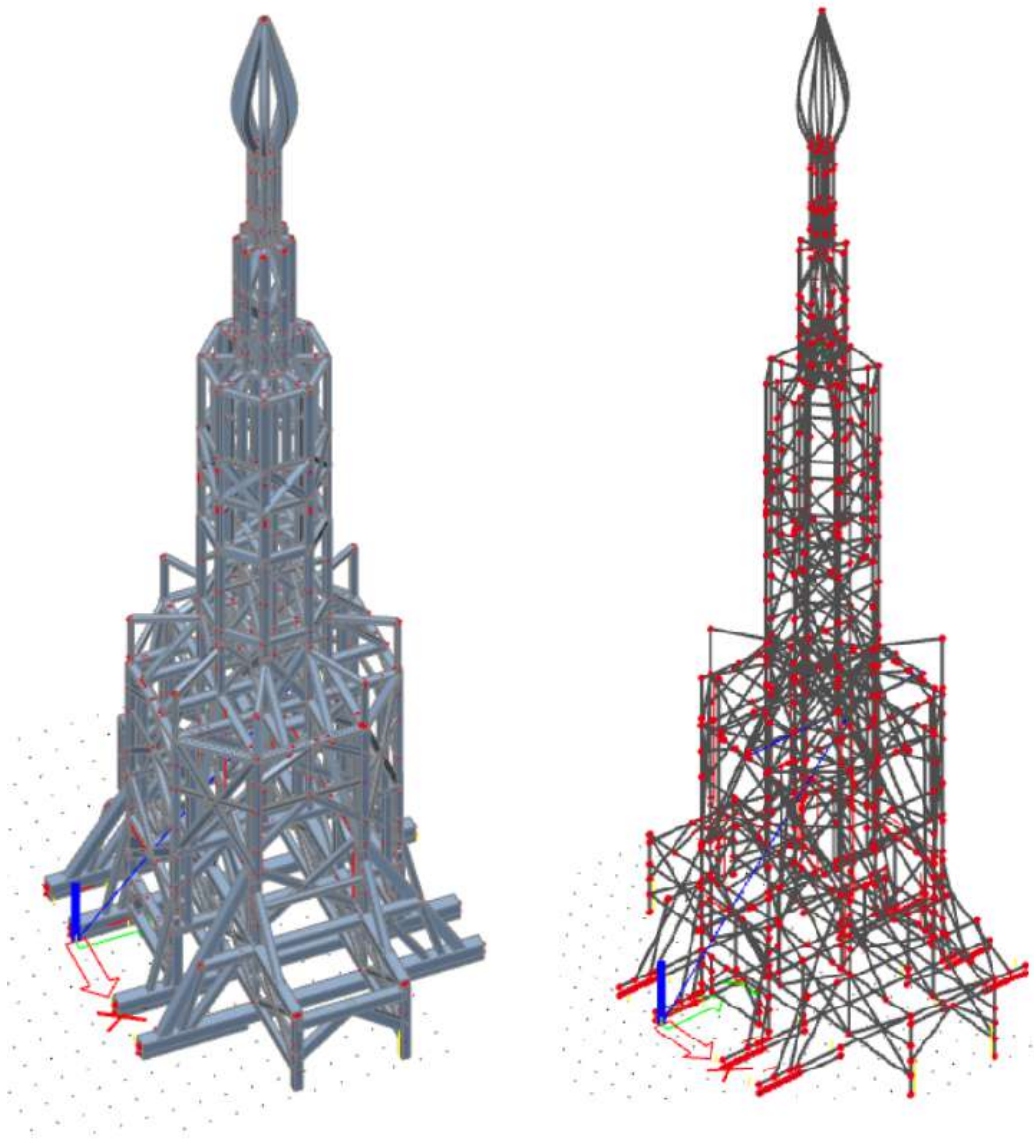

Figure 4.5: the Finite Element Model in Scia Engineer, left is the beam model and right is the rod model.

The model has been verified with the self-weight of the elements. For now, a random timber class was assigned for the mechanical properties, since the real mechanical properties are not known yet. The maximum deflection due to self-weight is 2.5mm, this can be seen in figure 4.6. The maximum deflections due to self-weight occurs in the cross-heads at the third and fourth floor. Only the base is visible in this figure because the picture would become unclear if the entire tower was visible.

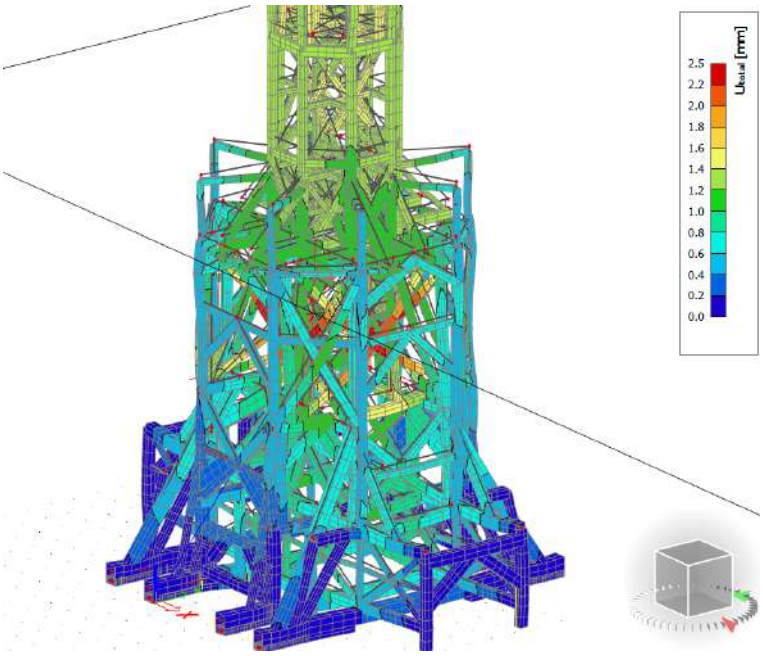

Figure 4.6: The deflections of the base of the tower.

Now the dimensions of the model are determined, only the loads have to be added and the mechanical properties should be changed to the correct values for a correct model in order to find the critical elements.

4.2. Discussion

In this chapter and in addition of appendix A the structure and the dimensions of all the structural elements in the tower are explained. As has been mentioned in the discussion of chapter 3, the geometry might have small errors, since the geometry is measured by hand. During the built-up of the finite element model, small modelling mistakes might be made. Since the finite element model is made by hand as well. On top of the small errors from determining the geometry, the model might be a bit off and it is possible to create a more accurate model. However, since the model is used as an indication, the small errors have been accepted.

5

Mechanical Properties of the Wood in the Tower

In order to determine the strength of the timber in the tower and finding representative values for the mechanical properties of the wood in the tower, a combination of longitudinal vibration tests and visual grading will be used. The longitudinal vibration tests will be used on the dismantled and replaced timber elements, stored in the tower, in order to find the dynamic modulus of elasticity. The dynamic modulus of elasticity will be converted to a modulus of elasticity at a moisture content of 12 %. The average moisture content in the tower will be measured by taking a few samples and measuring the moisture content of the samples with the FMD6 moisture meter. The average moisture content of the samples will be calculated and it is assumed that this is the moisture content for the entire tower. In total, nineteen suitable samples are present in order to test the dynamic modulus of elasticity with longitudinal vibration tests. The samples are shown in appendix B. Visual grading will be used to determine weaker elements in the tower. Elements which do not suffice the criteria of the NEN-EN 14081-1 for the knots on the face and on the edge of elements will be given a lower strength class than the other elements in the Finite Element Model. After performing both the grading methods, the results from the longitudinal vibration tests will be used as a global indication for all timber element in the tower. The average dynamic modulus of elasticity will be coupled to a strength class from Blass and Sandhaas (2017) with a comparable modulus of elasticity. The obtained strength class will be an indication for the entire tower. Visual grading will be used to determine weaker elements, which will be given lower strength properties than the strength class obtained from the longitudinal vibration tests, which is used for the other timber elements.

5.1. Longitudinal Vibration Tests

In order to perform longitudinal vibration tests on the stored elements, the elements should be lifted from the ground and placed on two supports. In this way, the elements are able to vibrate freely. In order to let the sensor measure the natural frequencies of the element, a flat surface is required. A sensor called Timber Grader is used to measure the vibration wave. The sensor will be held against the flat surface and a hammer will strike the flat surface, next to the sensor. The sensor will measure the response of the element and measure the vibration wave, induced by the hammer strike, going back and forth in the timber element. The sensor will send the results towards a connected computer and the results are immediately visible in a software program called Timber Grader. The program shows the response in a graph and one is immediately able to judge if the measured results are useable. The results require clear peaks, which represent the natural frequencies. Besides the peaks, it is preferable that the response in between the peaks is as flat as possible. The useable graphs and results are shown in appendix B. The test setup for test sample 12 is shown in figure 5.1. The test sample has been placed on two other timber beams, which acts as the supports.

Figure 5.1: The test setup for the longitudinal vibration test on test sample 12.

The first natural frequency is the required result from the longitudinal vibration tests. Only test samples 5,6,7,8,11 and 12 gave proper results, which can be used for the determination of the dynamic modulus of elasticity. Several measurements have been made in order to find the mean of the first frequencies. The other test samples were not use full because of different reason, namely: the length was too short, the required results were not useable or there was no flat surface present to strike with the hammer. With the obtained first natural frequencies, equation 5.1 is used to calculate the dynamic modulus of elasticity.

$$E_l = 4 * \rho * l^2 * f^2 \tag{5.1}$$

The density is determined by taking rectangular samples from the tower, where the volume is easily determined. The volume varies between 618.8 kg/m^3 and 690.5 kg/m^3. The huge difference is present due to cracks and holes created by insects in the timber. Some pieces are in worse conditions and have more voids inside. According to Sonderegger et al. (2015), the density of European oak, which is between 210 and 470 years old, is 668 kg/m^3 +/- 64 kg/m^3. The measured density from the tower lies in between the boundaries of 604 kg/m^3 and 732 kg/m^3 and therefore is assumed to be correct. The wood has dried for ages in the tower and therefore is assumed to be below equilibrium moisture content. Since the wood is dry, it is left out of the consideration in the calculation of the dynamic modulus of elasticity. Soaking the wood would increase the density of the wood, which would let the dynamic modulus of elasticity also increase, while the mechanical properties of the wood did not get stronger. Therefore, having a moisture content below equilibrium would negatively influence the dynamic modulus of elasticity and is therefore on the safe side of the calculations. The dynamic modulus of elasticity of each sample is calculated for the minimum, maximum and average measured density. The average first frequency is used for the calculations, all other values are shown in appendix B. The calculated moduli of elasticity are shown in table 5.1.

Table 5.1: The estimations of the dynamic modulus of elasticity of several test samples.

Test samples	5	6	7	8	11	12
Length (m)	5.45	5.25	5.63	5.25	2.30	3.46
Average first frequency (Hz)	335	349	615/2	343	723	574
Minimum modulus of elasticity (N/mm^2)	9207	9272	8278	8956	7638	10894
Maximum modulus of elasticity (N/mm^2)	8251	8310	7419	8026	6845	9763
Average modulus of elasticity (N/mm^2)	8729	8792	7849	8492	7242	10329

The average dynamic modulus of elasticity of all the elements follows from table 5.1 and is 8572 N/mm^2. According to Piazza and Riggio (2008), the dynamic modulus of elasticity is higher than the static modulus of elasticity, because of the viscous-elastic behaviour of wood. The minimum criteria is $E_{din} \geqslant 0.9 * E_{sta}$. Therefore the minimum average static modulus of elasticity is $E_{sta} = E_{din}/0.9 = 8572/0.9 = 9524 N/mm^2$. The modulus of elasticity for the lowest strength class of hardwoods (D18) is 9500 N/mm^2 (Blass and Sandhaas, 2017). This is almost equal to the obtained modulus of elasticity. In order to simplify the calculations, the strength class D18 is chosen in the Finite Element Model. After all, the Finite Element Model is used as an indication. Furthermore, The timber elements have been replaced, because they were most likely in worse condition than the elements which are still in use. Therefore, the assumption to give all elements in use a strength class of D18 is justified and the timber in the tower is probably in a higher strength class than D18.

The moisture content has been measured for 15 samples with the FMD6 Moisture Meter, the test setup is shown in figure 5.2. The samples have been picked randomly at floors 1 until 5a. The average moisture content of all samples was 16.85 % and ranged from 13.7 % to 19.3 %. The difference between the measurements is explained by the locations of the samples. For example, samples near the door to the balustrade are more exposed to moisture from the outside than others. The modulus of elasticity calculated with equation 5.1 are based on a moisture content of 12 %. According to Gerhards (1980), the moisture content negatively influences the mechanical properties. For instance, the modulus of elasticity is 13 % lower at a moisture content of 20 % and 6 % higher at a moisture content of 6 % in comparison to the modulus of elasticity at a moisture content of 12 %. This influence of moisture is tested by Gerhards (1980) for several species and is shown in figure 5.3. For the found moisture content of 16.85 %, a roughly estimated reduction of the mechanical properties is required by 6 %. However, since the results of the longitudinal vibration tests estimated strength class D18, which is the lowest strength class, the reduction due to the moisture content has not brought into consideration. Since the model is an indication, the simplification of taking strength class D18 is verified. Furthermore, the static relationship $E_{din} \geqslant 0.9 E_{sta}$ is a minimum criteria and the tested samples are replaced due to damage and are most likely in worse conditions than the timber still in use in the tower. Both these reasons can explain an underestimation, while the moisture content causes an overestimation. In future studies the results should be optimized by taking the moisture content into more consideration.

Figure 5.2: The FMD6 Moisture Meter during test setup.

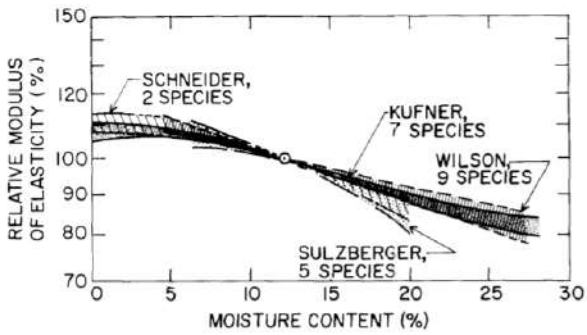

Figure 5.3: The relation between the mechanical properties and the moisture content (Gerhards, 1980).

5.2. Visual Grading

By performing a visual inspection on the elements in use in the tower, elements with significant defects are detected. The focus is placed on large knots present in the timber. The knots were treated as significant in case the knots diameter on the face is at least half of the width of the element or if the diameter of the knots on the edge was at least three-quarter of the thickness of the element. The criteria are shown in figure 2.4 and figure 2.5. The other demands will not be taken into consideration, because almost every member does not fulfil the demands for insect holes and fissures. If this is taken into consideration, barely any elements will give strength and the Finite Element Model will be useless and cannot be used in order to get an indication of the force distribution of the tower.

The visual inspection will only be done for reachable and visible elements and was only performed on floors 1 to 5a (see figure 1.1). Floors higher up than floor 5a are difficult to inspect, since the elements on floors 5b until floor 8 (besides floor 6a and 7a) are covered in lead and therefore are impossible to inspect. Furthermore, it is possible to inspect floor 6a and floor 7a, but this has been left out of consideration because supervision is required to inspect those floors.

During the visual inspection, 13 elements with significant defects were discovered. The locations and imperfections of the critical elements are shown in appendix C. Besides critical element 3.1 (critical element 3.1 has the width reduced by more than 50%, in order to make space for the carillon and therefore is assumed to be a critical element), all elements are stability elements and have knots, who do not suffice the criteria of the NEN-EN 14081-1. It is possible to conclude that the builders of the tower of the St. Bavochurch tower were aware of the lower mechanical properties of timber with the presence of large knots and therefore used the timber parts with large knots for stability purposes. However, in general the beams and columns have a larger width and thickness and the presence of knots is less significant in comparison to the thinner stability elements. In order to take the elements with large knots into consideration, the mechanical properties of the 13 ”defect” elements will be halved for the calculations in the Finite Element Model.

5.3. The Indicated Values for the Mechanical Properties

In short, all elements without significant defects are estimated to be of strength class D18. The mechanical properties of elements of strength class D18 are given in table 5.2. The strength class of D18 is an indication and has been based on the longitudinal vibration tests. The mechanical properties of elements with significant defects will be halved and are given in table 5.3. These elements are selected based on the visual inspection.

Material type	Timber
Thermal expansion ...	0.00
Unit mass [kg/m^3]	655.0
E modulus [MPa]	9.5000e+03
Poisson coeff.	0
Independent G mo...	☑
G modulus [MPa]	5.9000e+02
Log. decrement (no...	0.15
Colour	
Specific heat [J/gK]	6.0000e-01
Thermal conductivi...	4.5000e+01
Material behavi...	
Material behaviour	Elastic
EC5	
Bending (fm,k) [MPa]	18.0
Tension (ft,0,k) [MPa]	11.0
Tension (ft,90,k) [M...	0.6
Compression (fc,0,k...	18.0
Compression (fc,90,...	4.8
Shear (fv,k) [MPa]	3.5
Modulus (E0.05) [M...	8000.0
Modulus (E 90 mea...	630.0
Type of timber	Solid

Table 5.2: The mechanical properties under normal condition of the timber elements in use in the tower.

Material type	Timber
Thermal expansion ...	0.00
Unit mass [kg/m^3]	655.0
E modulus [MPa]	4.7500e+03
Poisson coeff.	0
Independent G mo...	☑
G modulus [MPa]	2.9500e+03
Log. decrement (no...	0.15
Colour	
Specific heat [J/gK]	6.0000e-01
Thermal conductivi...	4.5000e+01
Material behavi...	
Material behaviour	Elastic
EC5	
Bending (fm,k) [MPa]	9.0
Tension (ft,0,k) [MPa]	5.5
Tension (ft,90,k) [M...	0.3
Compression (fc,0,k...	9.0
Compression (fc,90,...	2.4
Shear (fv,k) [MPa]	1.8
Modulus (E0.05) [M...	4000.0
Modulus (E 90 mea...	315.0
Type of timber	Solid

Table 5.3: The mechanical properties of the element who did not full fill the demands of the NEN-EN 14081.

5.4. Discussion

The mechanical properties of all elements are based on longitudinal vibration tests on a few dismantled element (see appendix B). Most of the dismantled elements are replaced due to moisture damage and therefore probably have lower mechanical properties than the other elements in use in the tower. This probably causes the obtained mechanical properties to be underestimated from the real mechanical properties of the timber in use. Furthermore, the damage to the elements in use due to insects and ageing are not taken into consideration. However, in case wood is stored in dry conditions it barely undergoes any changes ((Nilsson and Rowell, 2012) and Niemz and Mannes (2012)). Therefore it is acceptable that damages due to insects and ageing are not taken into consideration. In order to optimize the results of the longitudinal vibration tests, the effect of the moisture content of the timber should be taken into consideration. This is left out of consideration, since the mechanical properties are used as an indication. The visual grading has only been done for reachable and visible elements. Therefore some major defects might have been missed. However, it is simply not possible to inspect these elements and therefore it has been left out of consideration.

6

The Inclination of the Tower

The tower is clearly inclined in the north-west direction as one can see with the naked eye. In order to calculate the inclination, the angle of inclination must be obtained. As shown in figure 6.3, the tower consists of a base and three separate roof lanterns. Every roof lantern is made out of an octagon.

6.1. Determination of the Inclination of the Tower

By laser scanning the tower from every angle with the Leica c10 scanstation, a pointcloud is obtained of the entire tower. In order to get the entire tower scanned, ten different scans from different locations were made during the fieldwork. The locations and sequence of the scans are given with the red crosses and red numbers in figure 6.1. The laser scanner during the field work on location 5 is shown in figure 6.3. In order to align the scans, targets have been placed (see figure 6.2) and have been scanned. The targets are magnetic and could be placed on metal objects (such as lampposts) or were placed on tripods. Two separate scans can be aligned by placing at least three targets (two targets are the minimum, but having at least one extra target in case a target got moved or the scanning of one target went wrong) in between the scan locations. The three targets have to be clearly visible from both scanning locations. The targets placed in order to align scan location 4 and scan location 5 are shown in figure 6.2. Two targets are placed on tripods and a third one can be seen on the lamppost just above the white van in the figure. The lamppost is octagonally shaped, so it was steadily attached to the lamppost. The round shape of regular lampposts might move the target due to the wind. However, the flat surface of the octagon-shaped lamppost was stable enough. By scanning the targets, the laser scanner knows the exact difference in the position of the separate scanning positions and can therefore align the results from each scanning location.

The obtained point cloud is shown in Figure 6.4. The excessive data is removed, since only the tower is required.

Figure 6.1: The scanlocations of the fieldwork

Figure 6.2: The targets to connect the different scans

Figure 6.3: The terrestrial laser scanner during the field work in Haarlem, operated by Linh Truong Hong

Figure 6.4: The obtained pointcloud from the field work by using the terrestrial laser scanner

In order to find the angle of inclination for the base and the three lanterns, two points are randomly selected in a straight line above each other on all eight seams of the octagons. The points create a parallel line to the facade. Since the points are chosen manually, human-made errors might occur. In order to minimize the human error, the procedure has been done three times. The point has been shuffled (for example the bottom point of measurement 1 with the top point of measurement 3) and a total of nine combinations has been made. This is done for the base and the three lanterns separately. In order to determine the angle of inclination, the horizontal displacement and the vertical displacement are used. The horizontal displacement is calculated with the Pythagorean theorem where the difference in x-coordinates and the difference in y coordinates is estimated according to equation 6.1. Thus, x_{11} is the top point and x_{12} is the bottom point of measurement 1. In this equation, the first number is the measurement and the second number indicates if it is a top point or and bottom point. The vertical displacement is the difference in z-coordinates and can be determined with equation 6.2. The angle of inclination α is calculated with simple geometry, which is shown in equation 6.3.

$$\delta_{xy} = \sqrt{(x_{11} - x_{12})^2 + (y_{11} - y_{12})^2} \tag{6.1}$$

$$\delta_z = z_{11} - z_{12} \tag{6.2}$$

$$\alpha = \arctan \delta_{xy}/\delta_z \tag{6.3}$$

With the obtained nine angles of inclination for each seam on the base and three lanterns, the average angle of inclination is determined per seam. The average, maximum and minimum inclination of the top of the tower can be determined. The inclination is calculated by multiplying the angle of inclination with the heights of the base and lanterns from figure 1.1. The different heights are given in table 6.1. The average angles of inclinations in ° of the base and three lanterns and the average, maximum and minimum inclination of the top of the tower (without the rooster on top of the tower) in mm are given in table 6.2. The letters in the first row indicate the wind direction of the seam.

Table 6.1: The heigths of the base and different lanterns

Location	Height (mm)
Base	15500
Lantern 1	12750
Lantern 2	6000
Lantern 3	11000

Table 6.2: The average angles of inclinations and average, maximum and minimum inclination of the top the tower, determined from the pointcloud

Location of the seam	1 SW	2 W	3 NW	4 N	5 NE	6 E	7 SE	8 S
Average angle of inclination (°) of the base	0.059	0.072	0.081	0.064	0.078	0.080	0.078	0.071
Average angle of inclination (°) of lantern 1	0.034	0.025	0.037	0.028	0.025	0.035	0.014	0.025
Average angle of inclination (°) of lantern 2	0.034	0.024	0.023	0.044	0.067	0.077	0.068	0.081
Average angle of inclination (°) of lantern 3	0.042	0.047	0.036	0.048	0.065	0.074	0.050	0.055
Average inclination (mm)	2020	2096	2259	2143	2650	2972	2345	2511
Maximum inclination (mm)	2456	2897	2688	2614	2962	3640	2942	2837
Minimum inclination (mm)	1633	1685	1986	1837	2117	2318	1946	2196

The obtained angles of inclination indicate that the tower is bent since the angle of inclination differs per lantern.The obtained angles of inclination and inclinations of table 6.2 are all absolute values and the direction of the inclination is not known. The inclination is tilted in the north-west direction, as one can see with the naked eye. Therefore, it is assumed that all inclination are in the north-west direction. The range of the inclination varies from 1633 mm for the seam in the south-west direction to 3640 mm in east direction. Therefore, it is possible to conclude that there is definitely a deformation. However, the obtained values are not written in stone and might have small errors within. The average of the average inclination for all seams is 2375 mm. In order to take the inclination of the tower into consideration in the Finite Element Model, the inclination is assumed to be approximately 2000 mm, which is in between the minimum and maximum estimated inclination and is on the lower side of the average inclination. At first, 2000 mm seems like a lot. However, the inclination is compared to the inclination of the bell tower of San Benedetto Church in Ferrara. The inclination of the bell tower of San Bendetto Church in Ferrare is 2530 mm (Furini and Russo, 2014). Furthermore, the Walfridus church in Bedum is the most inclined church in the Netherlands with an inclination of 2610 mm (Thijssen, 2011). The results of the bell tower of San Benedetto Church in Ferrara and the Walfridus Church in Bedum indicate that several churches suffer from an inclination of such a high magnitude. The main conclusion from the results is that the tower is significantly inclined. However, it is not possible with the used method to determine the precise inclination of the tower, partly due to the large difference in the minimum and maximum determined inclination.

In order to determine the cause of the inclination, the foundation of the tower is measured horizontal. With the horizontal measurements, one is able to verify if the tower starts of straight or the foundation

of the tower is already inclined, partly causing the observed inclination. This will be done with the obtained point cloud. The inclination of the base will be measured from the point cloud by taking the middle points of the clocks on each side. A line will be drawn from the parallel clocks on the opposite sides of the tower. The angle of inclination of the base will be determined in the same way as the total inclination of the tower. The method has been mentioned above. The horizontal and vertical difference between the middle points of the clocks will be stated in table 6.3. In order to minimize the error, the process will be repeated 3 times and will be combined with the other measurements, creating a total of 9 combinations. In total 9 combinations for the clocks on the South-West side and the North-East side will be determined and 9 combinations for the clocks on the North-West side and the South-East side. All 18 angles of inclinations indicate an angle of inclination of 1.5 °. Therefore, one is able to assume that the inclination is partly caused or perhaps completely caused by the inclination of the base of the tower.

Table 6.3: The angles of inclinations of the base of the tower, determined by using the middle of the clocks from the point cloud

combination	11	22	33	12	13	23	21	31	32
δ_{xy} SW to NE (m)	8.87	8.83	8.91	8.86	8.86	8.83	8.83	8.91	8.91
δ_z SW to NE (m)	0.005	0.015	0.049	0.003	0.001	0.019	0.023	0.045	0.053
angle SW to NE (°)	1.57	1.57	1.56	1.57	1.57	1.57	1.57	1.57	1.56
δ_{xy} NW to SE (m)	8.89	8.94	8.94	8.95	8.94	8.94	8.89	8.89	8.95
δ_z NW to SE (m)	0.060	0.012	0.003	0.013	0.003	0.022	0.085	0.060	0.013
angle NW to SE (°)	1.56	1.57	1.57	1.57	1.57	1.57	1.56	1.56	1.57

6.2. Possible Causes of the Inclination of the Tower

This section will briefly outline different possibilities for the inclination of the tower. The possibilities are additions or explanations to the inclined base, which resulted from the previous section. The inclination of the tower might be caused by settlements of the ground, man-made mistakes during the building process, shrinkage and swelling due to moisture, shrinkage and swelling due to heat radiation or another reason. A rough estimation of the difference in length of two sides can be made. This is applicable in case the inclination comes due to shrinkage or swelling of one side or due to man-made errors in the sawing process. The base of the tower has a width of approximately 16 m. If the middle of the tower is inclined 2 m in one direction and has a height of 49 m, the average angle of inclination will be $\arctan(2/49) = 0.041°$. This angle is used to calculate the difference in length for two sides. Over a width of 16 m, it requires the difference between two sides to be: $16 * \tan(0.041) = 0.65m$.

A common reason for the inclination of buildings is the settlement of the underlying ground layer. The church is built on a sand layer. The east side of the church is just on the border of the sand layer and has been anchored in order to prevent settlements. The settlements of the church are measured once every few years by the local municipality. The total settlements of the church, resulting from the measurements, are negligible and therefore settlements of the ground layer are excluded to cause the inclination of the tower.

Back in the 15th century, the beams and columns were sawn by hand (no machinery was present in order to accurately saw the timber). An accumulation of the man-made errors on the same side of the tower can cause an inclination. However, since the tower is still standing and built with a high level of precision, it is not likely that the man-made errors accumulate on one side of the tower to cause the entire inclination of the tower. Furthermore, if a large inclination was created during the building process, the workmen would notice the inclination by looking at the tower and perhaps took measurements to prevent further inclination of the tower.

Furthermore, the building process of the tower in the 15th century was most likely in open conditions. This means that the timber got wet during construction and could shrink or swell. In the worst case scenario, the rain came from the same direction all the time and only one side got wet. This means that the wet side has swollen more than the other side, causing an inclination of the tower. Shrinking and swelling due to moisture is different per direction. According to Kollmann and Côté (1968), shrinkage and swelling in the longitudinal direction can nearly always be neglected, since it is so small

in comparison to shrinkage and swelling in radial direction and tangential direction. The values from figure 6.5 of non-densified oak wood are applicable here. In radial direction, the wood can shrink/swell approximately 5 % and in tangential direction approximately 7 %. The difference between two sides of the entire tower can only be caused by shrinking and swelling in tangential direction of the beams present in the tower since the columns barely shrink and swell in longitudinal direction. A rough estimation of the built-up of the height is a contribution of 95% by the columns and the remaining 5 % of the height is established by the beams. The maximum difference between sides, due to shrinkage and swelling, is $7\% * 0.05 * 49 = 0.17m$. This assumption is a worst case scenario and is not even close to the 0.65 m, which is required to cause an inclination of 2 m. Therefore, the inclination is not caused by shrinkage and swelling due to moisture. However, the shrinking and swelling of timber might have contributed to the inclination.

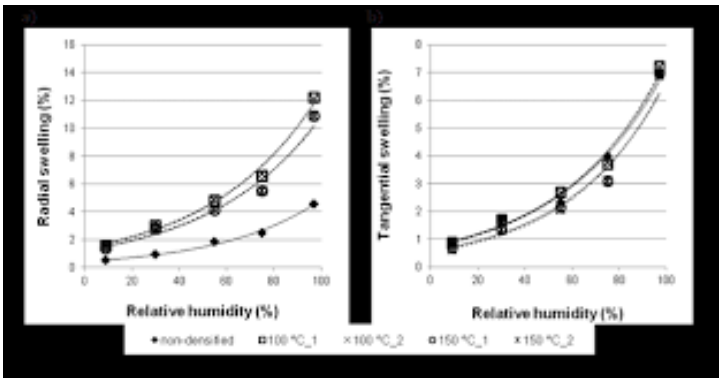

Figure 6.5: Shrinkage and swelling of oak wood in radial direction (left) and tangential direction (right) from Laskowska et al. (2018)

The side of the tower, facing the south, is exposed to more sunlight than the northern side. Therefore, there can be a temperature difference between the timber between the north and the south side. The thermal expansion coefficient of oak in parallel direction of the grain is $4.92 * 10^{-}6m/(m * K)$ and $54.4 * 10^{-}6m/(m * K)$ (Kollmann and Côté, 1968) in the perpendicular direction of the grain. An approximation of the temperature difference between the north and the south side is 10 °. This gives an expansion of $10 * 4.92 * 10^{-}6 = 0.0492mm$, this is a small length difference between the south and north side of the tower and is negligable compared to the total inclination of the tower. Apparently, the thermal expansion coefficient of oak is so low, that barely any expansion occurs. Furthermore, the lead cladding covers the timber and has a much higher thermal expansion coefficient than oak. However, the lead cladding is made with overlap and therefore the higher thermal expansion of lead will not affect the oak and will not contribute to the inclination of the tower. The overlap of the lead cladding is shown in figure 6.6.

Figure 6.6: The lead cladding, covering the timber parts of the tower.

The inclination might be made on purpose, in order to withstand North Western wind, which is the strongest wind direction in the Netherlands. This seems a bit far sketched. Another reason might be the inclination of one of the main pillars beneath the tower. the north-east pillar is clearly tilted, this was originally caused by the weight of the stone tower. This might be the cause of the inclination at the base of the tower. This was also the reason to break down the stone tower and replace it with a timber tower. Due to the heavy weight of the stone tower, some walls have been tilted as well. In order to put less weight on the damaged pillar and walls, the timber tower might be centred a bit away from the critical pillar and walls. However, this is not very likely either, since the tower is tilted in north-west direction and the critical pillar is the north-east pillar.

Most likely, the inclination is caused by a combination of an inclined base of the tower, the moisture differences during the open building phase back in the 15th century, human-made errors during the sawing process and perhaps other reasons, which have not been mentioned.

6.3. Discussion

The point cloud is made with the highest possible accuracy and only has an offset of approximately 2 mm. However, by measuring the angle of inclination with hand-picked points, small errors might occur. In order to minimize the errors, the procedure has been repeated several times. By repeating it even more, the error will become even smaller. This has not been done, due to the workload. The obtained results are an indication of the real inclination of the tower. However, an inclination of 2 m is significant but the exact inclination is not written in stone due to the large difference between the minimum and maximum determined inclination. Furthermore, another method might be more suitable in order to determine the inclination of the tower from the point cloud, but more research for such a method is required.

Furthermore, the angles of inclination of the base of the tower is based on vertical differences of 0.1 cm to 8.5 cm. These small vertical difference can easily be measurements errors, due to the small magnitude. The angles of inclination are based on the clocks on the outside of the tower. However, the clocks might not be symmetrically placed and do not necessarily represent the angles of inclination of the base of the tower. However, since only the outside of the tower was measured with the laser scanner, the clocks were the most suitable reference points and since the angles of inclination barely differ, it is assumed to be correct.

7

The Finite Element Model of the Tower

In this chapter, the results of the Finite Element Model will be presented. Furthermore, the impact of the inclination will be evaluated. For the dynamic behaviour of the tower, the natural frequencies are determined. With the natural frequencies, one is able to determine the impact of the wind on the dynamic behaviour of the tower. More information about the entire setup of the Finite Element Model is shown in appendix D.

With the obtained geometry in chapter 4 and the determined indication of the mechanical properties from chapter 5, the Finite Element Model is created with SCIA Engineer. Since the tower can be designed as a rod model and will only be linearly loaded, SCIA Engineer is a suitable solution to create a Finite Element Model of the tower. SCIA Engineer models the beams as rods and gives the rods a surface area and a moment of inertia according to the dimension. The database of SCIA Engineer consists of several wood strength classes, implemented according to the Eurocode. The strength class of D18 is also present in the database.

7.1. Results of the Finite Element Model in Straight Conditions

In order to verify the elements and connections, the stresses and shear forces have to be determined. The total stability of the tower will be verified with the total deflection of the tower and the dynamic behaviour of the tower.

Figure 7.1: The location of the highest stresses, shown in pink in the figure.

The deflection of the tower

In order to verify the maximum deflection of the tower, the tower is simplified to a cantilever beam. According to the euro code NEN-EN 1995-1-1 7.2 (table 7.2), the maximum allowed instantaneous deflection of the tower is l/250 = 49000/250 = 196 mm. The maximum allowed total deflection of the tower with the inclusion of creep is l/150= 326.67 mm. The creep factor $k_{def} = 0.8$ for sawn timber in climate class 2 (NEN-EN 1995-1-1 3.4, table 3.2). The deflection with inclusion of the creep factor $w_{final} = w_{instantaneous} * (1 + k_{def})$.The highest deflection in service limited state (SLS) occurs due to the wind, with combination 3.4. The deflection of the tower is shown in figure 7.2 and the top has a total deflection of 9.6 mm. The final total deflection will in this case be $w_{final} = 9.6 * (1 + k_{def}) = 16.92mm$. Both demands for service limit state amply suffice the demands. The

reason for the low deflections of the tower is due to the enormous mass of the entire tower, which makes the entire tower very rigid.

The highest Stresses in the tower

The stresses are used to verify the strength of the timber elements in the tower. The Finite Element Model is too complex to post all stresses in one figure. Therefore, the stresses have been studied and only the critical stresses will be reviewed in this chapter. During the study of the model, peak values at the supports and at connections are neglected. Since the tower is clamped at the bottom, high peak values occur. In reality, the high peak values are not present, because the bottom is not clamped in a single point and not fully clamped. SCIA Engineer models all the elements as rods (see figure 4.5). At the connections, the rods are connected in the middle points, which means that the 2D members interact and partly overlap in the model. At locations of overlap, high peak stresses occur. In reality, these peak stresses are not present and no overlap is present since one of the two members is just cut off in order to fit the connection.

The highest stresses occur in the outer trusses of the first floor. The truss is shown in pink in figure 7.1. The symmetrical truss has the same stress distribution. The highest compression stress is 7.7 N/mm^2 and the highest tension stress is 4.5 N/mm^2, the stress distribution is shown in figure 7.3. The peak value of 7.7 N/mm^2 is a bit too high, due to the overlap of the 2D members in the model. The highest compressive and tensile stresses both occur when the wind load is normative in ultimate limit state (ULS), see the combination in equation 3.2.

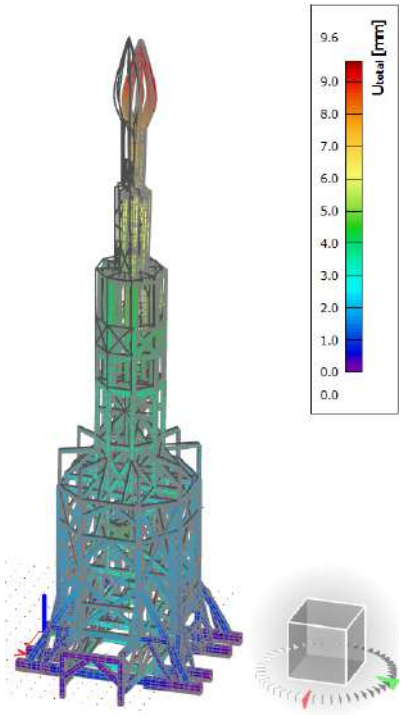

Figure 7.2: The deflection of the tower in SLS with wind as normative factors.

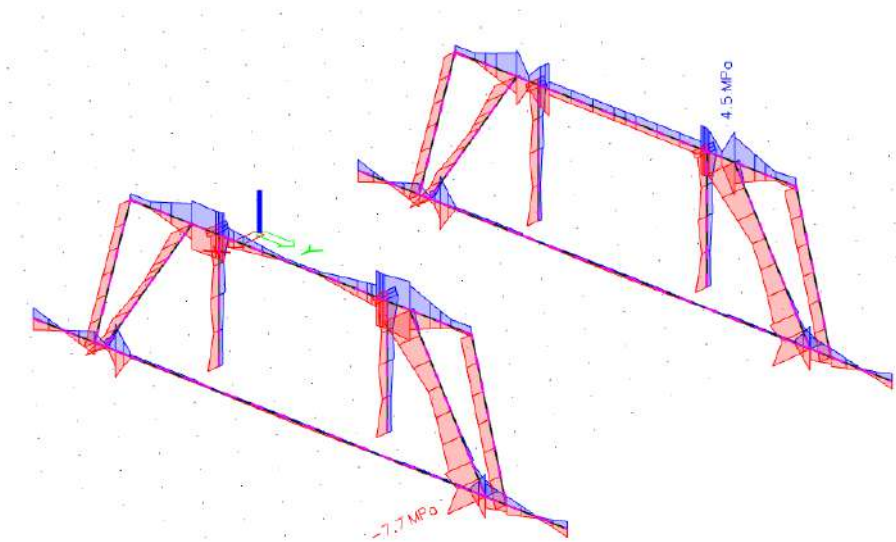

Figure 7.3: The highest and lowest stresses in the tower, occur in the trusses on the first floor.

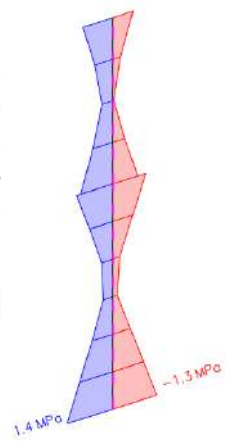

Figure 7.4: The stress distribution in the defect element 3.1 (see Appendix C

The only element with significant defects, which is used as a structural element, is the column on the third floor. The element is shown in appendix C and is named defect element 31. Since the mechanical properties of this element are lower, the column has to be checked as well. The maximum stresses occur when the combination for imposed floor loads are normative (see equation 3.3). The stress distribution is shown in figure 7.4.

The highest shear forces in the tower

The shear forces are used to verify the connections. Not all shear forces on the tower are shown in a figure because the tower is too complex to visualize all shear forces. Only the highest shear forces are reviewed. In order to verify the connections, the jump in shear force is used. In total 16 connections are critical. The trusses, where the maximum stresses occur, also have 2 critical connection each. The location of the connections is shown in figure 7.1. The jump in the shear force in these 4 connections is 90.73 + 18.74 = 109.47 kN. The shear force line is given in figure 7.7. Four other critical connections are present on the second floor. One connection is shown in figure 7.5. The jump in shear force in these connections is 35.56+8.15=43.71 kN and is shown in figure 7.8. The other eight connections are on the fourth floor, see figure 7.5 for the location of the connections. Since the beams are not in line with each other, large shear forces are created by the wind on the connection on the column in between the beams. The jump in shear force is approximately 99.82 kN. The shear force line of the connections on the fourth floor is shown in figure 7.9. All peak shear forces occur when the wind load is normative in ultimate limit state (ULS), see combination 3.2.

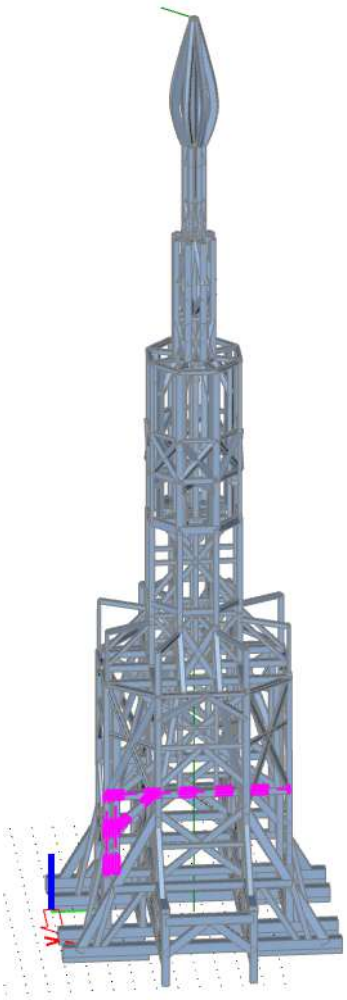

Figure 7.5: The location of the peak shear forces in the connection on the second floor.

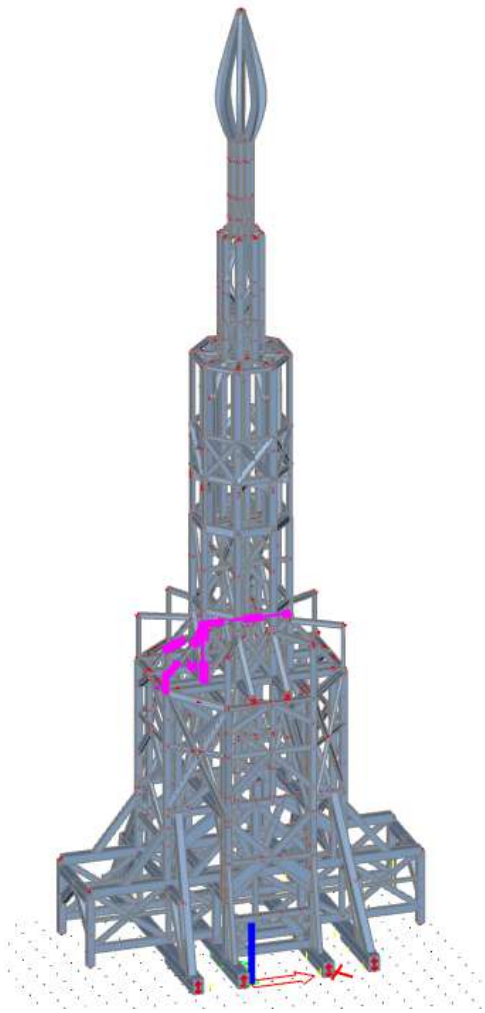

Figure 7.6: The location of the peak shear forces in the connections on the fourth floor.

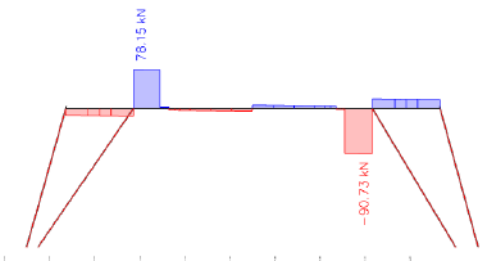

Figure 7.7: The peak shear forces in the connections on the first floor.

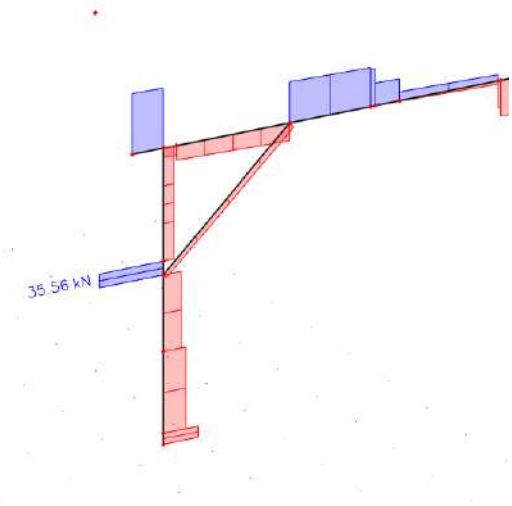

Figure 7.8: The peak shear forces in the connections on the second floor.

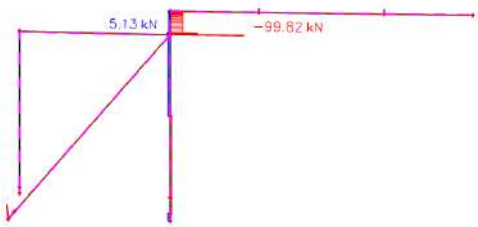

Figure 7.9: The peak shear forces in the connections on the fourth floor.

7.2. Results of the Finite Element Model with Inclusion of the Inclination

In the previous section the critical stresses and shear forces where found with the wind as the normative factor in the ULS combinations. In order to take the inclination into consideration, a non-linear combination is created with the values of combination 3.2. The non-linear combination takes the inclination into consideration, by implementing an angle of inclination over the entire tower. In short, the entire tower is under the same angle of inclination. The total inclination is $\sqrt{2}m$ in both x and y-direction, making the total horizontal inclination 2 m. Since the deflection criteria were more than satisfied, no non-linear SLS combination was created in order to determine the deflection with the inclusion of the inclination to the model. The same procedure has been used as in the previous section and only the critical stresses and shear forces will be shown.

The highest Stresses in the tower with the inclusion of the inclination

The highest stresses still occur in the trusses on the first floor, see figure 7.1. The magnitude of the stresses has changed though. Higher tensile stresses occur on the opposite side of the inclination (in the south-east, while the tower inclines towards the north-west). The highest tensile stresses in the tower are 5.2 N/mm^2 and the highest compressive stresses are 6.7 N/mm^2. Both peak values are a bit off, due to the overlap in reality of the 2D members. The stresses can be seen in figure 7.10.

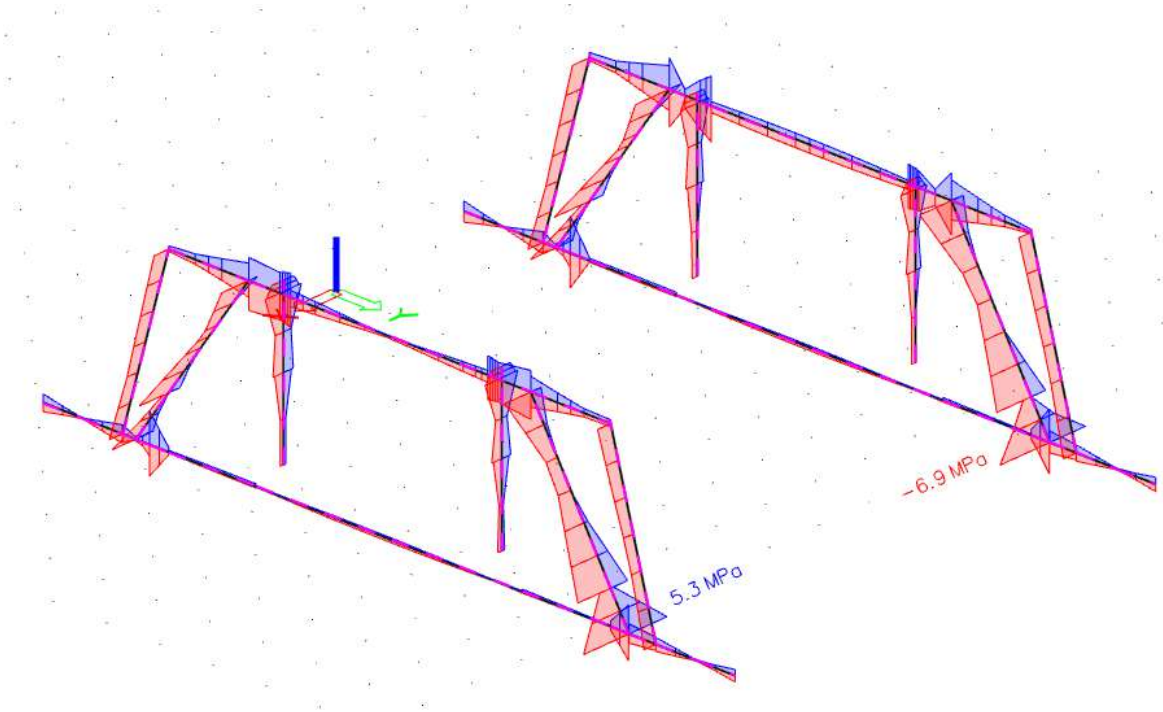

Figure 7.10: The highest stresses in the tower, with inclusion of the inclination of the tower

The highest shear forces in the tower with the inclusion of the inclination

The locations of the critical shear forces is unchanged from the previous section. However, the magnitude of the shear forces has changed. All values have decreased in comparison to the previous section. This is most likely due to the fact that the wind is not completely perpendicular on the planes anymore and therefore the shear forces will decrease in comparison to the previous section. The connections on the first floor will have a jump in the shear force of 55.69+8.22 = 63.91 kN and are shown in figure 7.11. The connections on the second floor will have a jump in the shear force of 30.54+8.98 = 39.52 kN and are shown in figure 7.12. The connections on the fourth floor have a jump in the shear force of approximately 70.36 kN and are shown in figure 7.13.

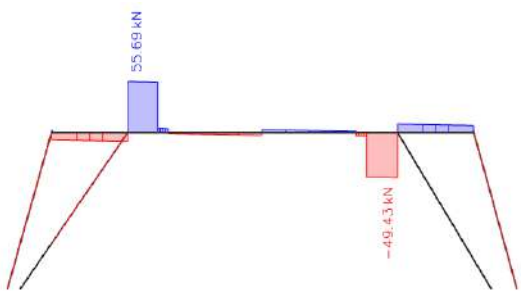

Figure 7.11: The peak shear forces in the connections on the first floor, with inclusion of the inclination of the tower.

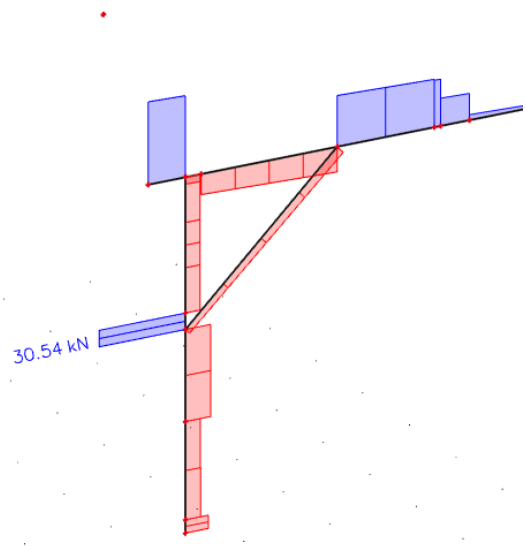

Figure 7.12: The peak shear forces in the connections on the second floor, with inclusion of the inclination of the tower.

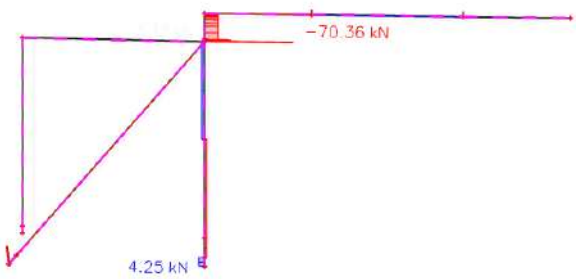

Figure 7.13: The peak shear forces in the connections on the fourth floor, with inclusion of the inclination of the tower.

7.3. The natural frequencies of the tower

Scia Engineer easily calculates the natural frequencies of the entire tower. The first until the tenth natural frequency are given in table 7.1. The boundaries for the natural frequencies is 1 Hz for storms and 10 Hz for earthquakes (Hoogenboom, n.d.). The lowest natural frequency is 1.65 Hz, which means the tower is not sensitive for storms and wind loads. The tower is sensitive to earthquakes. However, one can see in figure 7.14 , that Haarlem does not lay in an earthquake-sensitive area. Therefore no problems with the dynamics of the tower are present.

Table 7.1: the natural frequencies of the tower obtained from SCIA Engineer

Natural frequency	Value (Hz)
First	1.65
Second	1.69
Third	3.71
Fourth	3.85
Fifth	4.4
Sixth	4.5
Seventh	5.96
Eighth	5.99
Ninth	6.22
Tenth	7.42

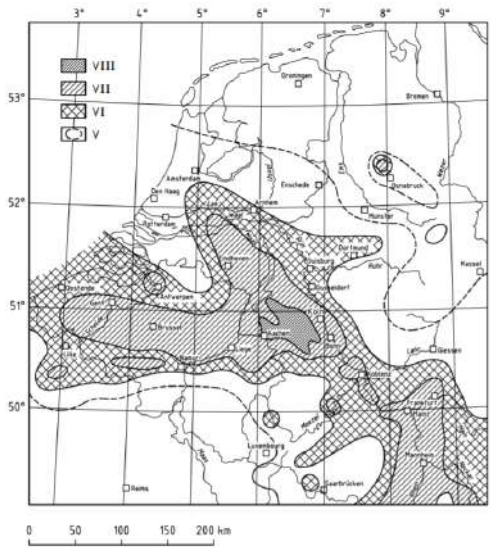

Figure 7.14: Earthquake sensitive areas in the Netherlands from NEN-EN 1991-1-7 +C1/NB table NB.4

7.4. discussion

The peak values of the stresses and shear forces are determined on personal knowledge. Abnormal peak values, due to small modelling errors or overlap between 2d elements are neglected. However, the decisions for abnormal peak values are based on personal knowledge. Important peak values, which might occur in reality, might have been overlooked. It is assumed that the personal made decisions are correct and give a good indication of the peak stresses and shear forces in reality.

8

Strength and Stability Verifications

The resistance of the connections and elements will be determined in this Chapter and will be compared to the obtained shear forces and stresses, which will occur in the tower from chapter 7. Conclusions about the strength and stability of the tower are drawn from the comparisons made.

8.1. Structural Elements

In order to determine the resistance of the structural elements, the material factor γ_m and modification factor k_{mod} are required. According to the NEN-EN 1995-1-1 +C1+A1 table 2.3 the material factor $\gamma_m = 1.3$ for sawn timber. The modification factor $k_{mod} = 0.6$ for permanent loads according to the NEN-EN 1995-1-1 +C1+A1/ Table 3.2. The modification factor $k_{mod} = 0.9$ for short term loads such as wind and $k_{mod} = 0.8$ for average term loads such as imposed floor loads. The modification factor for the resistance depends on the normative load.

The mechanical properties of most elements are of strength class D18. The resistance to compressive stresses, tensile stresses and shear stresses is respectively $f_{c0k} = 18N/mm^2$, $f_{t0k} = 11N/mm^2$ and $f_{vk} = 3.5N/mm^2$ (see figure 5.2). The highest compressive stresses occur in the trusses on the first floor without taking the inclination in consideration and is $\sigma_c = 7.7N/mm^2$. The highest tensile stresses occur on one of the same trusses but appear with the inclusion of the inclination in the south-east connection of the truss only and is $\sigma_t = 5.2N/mm^2$ (see figure 7.3 and 7.4). The highest shear stresses occur at the connections and will be calculated in that section. The unity checks (UC) are performed in equations 8.1 and 8.2 and include the material factor and modification factor. The wind is the normative load in almost all cases and the $k_{mod} = 0.9$ will be used. The self weight is normative for the defect element on the third floor and $k_{mod} = 0.6$ will be used here. The compression and tensile stresses suffice. Since the rest of the entire tower amply suffices the demands, it can be concluded that the elements have sufficient resistance and no problems occur.

$$UC_{compression} = \sigma_c/(k_{mod} * f_{c0k}/\gamma_m = 7.7/(0.9 * 18/1.3) = 0.62 \tag{8.1}$$

$$UC_{tension} = \sigma_t/(k_{mod} * f_{t0k}/\gamma_m = 5.3/(0.9 * 11/1.3) = 0.7 \tag{8.2}$$

Besides the column on the third floor, the elements with significant defects are all stability members and therefore do not require to be checked. The highest stresses on the column (defect element 3.1, see appendix C) are tensile stresses of $1.4N/mm^2$ and a compressive stresses of $1.3N/mm^2$. The resistance of the defect members to compressive stresses, tensile stresses and shear stresses is respectively: $f_{c0k} = 9N/mm^2$, $f_{t0k} = 5.5N/mm^2$ and $f_{vk} = 1.75N/mm^2$ (see figure 5.3). The unity checks are performed in equation 8.3 and 8.4 and all suffice easily. The shear stresses are not verified, because the magnitude of the shear forces is negligible on this specific column.

$$UC_{compression} = \sigma_c/(k_{mod} * f_{c0k}/\gamma_m = 1.3/(0.6 * 9/1.3) = 0.24 \tag{8.3}$$

$$UC_{tension} = \sigma_t/(k_{mod} * f_{t0k}/\gamma_m = 1.4/(0.6 * 5.5/1.3) = 0.55 \tag{8.4}$$

8.2. Connections

Almost all connections are realised by interlocking the timber elements and using timber dowels through the interlocking parts of the elements for stability. The interlocking makes the force distribution between the elements possible. A sketch of the interlocking critical connection on the second floor is shown in figure 8.1. Since the elements are interlocked in each other, the elements cannot slip off and there is no need to verify the dowels in these types of connection. In case the connection is loaded in tension and the dowels have to prevent the pull out of interlocking connection, the dowels will be heavily loaded and have to be verified. However, almost all connections in the tower are loaded in compression. All the critical connections will be individually verified and discussed below.

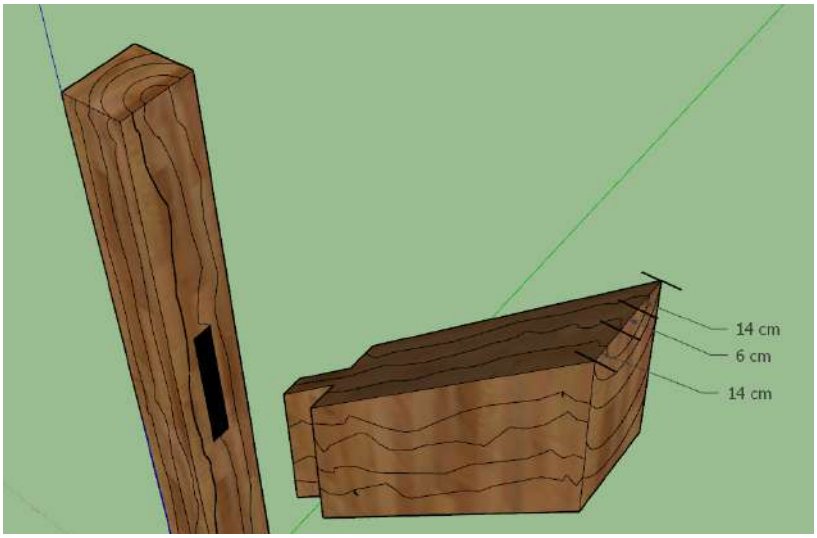

Figure 8.1: A 3D sketch of the critical connection on the second floor

One of the critical connections on the first floor is shown in figure 8.2. The high shear forces (see figure 7.7) on the connection do not load the dowel connection. The dowels are used for stability in such a way that the columns under an angle do not fall. However, since the beam and columns are stacked on each other and interlocked in between, the shear force will directly be transferred to the column and no high forces will occur on the dowels. This connection is loaded in compression. The cross section of the beam has to be verified on shear stresses. The cross section of the beam is 380 mm (width) by 330 mm (height). The shear force is $F_V = 109.47kN$ and will be equally divided over this cross-section and is compared to the shear stress resistance. The unity check is given in equation 8.5. This demand suffices and it can be concluded that these connections have sufficient resistance.

$$UC_{shear} = (F_V * 1000/A)/f_{vk} = (109.47 * 1000/(380 * 330))/3.5 = 0.25 \tag{8.5}$$

Figure 8.2: The critical connection on the first floor.

The critical connection on the second floor, see figure 8.3, is originally built up with 3 timber dowels with a diameter o f 25 mm. However, one of the connections is missing one dowel and will therefore be critical. Since the shear force on this connection is way lower than the shear force on the critical connection on the first floor, the shear stresses will not be critical and there is no need to verify them. Since the shear force loads the connection in compression (see figure 7.9) the connection is a stability connection. The connection is simplified in figures 8.1. The interlocking part in the connection realises the force distribution and the dowels improve the stability of the joints. Therefore the connection does not have to be checked on shear forces and has sufficient strength. The missing dowel in the connection does not have any influence on the stability of the connection.

Figure 8.3: The critical connection on the second floor of the tower

H

Figure 8.4: The critical connection on the fourth floor

The critical connection on the fourth floor is shown in figure 8.4. Apparently, someone else thought of the connection on this floor to be critical and fully anchored the connection. Since the connection is fully anchored, no risks occur due to the heavy shear forces. The anchor will not be normative in this connection, but the wood will be normative. The wood will be checked with the shear stress resistance. The anchor is not brought into consideration by verifying the shear stress. The shear force is $F_V = 99.82kN$. This force will be equally divided over the cross-section of the column. The cross-section of the column is 250 mm by 300 mm. The unity check is shown in equation 8.6. It is concluded that the fourth connection suffices the demands and has enough resistance.

The bolt threat which goes through the column and is bolted on the other side is clearly fabricated with machinery. Therefore, the reinforcement of the connection has probably been made in the previous era. The exact age of the anchor is unknown.

$$UC_{shear} = (F_V * 1000/A)/f_{vk} = (99.82 * 1000/(250 * 300))/3.5 = 0.38 \tag{8.6}$$

8.3. discussion

The critical connections and critical elements are based on the peak shear forces and peak stresses. As has been mentioned in the discussion of chapter 7, the peak values are based on personal knowledge. Therefore, the critical connections and critical elements are also determined on personal knowledge. It might be possible that other critical connections and critical elements have been neglected. However, it is assumed that the decisions on personal knowledge are correct.

Furthermore, the strength class D18 is based on a few tests and is applied to almost all structural elements. In reality, the strength of some elements might be even lower than the considered strength class D18. However, the elements would also suffice the unity checks in case lower strength properties are used since all unity checks now amply suffice the demands.

9 Discussion

This discussion is aimed to discuss the addition of modern technologies on top of the regular assessment methods which have been described in section 2.1.1. In addition to some of the regular assessment methods, this study also used a terrestrial laser scanner, investigated the use of the U-BLOX and verified the entire structure with finite element software.

The initial idea to obtain the geometry of the tower was by using the terrestrial laser scanner to create a point cloud of the scale model, made by Theo van Paradijs. Since the scans are made from the outside of the scale model, not all of the internal components were scanned and some important information was missing. This is because the external components block the view for the laser scanner and some parts are not visible from the outside. Therefore, the obtained point cloud of the scale model was of no use. In order to obtain the dimensions, one should use the terrestrial laser scanner through the entire tower. This brings a large workload but gives the most accurate representation of the geometry of the tower. A more suitable solution is using the handheld laser scanner. This method is still much more accurate than measuring the geometry by hand and it is easier manageable in comparison to the terrestrial laser scanner. The terrestrial laser scanner is preferred in case the cracks and defects should also be clearly mapped, since the terrestrial laser scanner has a higher accuracy than the handheld laser scanner. By obtaining the exact geometry of the tower, an accurate representation of the structural behaviour could be modelled and more accurate calculations could be performed. Moreover, the additional value of using the 3D Lidar scanning techniques to measure the geometry will be further discussed in the part about the finite element software below.

The terrestrial laser scanner was also used to measure the total inclination of the tower. In order to measure the angle of inclination, the accuracy is important. Since the scanner will be approximately 80 m away from the top of the tower, the most accurate laser scanner is preferable. The obtained point cloud from laser scanning is of high accuracy and the inclination could precisely be measured. However, the method of measuring the inclination by hand brings human-made errors into the process. Small measurement errors might significantly influence the results of the total inclination. The obtained results from the hand measurements from the point cloud can only be used as approximations of the total inclination of the tower and inclination of the base of the tower. In order to determine the total inclination, research for a more suitable method to obtain the inclination from the point cloud is required.

In order to precisely determine the structural reliability of the entire tower, a Finite Element Model has been created. The Finite Element Model is based on the obtained results of the geometry, the determined mechanical properties and the maximum loads according to the Eurocode. The Finite Element Model shows the force and stress distribution in the entire structure. In this way, critical connections and elements, which suffer from high forces or stresses, could be verified. The Finite Element Model also provides information about the importance of structural elements. For example, an element appears to be in critical condition due to decay. However, the Finite Element Model shows that the element is of no importance for the load-carrying capacity of the entire structure and the element is redundant. Therefore, the element does not contribute to the current state of the entire tower. The

Finite Element Model improves the regular assessment methods by determining the importance of all elements. Moreover, the stress and force distribution can also be used to verify the elements and connections according to the Eurocode. The verification according to the Eurocode gives insight if the elements and connections have enough load carrying capacity. Furthermore, using a laser scanner to obtain the geometry gives a higher accuracy to the Finite Element Model and it also improves the regular assessment methods by substantiating the Finite Element Model.

Additionally, the U-BLOX could be used to measure the deflections of the top of the tower due to the wind. It should be installed for several weeks and the maximum deflections could be coupled to the wind forces on that day. The deflections of the top of the tower could be used for a more precise estimation of the dynamic behaviour of the tower and also in order to help verifying the results of the Finite Element Model. The results were of low priority in this research, since the tower of the Grote of St. Bavochurch is very rigid. However, for more slender structures, it might be a good addition to the regular assessment methods. Furthermore, the U-BLOX requires access to the power net, which was not possible in this study. Another solution is using a car battery, but carrying a car battery to the top of the tower was dangerous in this case. Therefore, this was no consideration in this specific study, but it could be useful in other cases.

All in all, the addition of this study to regular assessment methods, creating a Finite Element Model of the structure gives a lot of insight into the importance of all structural elements. The built-up of this study from section 1.4 is aimed to perform a structural analysis in order to obtain the required input results for the Finite Element Model. The Finite Element Model is used to draw conclusions on the structural reliability of the entire structure.

10

Conclusion

This master thesis, on behalf of the Council of the Grote of St. Bavo Kerk, investigated the structural reliability of the wooden tower of the Grote of St. Bavo Kerk. A Finite Element Model is created to investigate the structural reliability of the tower. The Finite Element Model is supposed to give information about the flow of forces and the critical locations in the tower. The Finite Element Model is created by measuring the geometry of all elements in the tower by hand, performing longitudinal vibration tests and visual grading the timber in the tower in order to determine the mechanical properties. Finally, 3D Lidar scanning technologies is used to determine the inclination of the tower.

The results of the longitudinal vibration tests indicate that the strength of the 500 year old oak wood is approximately of strength class D18. Whereas the mechanical properties of the elements with significant defects, determined from the visual inspection, are halved. Furthermore, the total inclination of the tower is determined. By using a terrestrial laser scanner, an accurate point cloud of the tower is obtained. Lines perpendicular to the facade are drawn in the point cloud in order to measure the angle of inclination of the tower. The total inclination is approximately $2m$ and is partly caused by an inclination of the base of the tower. Subsequently, after obtaining the geometry, mechanical properties and the inclination of the tower, The Finite Element Model is created. The peak stresses and shear forces have been determined in order to verify the connections and elements. From the unity check, it follows that all element and connection amply suffice the demands.

One should bear in mind that the measurements of the geometry, the drawn lines perpendicular to the facade in order to determine the angle of inclination and the Finite Element Model are all determined or created by hand and therefore might have small errors. Hence, all the results are a proper indication of the real results, but not necessarily of a high accuracy.

Nevertheless one is able to conclude that the tower is structurally reliable since the unity checks amply suffice the demands. Furthermore, the tower is heavily over-designed and in most places, the structure is not in danger. Therefore, several elements could have been designed thinner in the design process and some elements are even redundant for the strength and stability of the tower.

Furthermore, the determined inclination of $2m$ is only an approximation, but due to the large magnitude of the inclination, one is able to conclude that the tower is in fact inclined. Lastly, the Finite Element Model is also used to determine the natural frequencies of the tower. Since the obtained natural frequencies of the tower are above the frequency range of wind loads, one is able to conclude that the tower will not have dynamic problems due to wind loads.

This report shows the possibility to use modern technologies, such as Finite Element Analysis and 3D Lidar scanning technologies, to assess old timber buildings. In addition to the regular assessment methods, these modern technologies are able to assess old timber buildings more precise and give more detailed information.

11 Recommendation

In this chapter, several recommendations for future studies are stated below.

- In this study the geometry of all elements in the tower is obtained by measuring the elements by hand. In order to get more accurate results for the geometry, laser scanning is recommended. In case only the geometry is required, the hand held laser scanner is a proper method to obtain a more accurate representation of the geometry of the entire tower. The hand held laser scanner has a lower accuracy in comparison to the terrestrial laser scanner, but is a faster solution. In case one is also interested in the cracks and defects and prefers an even high accuracy level, the terrestrial laser scanner is recommended. Since the timber in the tower is over 500 years old, a lot of cracks are present. In order to optimize the model of the entire tower and get the most accurate results, the terrestrial laser scanner is the best solution to measure all the geometry.
- The mechanical properties are obtained with a combination of longitudinal vibration tests and visual grading. The strength class of all timber elements in the tower is an indication based on the obtained dynamic modulus of elasticity with longitudinal vibration tests on several dismantled elements. In order to optimize the results, several other non-destructive tests (such as acoustic tests) might be used and be compared to the results of the longitudinal vibration tests. Hence, the results might be verified.
- The moisture content has not been brought into consideration. The effect of the moisture content on the mechanical properties should be carefully determined in order to optimize the results.
- The static and variable loads are simplified in this study. In order to create representative behavior of the entire tower, the loads should be implemented as precise as possible. Especially the wind loads should be implemented as a dynamic load instead of a static load in future studies.
- The inclination of the tower has been determined by using the terrestrial laser scanner to create a accurate point cloud of the entire tower. The inclination has been measured from the points cloud by drawing a line perpendicular to the facade of every lantern of the tower. The angle of inclination of the line is measured for each lantern and the total inclination is calculated. Since the line is drawn by hand and the process has only been repeated 3 times and a total of 9 combinations is created to minimize the error, errors might still be present. In future studies it is recommended to repeat the hand drawn lines even more often or research for a more suitable method to determine the inclination from a point cloud is required.
- The inclination of the base of the tower is also obtained from the point cloud from the previous item. The angle of inclination has been determined by hand drawing a line between the two clocks parallel to each other. The angle of inclination is determined from the line. The process has only been repeated 3 times and a total of 9 combinations per opposing clock pair is created to minimize the error. However, the lines are drawn by hand and errors might therefore still be present. in addition, the vertical difference, where the angles of inclination are based on, only

vary between 0.1 cm and 8.5 cm. Since the magnitude of the vertical difference is so low, small errors could have a large impact. Moreover, the clocks might not be symmetrically placed and do not necessarily represent the angles of inclination of the base of the tower. In order to verify the results, the base of the tower has to be scanned from the inside with the terrestrial laser scanner. In this way, more accurate results of the inclination of the base of the tower could be determined. Furthermore, the more suitable method to determine the inclination from the point cloud could be applied in this scenario as well.

- In this study the Finite Element Model is created by hand. The precision level of a hand made model is a bit lower in comparison to fully programmed models. Nowadays, the possibility exist to fully write a code for a Finite Element Model. This has a higher work load for someone who lacks the experience to program it but has a higher accuracy. Furthermore, in case one decided to measure the geometry with the laser scanning devices, the obtained cloud points might be converted immediately to a finite element model. This method creates the most accurate models. However, this requires a lot of work due to the complicity of the structure of the tower. A lot of redundant elements should be removed from the point cloud and the converting process might be difficult. In future studies a research should be done to determine the best suitable method to create an accurate Finite Element Model of a complex structure such as the tower of the Grote of St. Bavochurch.

- In this study it is assumed that the force distribution in the connection occurs due to the interlocking of the elements. The timber dowels in the construction only provide stability for the connection. In order to assess the connections more carefully, a scale model (1:1) of several connections in the tower should be made. The scale models should be tested on shear forces in the same direction as in reality and the total resistance might be measured. In this way one is able to conclude the real resistance of these joints and determine if the statements about the connections are correct.

All in all, all obtained results are still a proper indication of reality and the unity checks all amply suffice the demands. The simplifications and lower accuracy of some results are approved since the unity checks would still amply suffice all demands in case the obtained results are a bit off.

Bibliography

Blass, H., Aune, P., Choo, B., Görlacher, R., Griffiths, D., Hilson, B., Racher, P. and Steck, G. (1995), *Timber Engineering STEP 2, Design- Details and structural systems*, Centrum Hout, 1300 BJ Almere, The Netherlands.

Blass, H. and Sandhaas, C. (2017), *Timber Engineering*, KIT Scientific Publishing, Strasse am Forum 2, D-76131 Karlsruhe.

Cavalli, A., Bevilacqua, L., Capecchi, G., Cibecchini, D., Fioravanta, M., Goli, G., Togni, M. and Uzielli, L. (2016), Moe and mor assessment of in service and dismantled old structural timber., Technical report, Department of Agricultural, Food and Forestry systems, University of Florence.

Ceccittu, A. and Togni, M. (1996), Ndt on ancient timber beams: assessment of strength/stiffness properties combining visual and instrumental methods, Technical report, Department of Civil Engineering, Florence University & institute for Forest Management and Technology, Florence University.

De Boer, J., Delleman, A., Phaff, H., Snoep, D., van der Steur, A. and Temminck, J. (1985), *De Bavo te boek.*, Haarlem, The Netherlands.

De bouw van de Grote Kerk (n.d.), https://www.bavo.nl/over-de-bavo-en-de-nieuwe-kerk/grote-of-st-bavokerk/geschiedenis/. Accessed: 2019-03-01.

Emmens, K., Enderman, M., Van Hemert, R., Kluft, R., Prins-Schimmel, M., Rodenburg, R., Sietsma, W. and Vink, E. (2002), *De toren van de grote of Sint-Bavokerk*, Haarlem, The Netherlands.

FLP (1999), Wood handbook-wood as an engineering material, Technical report, Department of Agriculture, Forest Service, Forest Products Laboratory: USA.

Frese, M. (2008), Visual strength grading supported by mechanical grading, Technical report, University of Karlsruhe (TH).

Furini, A. and Russo, P. (2014), Earthquakes and ancient leaning towers: Geodetic monitoring of the bell tower of san benedetto church in ferrara (italy), Technical report, Engineering department in Ferrara, University of Ferrara.

Gerhards, C. (1980), Effect of moisture content and temperature on the mechanical properties of wood: an analysis of immediate effects., Technical report, Forest Products laboratory. Forest Service, U.S. Department of Agriculture.

Hoogenboom, P. C. J. (n.d.), 'Note on stresses in shells', http://homepage.tudelft.nl/p3r3s/b17_schedule.html. Accessed: 2019-23-04, handout 9 on the website.

Kamphuis, b. v. b. (2001), *De vieringtoren van de grote of St. Bavokerk.*, Bureau monumentenzorg, Delft, The Netherlands.

Kollmann, F. P. and Côté, W. (1968), *Principles of Wood Science and Technology*, Springer-Verlag Berlin, Heidelberg, Germany.

Laskowska, A., Marchwicka, M., Boruszewski, P. and Wyszyńska, J. (2018), Chemical composition and selected physical properties of oak wood (quercus robur l.) modified by cyclic thermo-mechanical treatment., Technical report, BioResources.

Leica-geosystems (Unknown), https://w3.leica-geosystems.com/downloads123/hds/hds/ScanStation

Niemz, P. and Mannes, D. (2012), Non-destructive testing of wood and wood-based materials, Technical report, ETH Zurich, institute for Building Materials.

Nilsson, A. and Rowell, R. (2012), Historic wood - struccture and properties, Technical report, Faculty of Forest Sciences SLU Stockholm & University of Wisconsin.

OpticalSurveyequipment (2018), https://surveyequipment.com/geoslam-zeb-revo-3d-laser-scanning-system/.

Piazza, M. and Riggio, M. (2008), Visual strength-grading and ndt of timver in traditional structures, Technical report, Trento University, department of mechanical and structural engineering.

Ridley-Ellis, D., Stapel, P. and Baño, V. (2016), Strength grading of sawn timber in europe: an explanation for engineers and researchers., Technical report, European Journal of Wood and Wood Products.

Riggio, M., D'Ayala, D., Parisi, M. A. and Tardini, C. (2017), Assessment of heritage timber strutures: Review of standards guidelines and procedures., Technical report, Oregon State University, Department WSE & University college London, Department CEGE & Politecnica di Milano, Department ABC.

Selassa, R. (2011), 'Deformatiemeting toren sint bavo kerk'.

Sonderegger, W., Kránitz, K., Bues, C. T. and Niemz, P. (2015), Aging effects on physical and mechanical properties of spruce, fir and oak wood, Technical report, ETH Zurich, institute for Building Materials & Dresden University of Technology, Faculty of Environmental Sciences, Institute of Forest Utilization and Forest Technology, Chair of Forest Utilization.

Thijssen, W. (2011), 'Wie heeft de scheefste?', *volkskrant* .

Von der Dunk, T. (2016), *Haarlem als Hollands Jeruzalem*, Hilversum, The Netherlands.

Vosselman, G. and Haas, M. (2010), *Airborne and terrestrial laser scanning*, Whittless publisher, Dunbeath, Scotland.

ZEB-REVO-User-Guide (2017).

List of Figures

1.1 The scale model of the St. Bavochurch (1:25), made by Theo van Paradijs, 2017 2
1.2 The outline of the thesis 5

2.1 Principle of airborne laser scanning by Vosselman and Haas (2010) 14
2.2 The Leica c10 Scan station on a tripod (Leica-geosystems, Unknown) 15
2.3 The Zeb-Revo handheld scanner (OpticalSurveyequipment, 2018) 15

4.1 The structure of the 1st floor by Kamphuis (2001) 23
4.2 The structure of the 2nd floor by Kamphuis (2001) 24
4.3 The structure of the 3rd and 4th floor by Kamphuis (2001) 24
4.4 The sketch model made in Autodesk Revit 25
4.5 the Finite Element Model in Scia Engineer, left is the beam model and right is the rod model. 26
4.6 The deflections of the base of the tower. 27

5.1 The test setup for the longitudinal vibration test on test sample 12. 30
5.2 The FMD6 Moisture Meter during test setup. 31
5.3 The relation between the mechanical properties and the moisture content (Gerhards, 1980). 31

6.1 The scanlocations of the fieldwork 35
6.2 The targets to connect the different scans 35
6.3 The terrestrial laser scanner during the field work in Haarlem, operated by Linh Truong Hong 36
6.4 The obtained pointcloud from the field work by using the terrestrial laser scanner . . . 36
6.5 Shrinkage and swelling of oak wood in radial direction (left) and tangential direction (right) from Laskowska et al. (2018) 39
6.6 The lead cladding, covering the timber parts of the tower. 39

7.1 The location of the highest stresses, shown in pink in the figure. 41
7.2 The deflection of the tower in SLS with wind as normative factors. 42
7.3 The highest and lowest stresses in the tower, occur in the trusses on the first floor. . . 42
7.4 The stress distribution in the defect element 3.1 (see Appendix C 42
7.5 The location of the peak shear forces in the connection on the second floor. 43
7.6 The location of the peak shear forces in the connections on the fourth floor. 43
7.7 The peak shear forces in the connections on the first floor. 44
7.8 The peak shear forces in the connections on the second floor. 44
7.9 The peak shear forces in the connections on the fourth floor. 44
7.10 The highest stresses in the tower, with inclusion of the inclination of the tower 45
7.11 The peak shear forces in the connections on the first floor, with inclusion of the inclination of the tower. 45
7.12 The peak shear forces in the connections on the second floor, with inclusion of the inclination of the tower. 45
7.13 The peak shear forces in the connections on the fourth floor, with inclusion of the inclination of the tower. 46
7.14 Earthquake sensitive areas in the Netherlands from NEN-EN 1991-1-7 +C1/NB table NB.4 46

8.1 A 3D sketch of the critical connection on the second floor 50
8.2 The critical connection on the first floor. 51

8.3 The critical connection on the second floor of the tower 51
8.4 The critical connection on the fourth floor 52

A.1 The sketches of floor 1 1 67
A.2 The sketches of floor 1 2 68
A.3 The sketches of floor 2 1 69
A.4 The sketches of floor 2 2 70
A.5 The sketches of floor 3 1 and 4 1 71
A.6 The sketches of floor 3 2 and 4 2 72
A.7 The sketches of floor 5 73
A.8 The sketches of floor 6 1 74
A.9 The sketches of floor 6 2 75
A.10 The sketches of floor 7 1 76
A.11 The sketches of floor 7 2 77
A.12 The sketches of floor 8 1 and 9 1 78
A.13 The sketches of floor 8 2 and 9 2 79
A.14 The sketches of floor 8 3 and 9 3 80
A.15 The sketches of floor 8 4 and 9 4 81
A.16 The sketches of floor 10 1 and 11 1 82
A.17 The sketches of floor 10 2 and 11 2 83
A.18 The sketches of floor 12 84

B.1 Test samples 1 86
B.2 Test samples 2 87
B.3 Test samples 3 88
B.4 Test samples 4 89
B.5 Test samples 5 90
B.6 Test sample 6 (left) and test sample 7 (right) 91
B.7 Test samples 8 92
B.8 Test samples 9 93
B.9 Test samples 10 94
B.10 Test samples 11 95
B.11 Test samples 12 96
B.12 Test samples 13 97
B.13 Test samples 14 (left) and test sample 15 (right) 98
B.14 Test samples 16 99
B.15 Test samples 17 100
B.16 Test samples 18 101
B.17 Test samples 19 102
B.18 The longitudinal vibration test results of sample 5. 103
B.19 The longitudinal vibration test results of sample 6. 104
B.20 The longitudinal vibration test results of sample 6. 105
B.21 The longitudinal vibration test results of sample 8. 106
B.22 The longitudinal vibration test results of sample 11. 107
B.23 The longitudinal vibration test results of sample 12. 108

C.1 The defect elements on the first floor of the tower. 110
C.2 The first defect element on floor 1. 111
C.3 The second defect element on floor 1 112
C.4 The third defect element on floor 1. 113
C.5 The defect element on the second floor of the tower. 114
C.6 The first defect element on floor 2. 115
C.7 The second defect element on floor 2. 116
C.8 The third defect element on floor 2. 117
C.9 The defect elements on the third floor. 118
C.10 The first defect element on floor 3a. 119
C.11 The second defect element on floor 3a. 120

C.12 The third defect element on floor 3a. 121
C.13 The fourth defect element on floor 3a. 122
C.14 The first defect element floor 3b. 123
C.15 The defect elements on the fourth floor. 124
C.16 The first defect element floor 4. 125
C.17 The defect elements on the first half of the fifth floor. 126
C.18 The first defect element floor 5a. 127

List of Tables

2.1 Major degradation pathways and chemistries by Nilsson and Rowell (2012). 7
2.2 Operational categories for the assessment of timber structures by Riggio et al. (2017). 8
2.3 The formulas to derive the other mechanical properties from the NEN-EN 384 11
2.4 The first part of guidelines for visual grading according to the NEN-EN 14081-1 12
2.5 The second part of guidelines for visual grading according to the NEN-EN 14081-1 . . . 12

3.1 The magnitude of the forces used in the Finite Element Model 20
3.2 The required results with the chosen methods to obtain the results. 22

5.1 The estimations of the dynamic modulus of elasticity of several test samples. 30
5.2 The mechanical properties under normal condition of the timber elements in use in the tower. 33
5.3 The mechanical properties of the element who did not full fill the demands of the NEN-EN 14081. 33

6.1 The heigths of the base and different lanterns 37
6.2 The average angles of inclinations and average, maximum and minimum inclination of the top the tower, determined from the pointcloud 37
6.3 The angles of inclinations of the base of the tower, determined by using the middle of the clocks from the point cloud 38

7.1 the natural frequencies of the tower obtained from SCIA Engineer 46

B.1 The dimensions of the test samples 85
B.2 The first frequencies measurements from the longitudinal vibration tests 103

A

Geometry Sketches

In this appendix, all the sketches made from measurements in the tower are stated. Note, the fifth floor was forgotten in the sketch model from Autodesk Revit and has been made on blank paper.

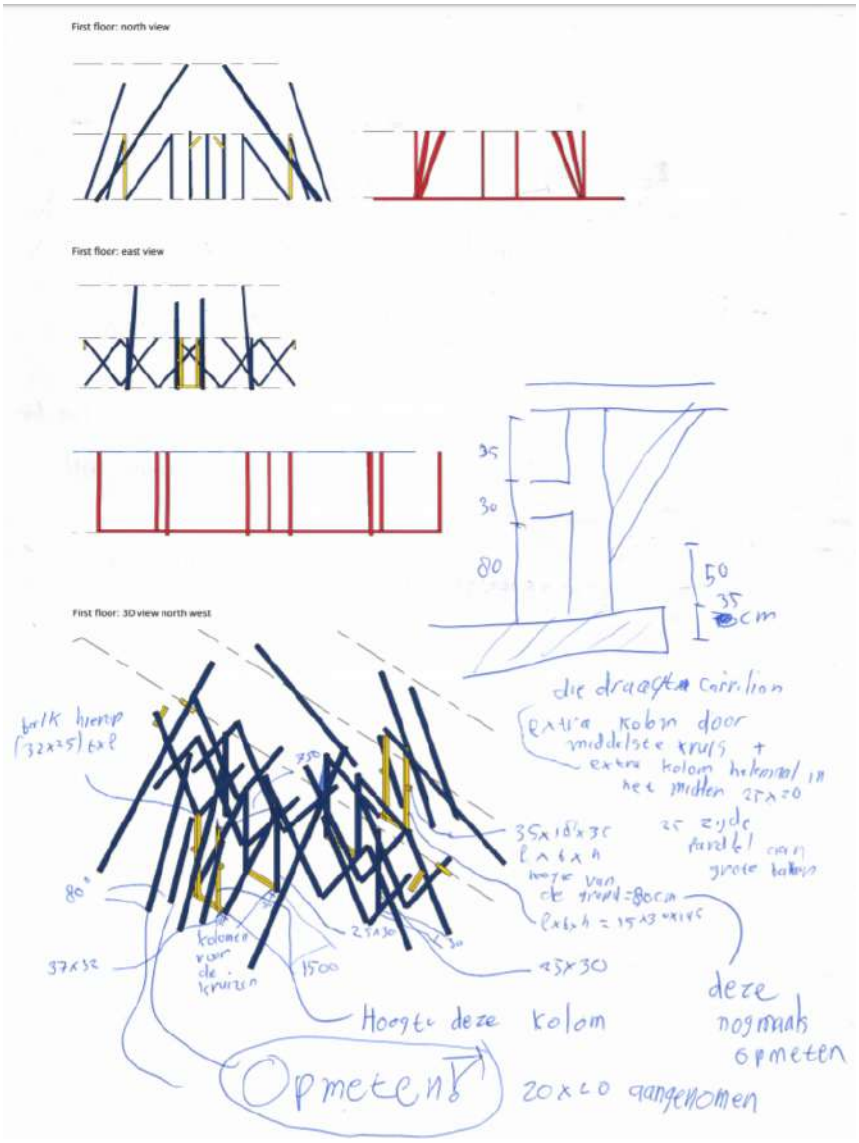

Figure A.1: The sketches of floor 1 1

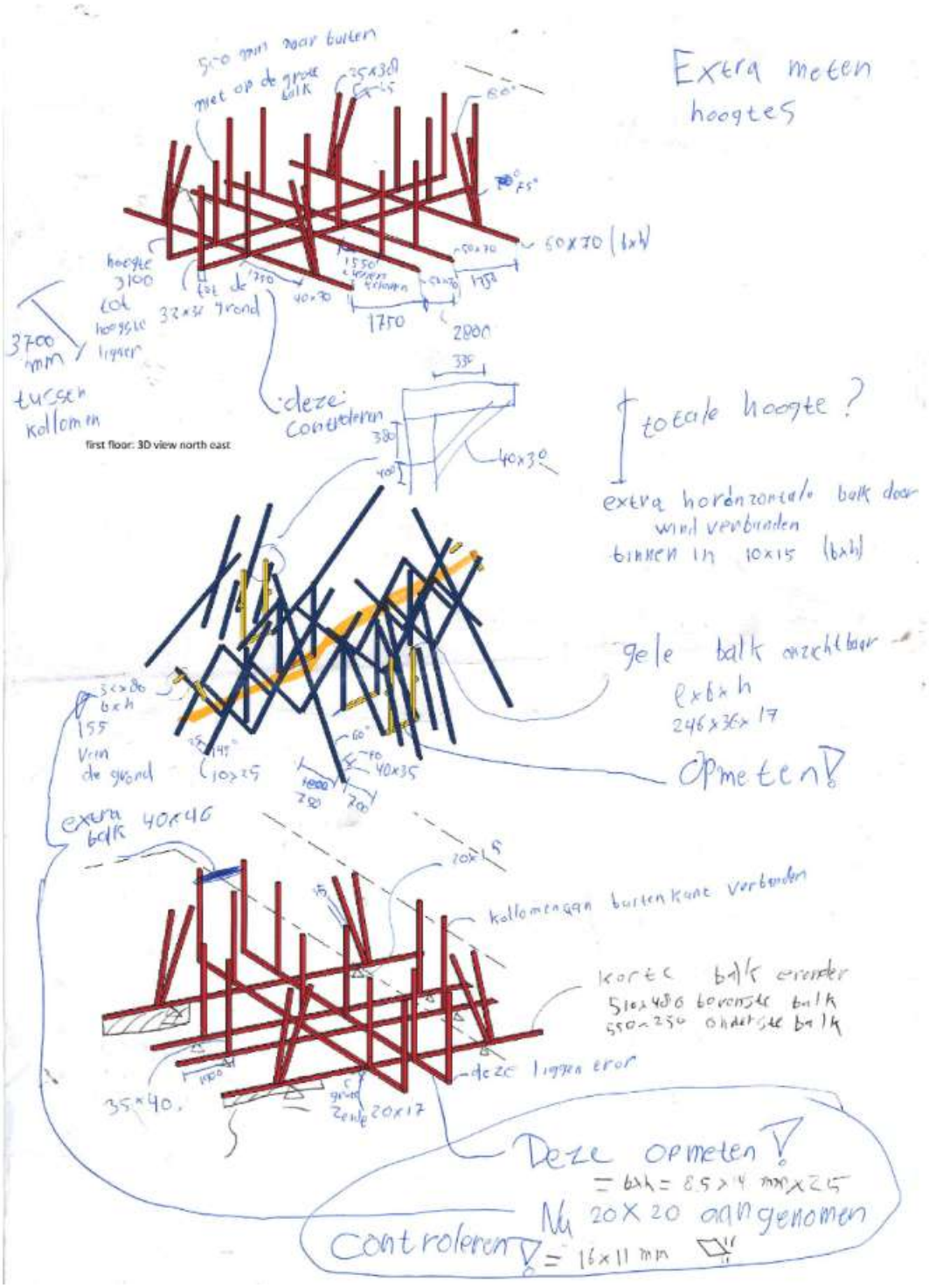

Figure A.2: The sketches of floor 1 2

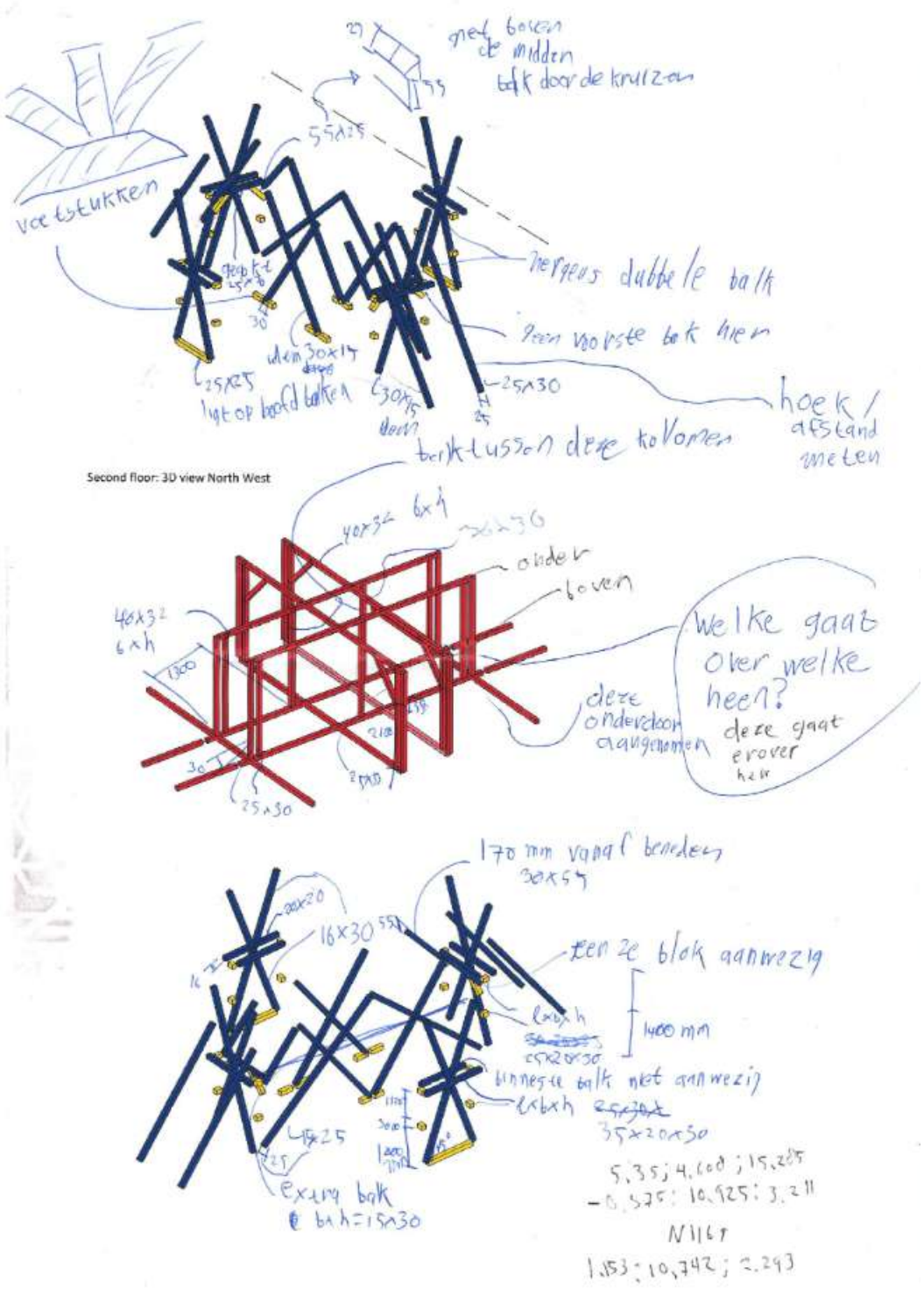

Figure A.3: The sketches of floor 2 1

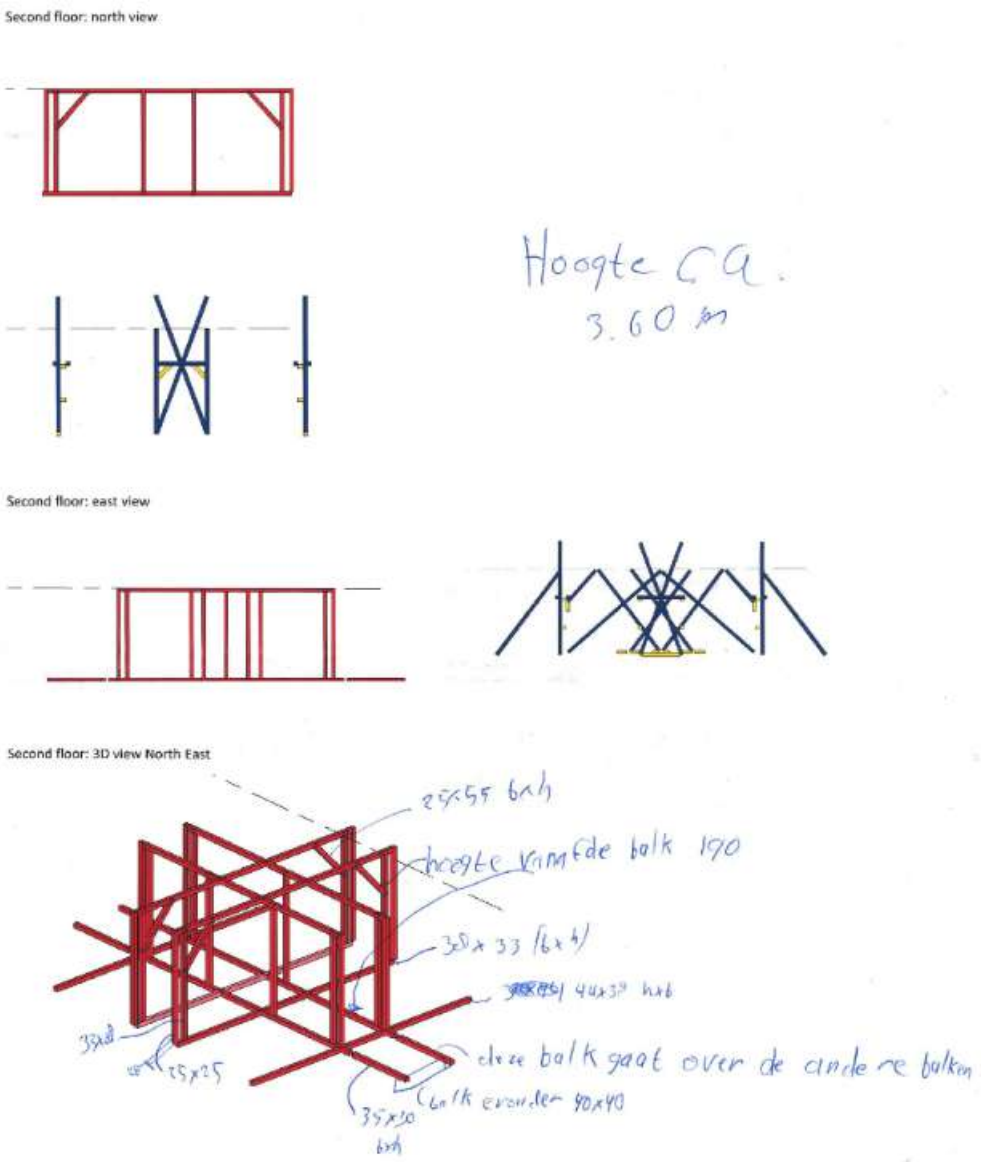

Figure A.4: The sketches of floor 2 2

Figure A.5: The sketches of floor 3 1 and 4 1

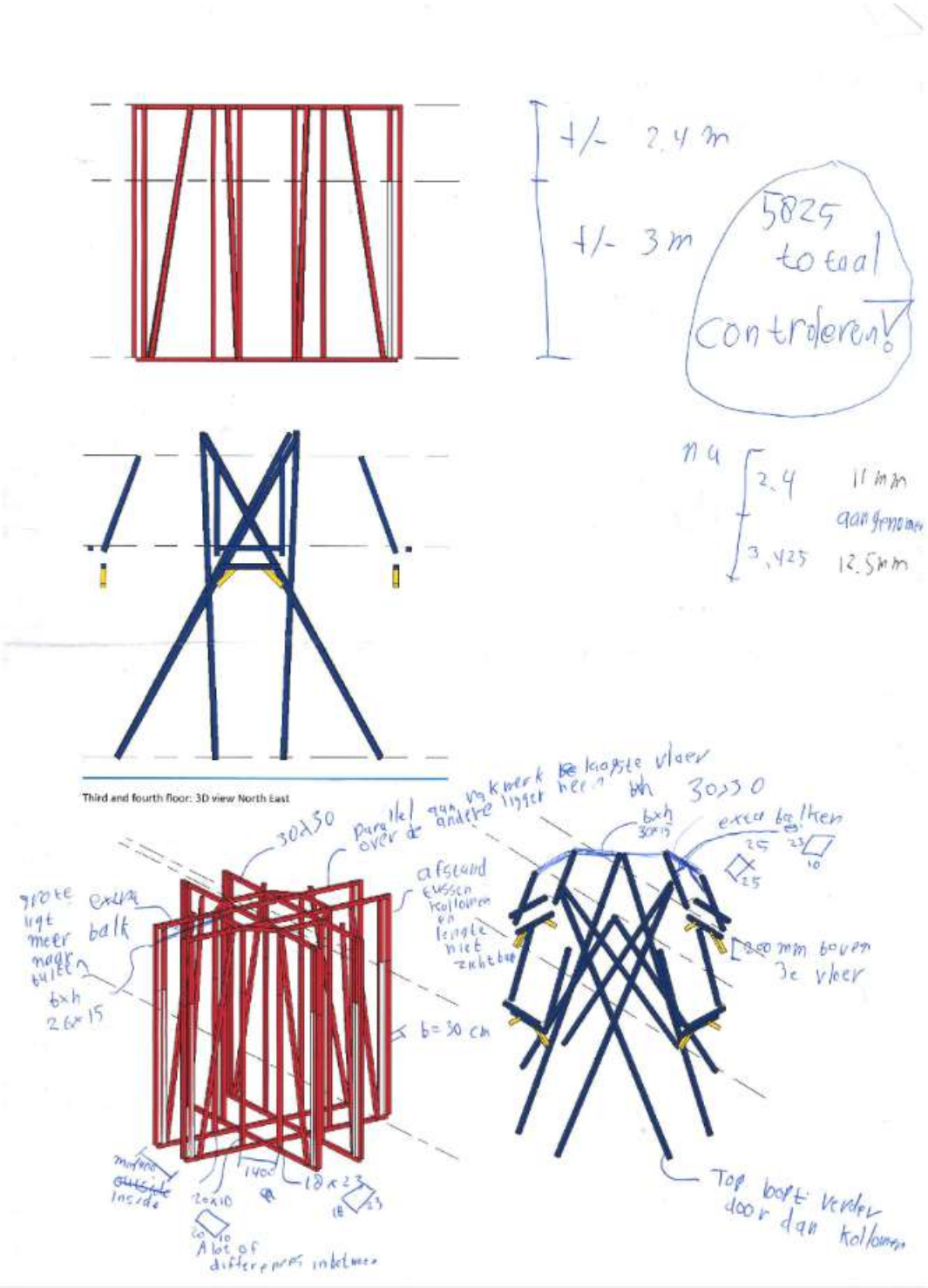

Figure A.6: The sketches of floor 3 2 and 4 2

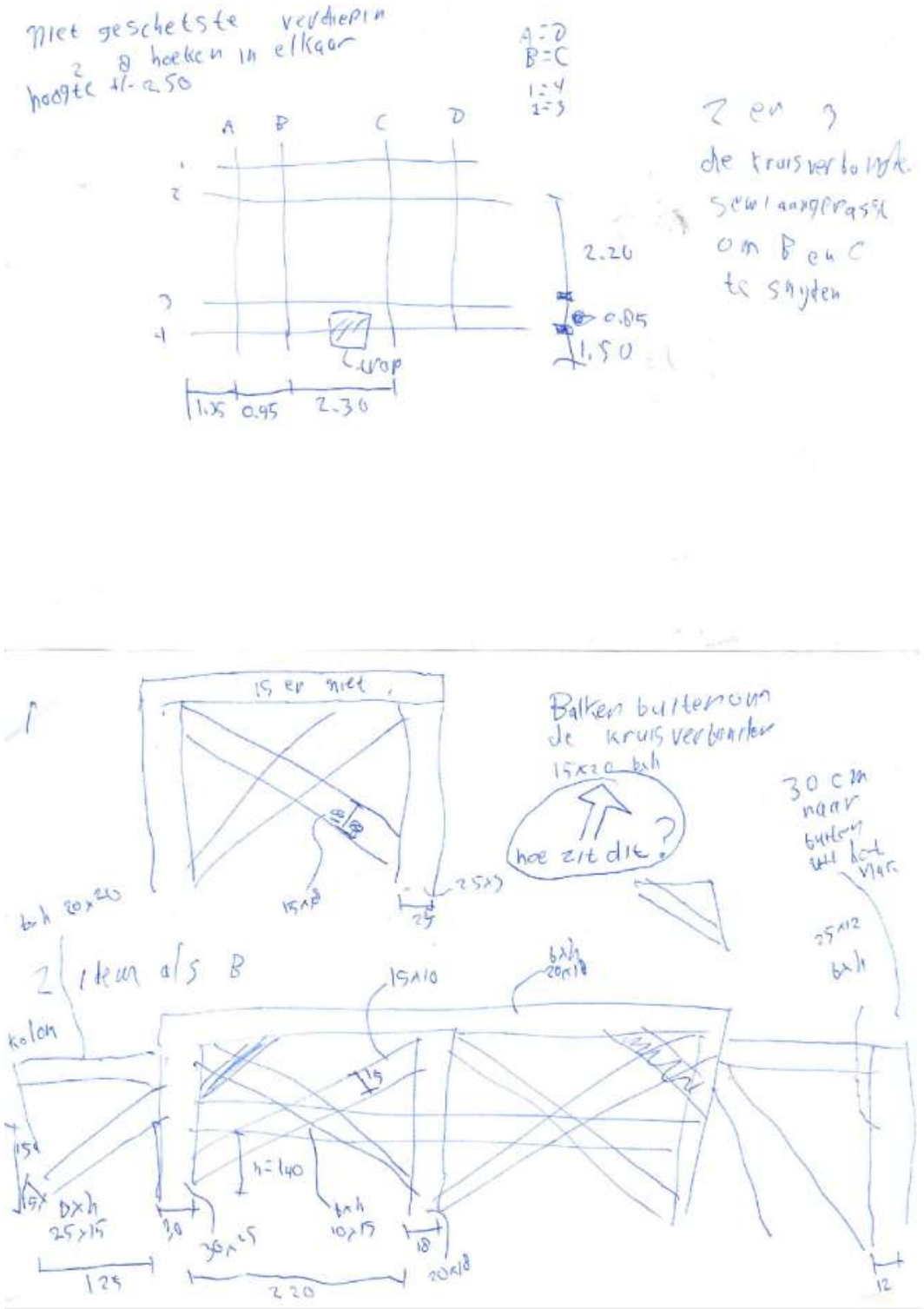

Figure A.7: The sketches of floor 5

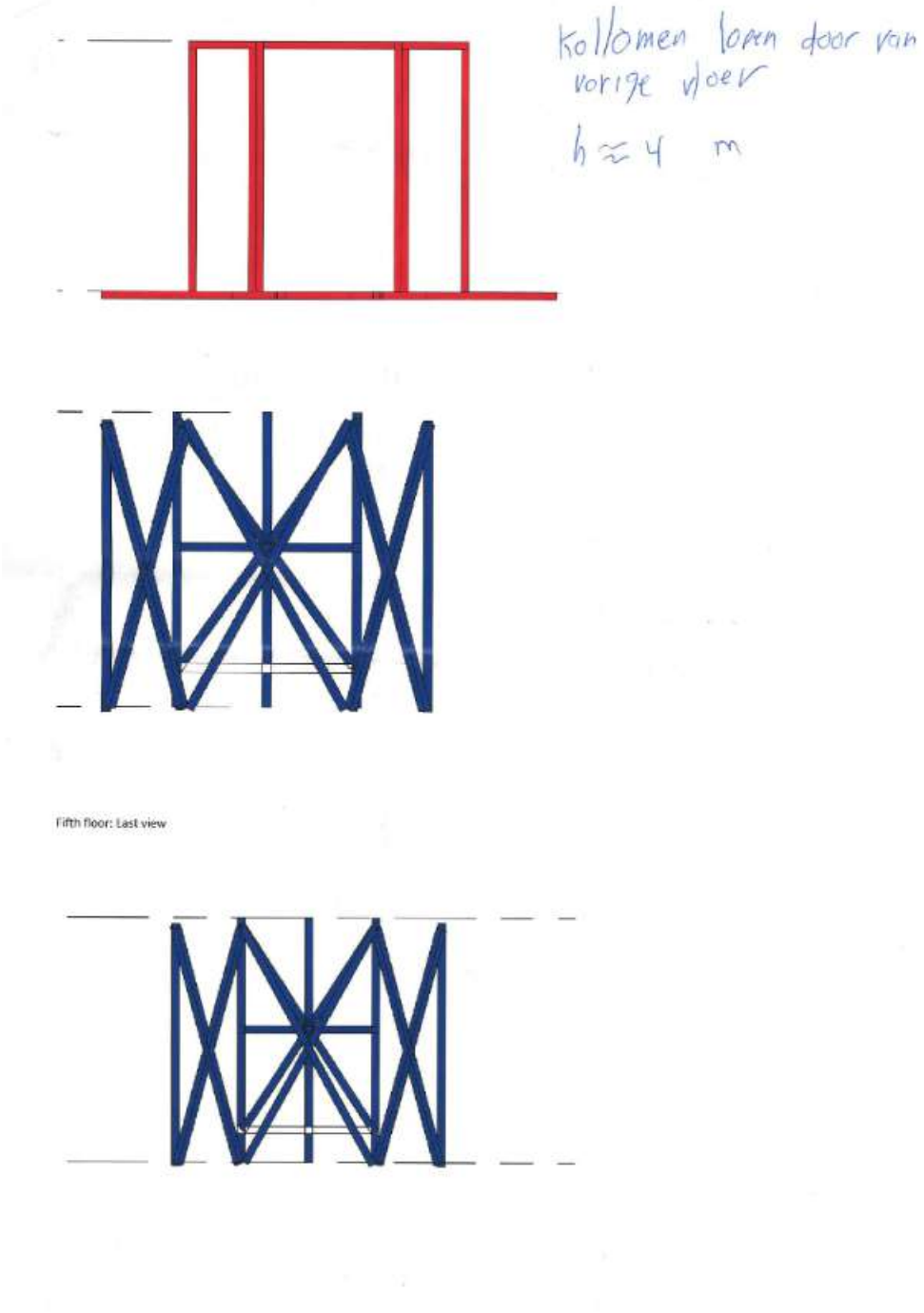

Figure A.8: The sketches of floor 6 1

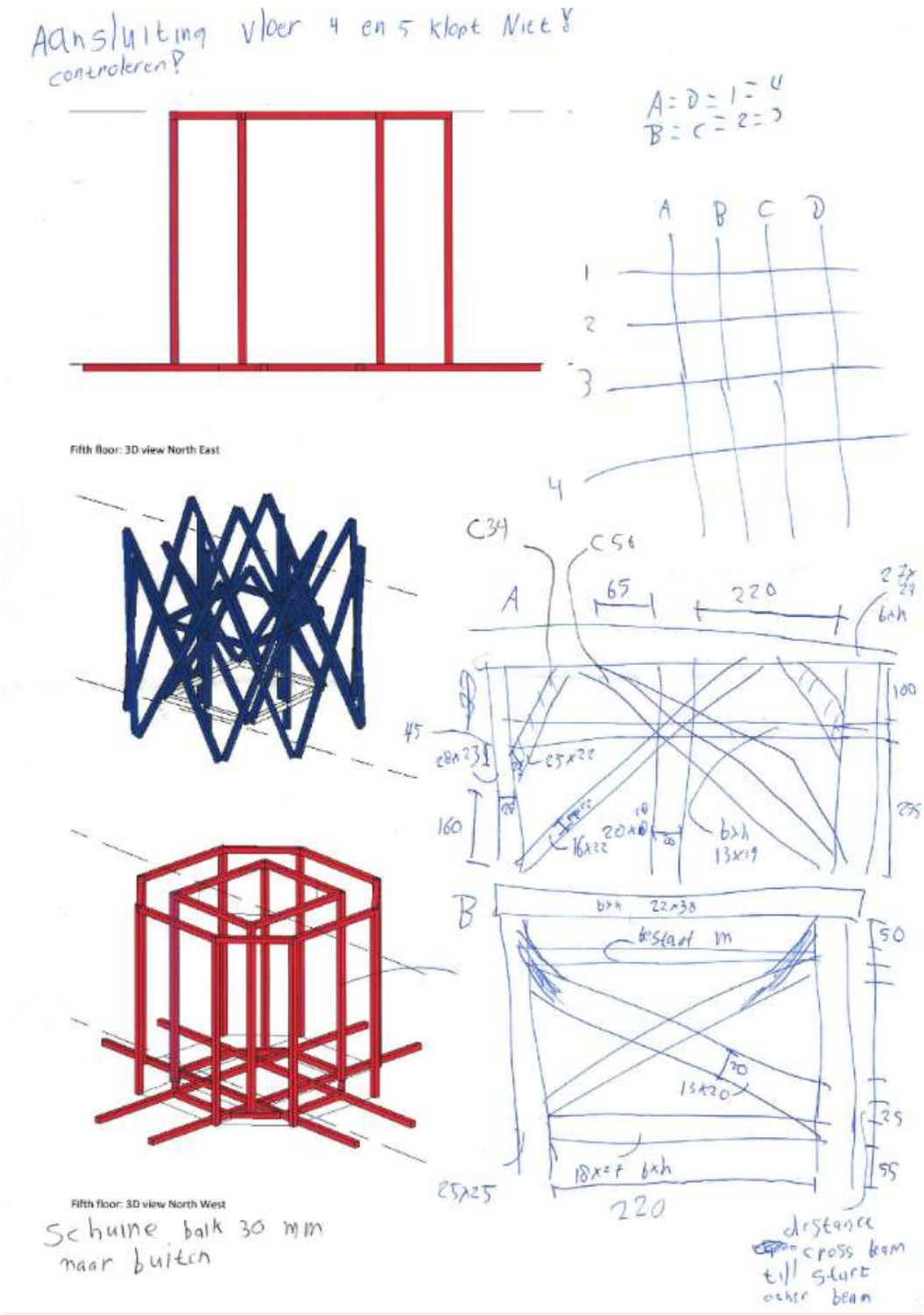

Figure A.9: The sketches of floor 6 2

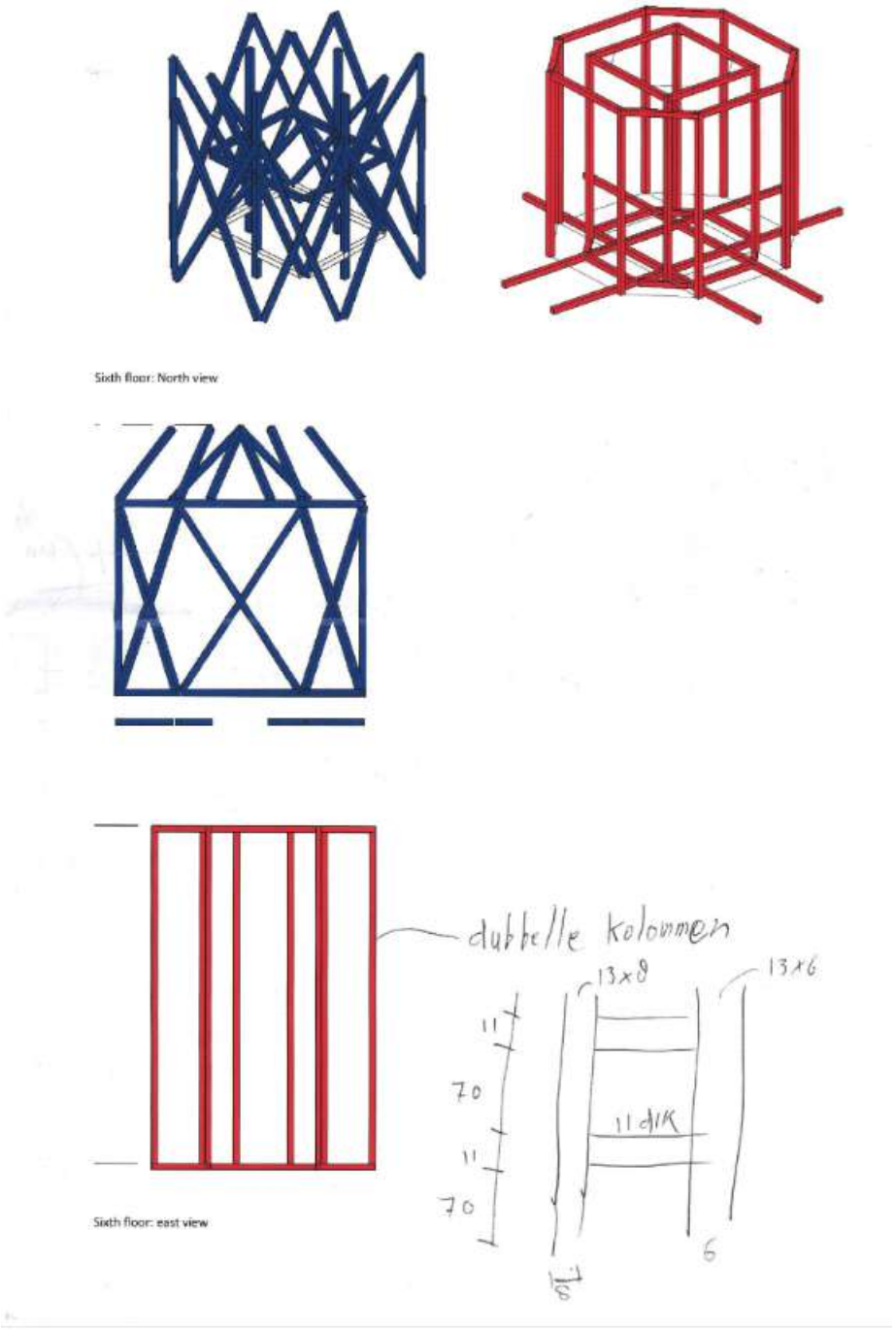

Figure A.10: The sketches of floor 7 1

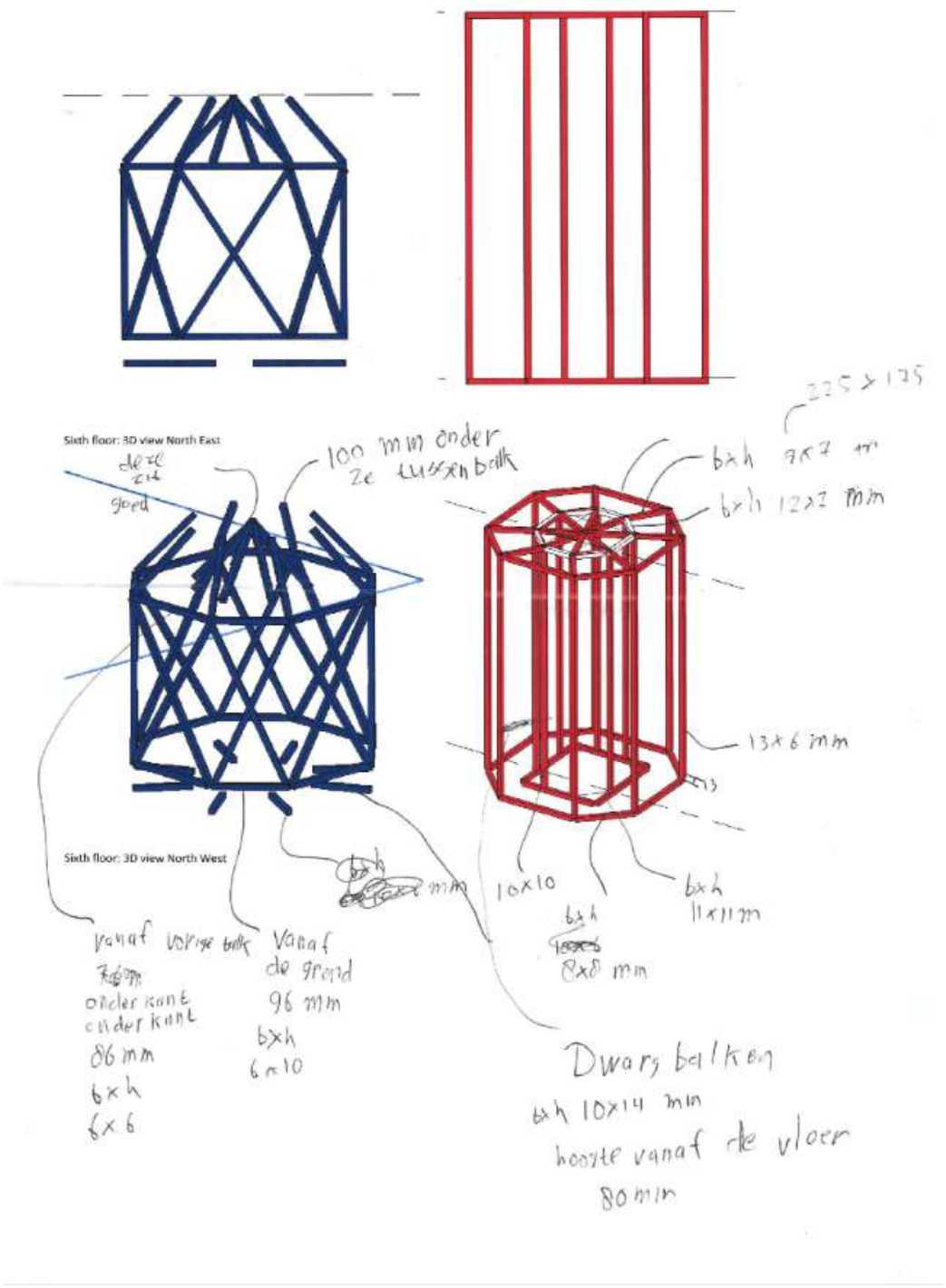

Figure A.11: The sketches of floor 7 2

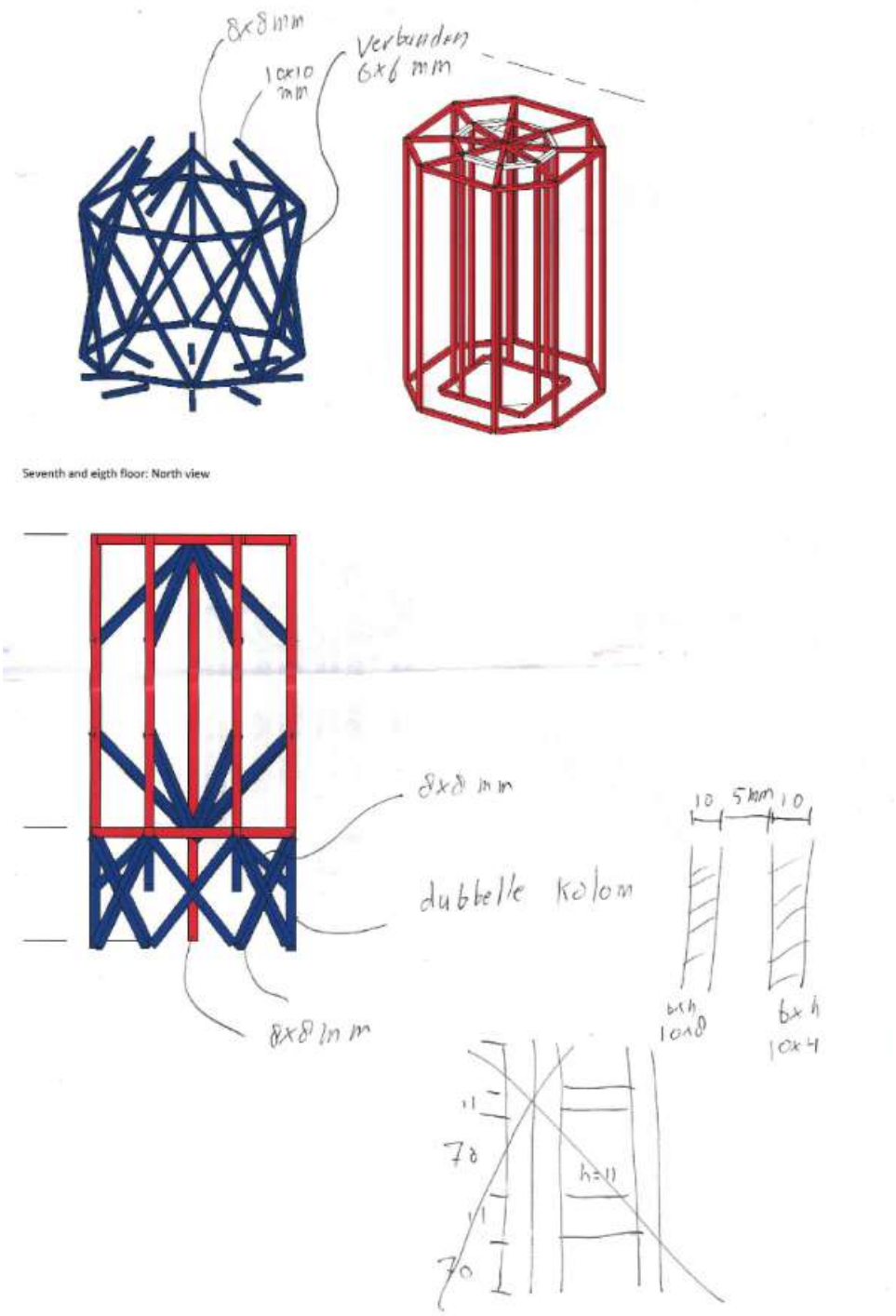

Figure A.12: The sketches of floor 8 1 and 9 1

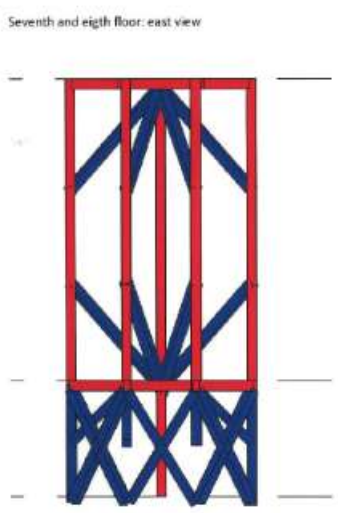

Figure A.13: The sketches of floor 8 2 and 9 2

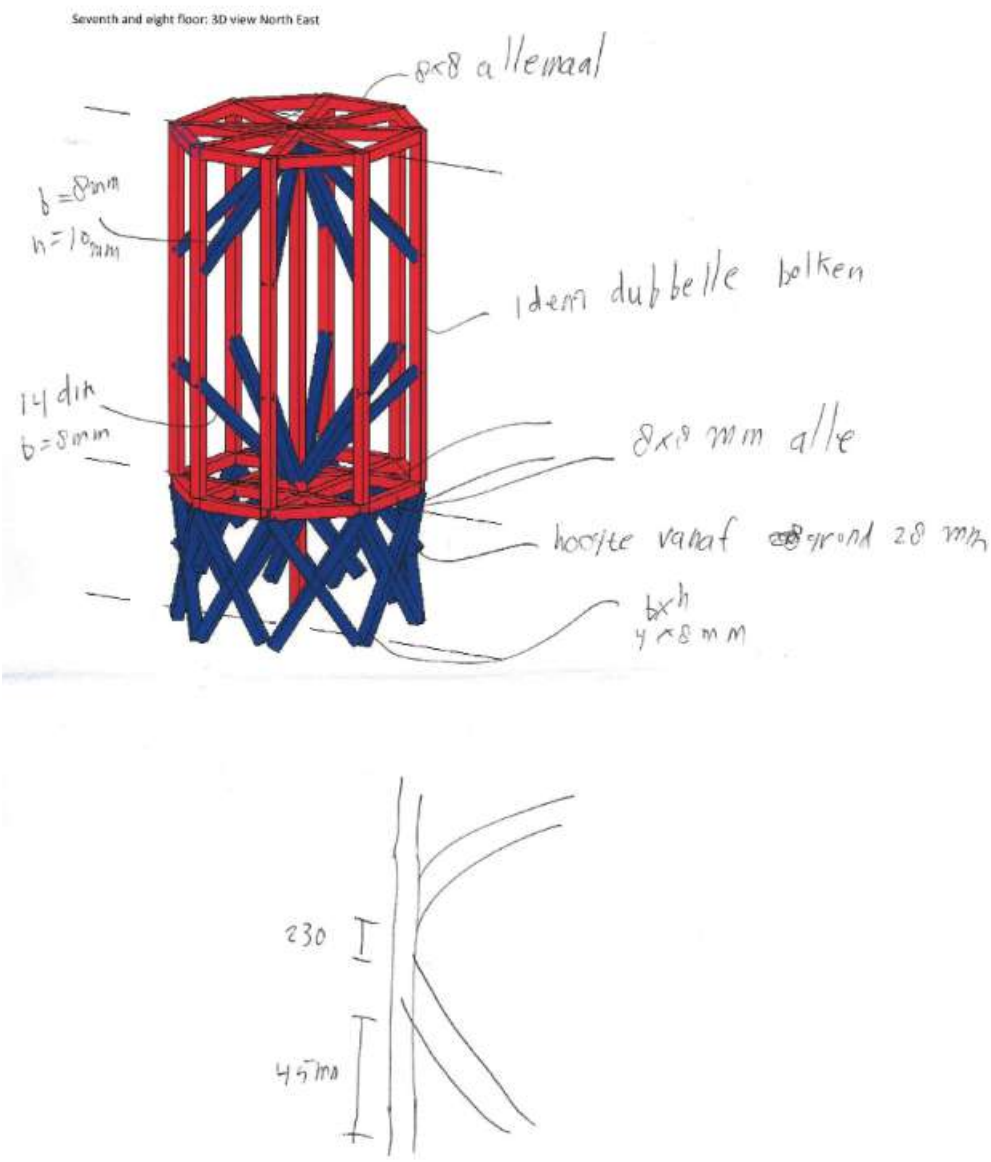

Figure A.14: The sketches of floor 8 3 and 9 3

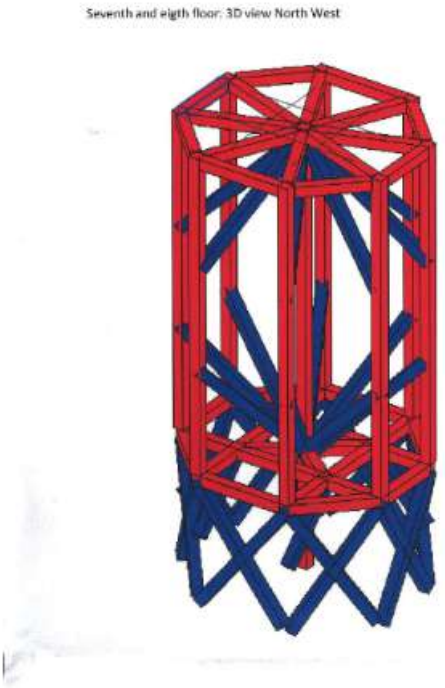

Figure A.15: The sketches of floor 8 4 and 9 4

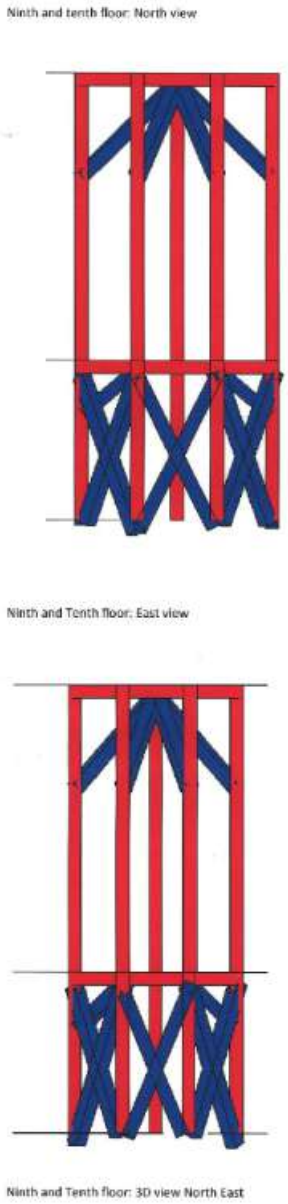

Figure A.16: The sketches of floor 10 1 and 11 1

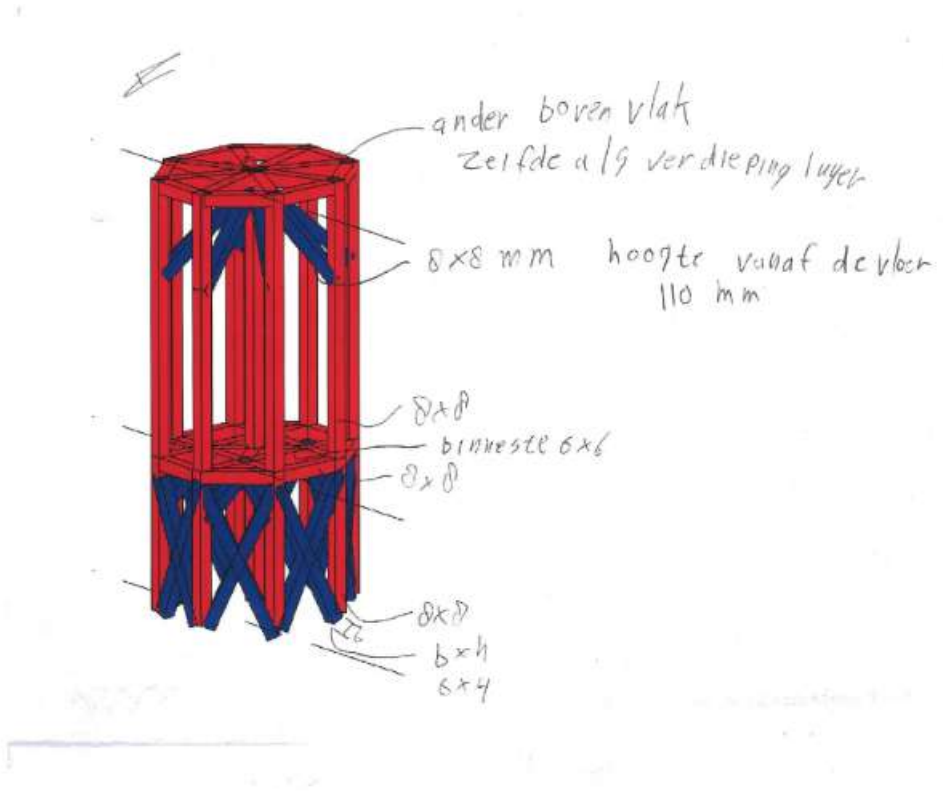

Figure A.17: The sketches of floor 10 2 and 11 2

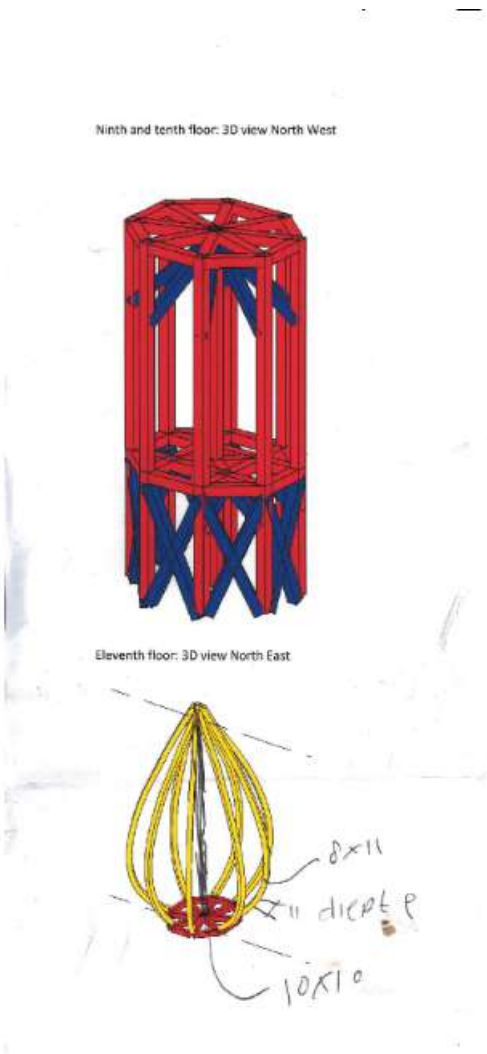

Figure A.18: The sketches of floor 12

B

Longitudinal Vibration Tests

B.1. Test Samples

In total 19 test samples are present in the tower. The test samples have been replaced and are out of use nowadays. The samples are stored in the tower. Only the usable pieces are considered. The dimensions of the test samples are given in table B.1.

Table B.1: The dimensions of the test samples

Test Sample number	Length (cm)	Width (cm)	Height (cm)
1	115	22	17
2	86	20	11
3	90	19	13
4	55	20	13
5	545	25	25
6	525	25	25
7	563	25	25
8	525	25	25
9	328	17	13
10	217	25	15
11	230	15	12
12	346	20	20
13	273	18	18
14	367	15	15
15	373	15	15
16	588	25	25
17	409	8	30
18	420	8	30
19	470	20	20

All the test samples are shown in the figures below.

Figure B.1: Test samples 1

Figure B.2: Test samples 2

Figure B.3: Test samples 3

Figure B.4: Test samples 4

Figure B.5: Test samples 5

Figure B.6: Test sample 6 (left) and test sample 7 (right)

Figure B.7: Test samples 8

Figure B.8: Test samples 9

Figure B.9: Test samples 10

Figure B.10: Test samples 11

Figure B.11: Test samples 12

Figure B.12: Test samples 13

Figure B.13: Test samples 14 (left) and test sample 15 (right)

Figure B.14: Test samples 16

Figure B.15: Test samples 17

Figure B.16: Test samples 18

Figure B.17: Test samples 19

B.2. Results of the Longitudinal Vibration Tests

Only samples 5,6,7,8,11 and 12 gave use full results for the determination of the modulus of elasticity. The longitudinal vibration tests require a flat surface to strike with the hammer at the ends and some samples could not give proper results. The measurement device immediately transports the results towards a computer. The computer can plot a graph, which shows the frequencies. One can directly see if the hit and results were correct in this way. Preferable, only high peaks occur and the rest is flat. Every peak is an eigenfrequency (the first peak is the first eigenfrequency, the second peak is the second eigenfrequency, etc). The first eigenfrequency is the required frequency, which can be used to calculate the modulus of elasticity. Test sample 7 has very high peaks for the second eigenfrequency, only the results of the second eigenfrequency have been noted during the field work. According to the theorem, the first eigenfrequency is half the second eigenfrequency. By dividing the second eigenfrequency by 2, the first eigenfrequency was determined. The first eigenfrequency results can be seen in table B.2. The results can be seen in the figures below.

Table B.2: The first frequencies measurements from the longitudinal vibration tests

Test sample	frequency tests (f t) 1 (Hz)	f t 2 (Hz)	f t 3 (Hz)	f t 4 (Hz)	average frequency
5	326	342	-	-	335
6	351	346	346	351	349
7	615	615	615	615	615
8	346	317	366	-	343
11	722	727	722	722	723
12	595	556	556	590	574

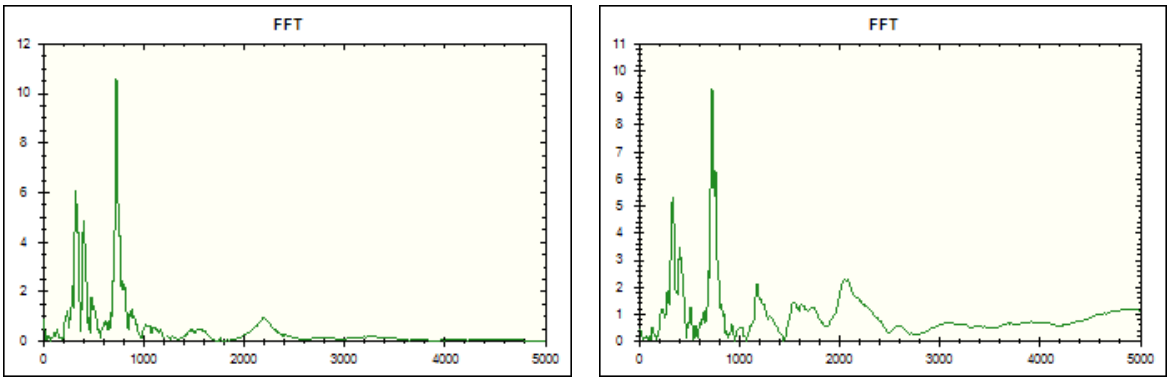

(a) First test of sample 5

(b) Second test of sample 5

Figure B.18: The longitudinal vibration test results of sample 5.

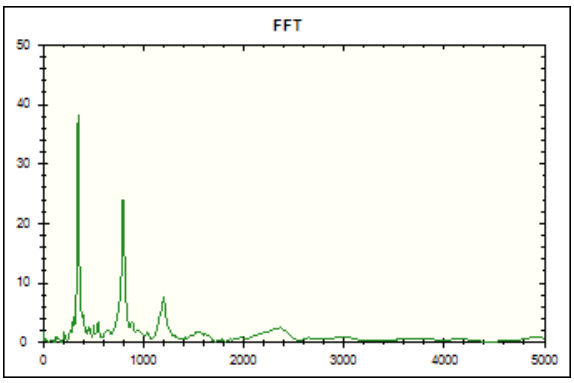

(a) First test of sample 6

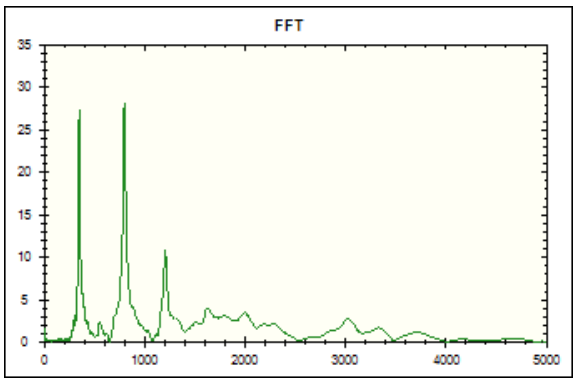

(b) Second test of sample 6

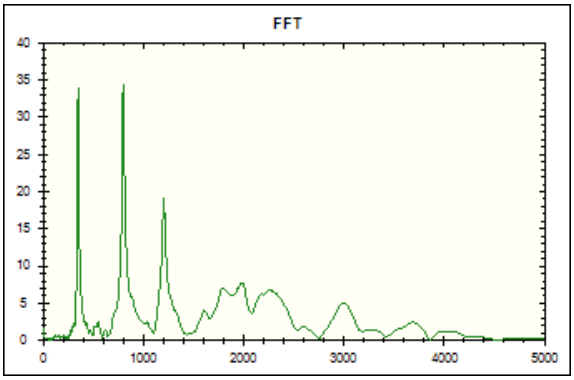

(c) Third test of sample 6

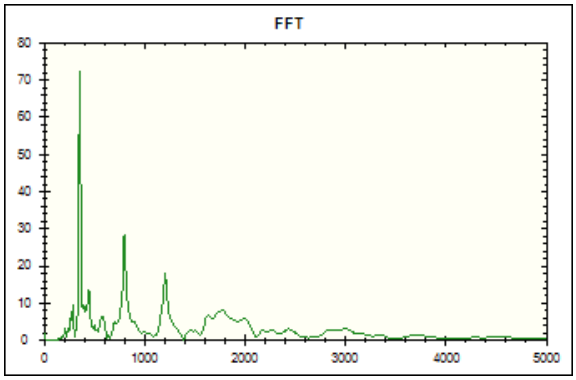

(d) Fourth test of sample 6

Figure B.19: The longitudinal vibration test results of sample 6.

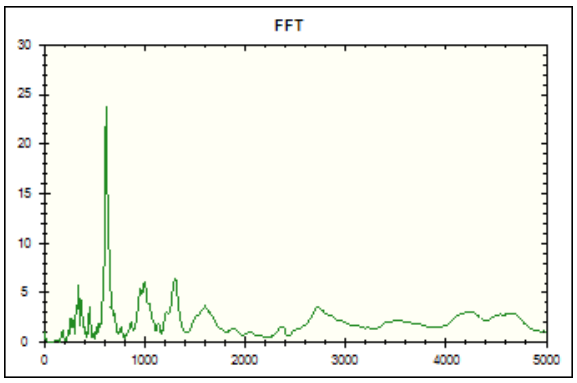

(a) First test of sample 7

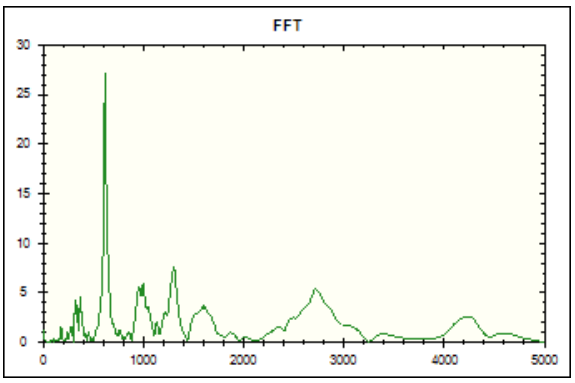

(b) Second test of sample 7

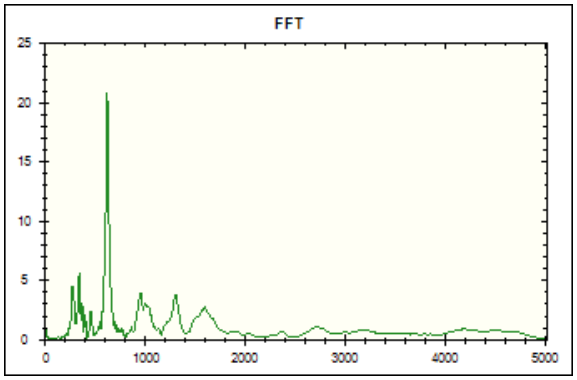

(c) Third test of sample 7

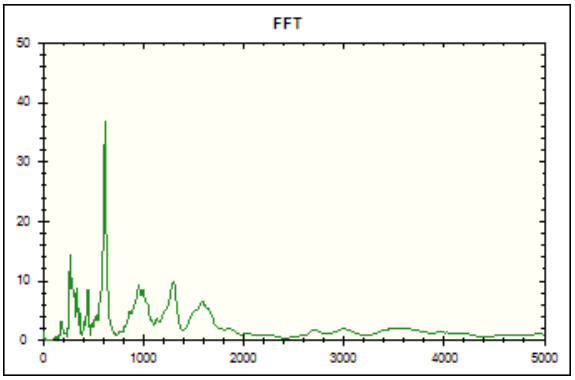

(d) Fourth test of sample 7

Figure B.20: The longitudinal vibration test results of sample 6.

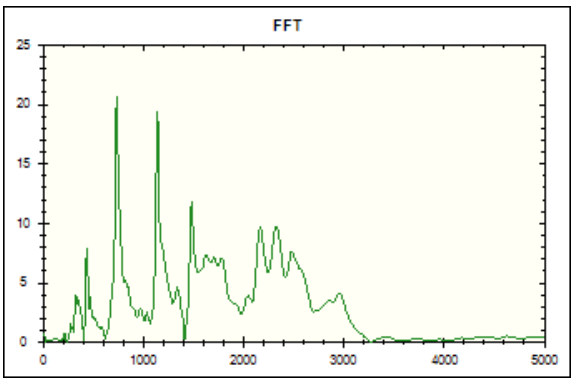

(a) First test of sample 8

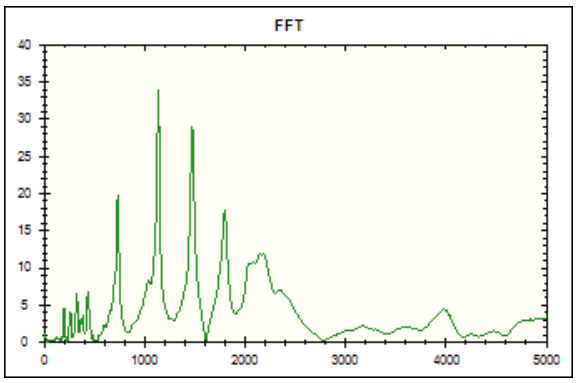

(b) Second test of sample 8

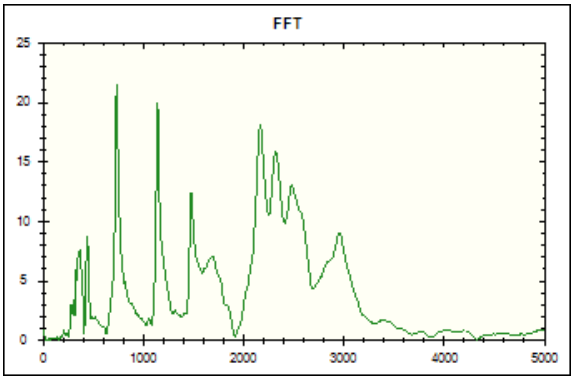

(c) Third test of sample 8

Figure B.21: The longitudinal vibration test results of sample 8.

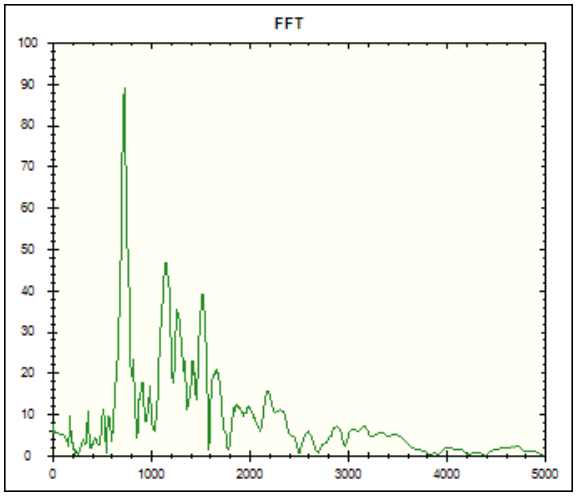

(a) First test of sample 11

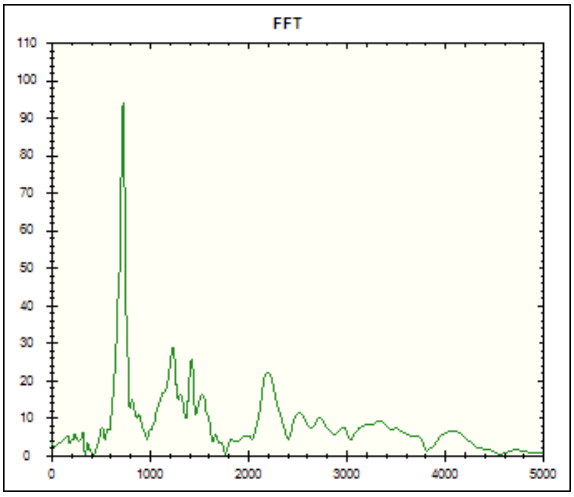

(b) Second test of sample 11

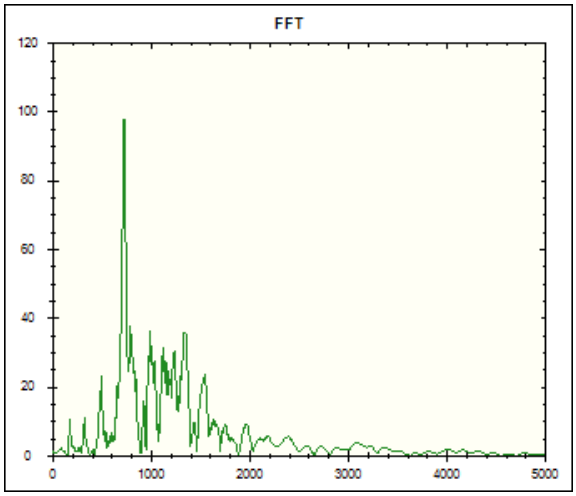

(c) Third test of sample 11

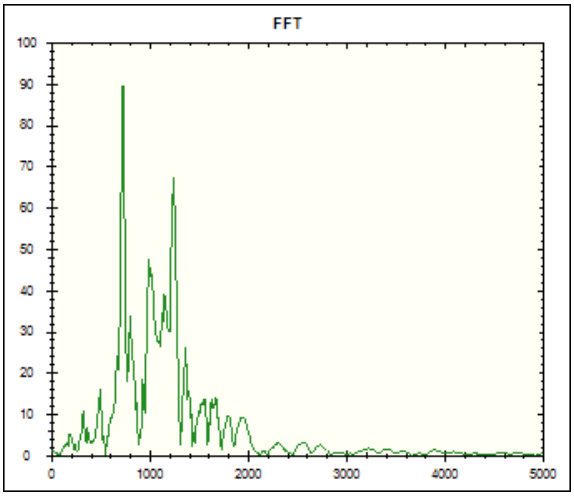

(d) Fourth test of sample 11

Figure B.22: The longitudinal vibration test results of sample 11.

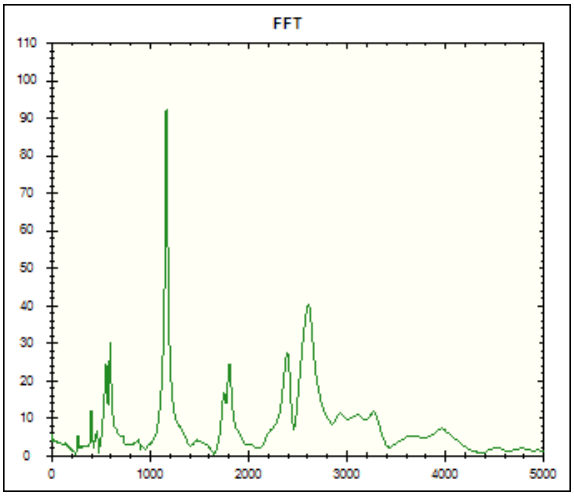

(a) First test of sample 12

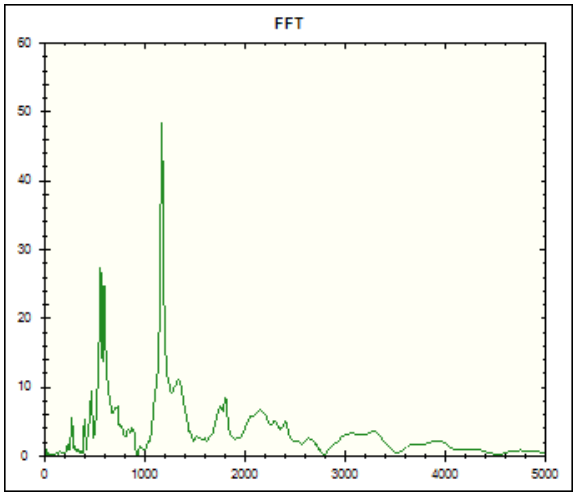

(b) Second test of sample 12

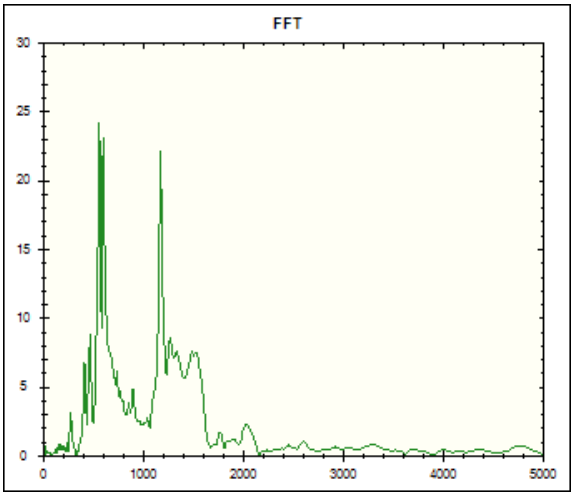

(c) Third test of sample 12

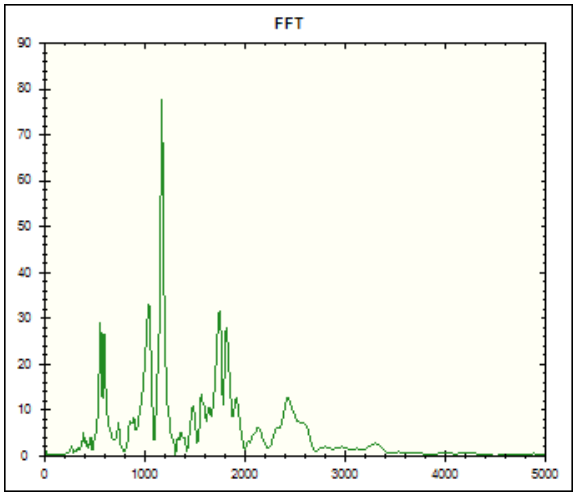

(d) Fourth test of sample 12

Figure B.23: The longitudinal vibration test results of sample 12.

C

Visual Grading

13 defect elements were discovered in the tower. The numbering in figures C.1, C.5, C.9, C.15 and C.17 is done with two number. The first number indicates the floor and the second number indicates an assigned number.

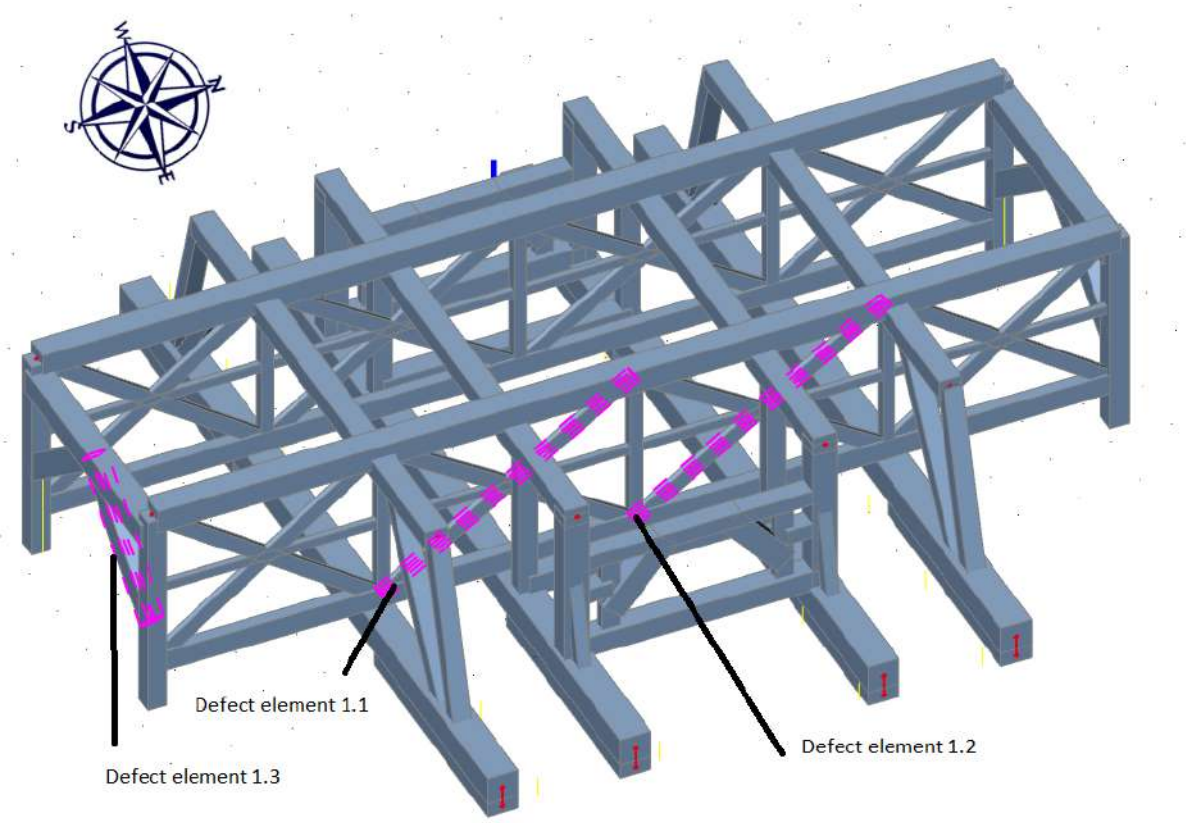

Figure C.1: The defect elements on the first floor of the tower.

Figure C.2: The first defect element on floor 1.

Figure C.3: The second defect element on floor 1 .

Figure C.4: The third defect element on floor 1.

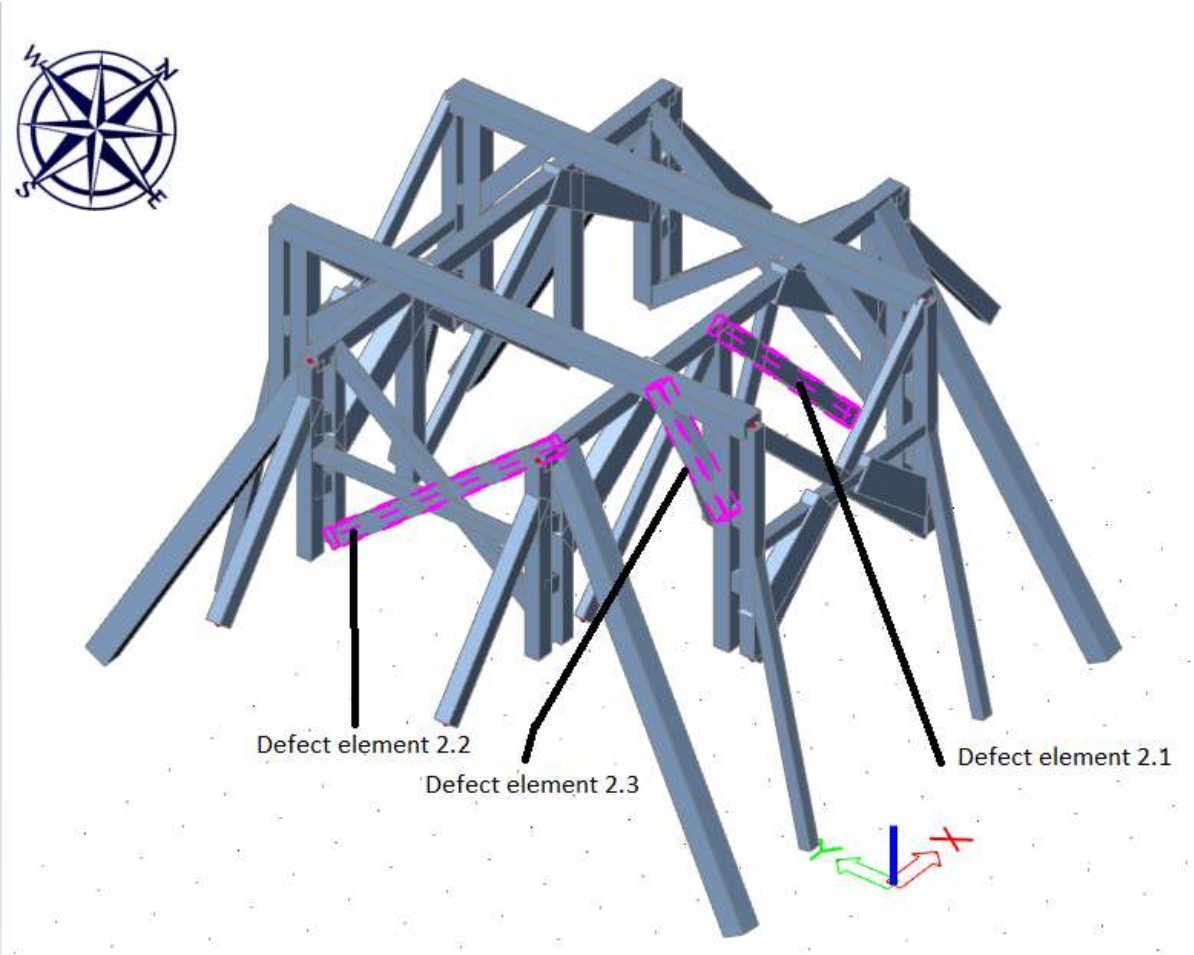

Figure C.5: The defect element on the second floor of the tower.

Figure C.6: The first defect element on floor 2.

Figure C.7: The second defect element on floor 2.

Figure C.8: The third defect element on floor 2.

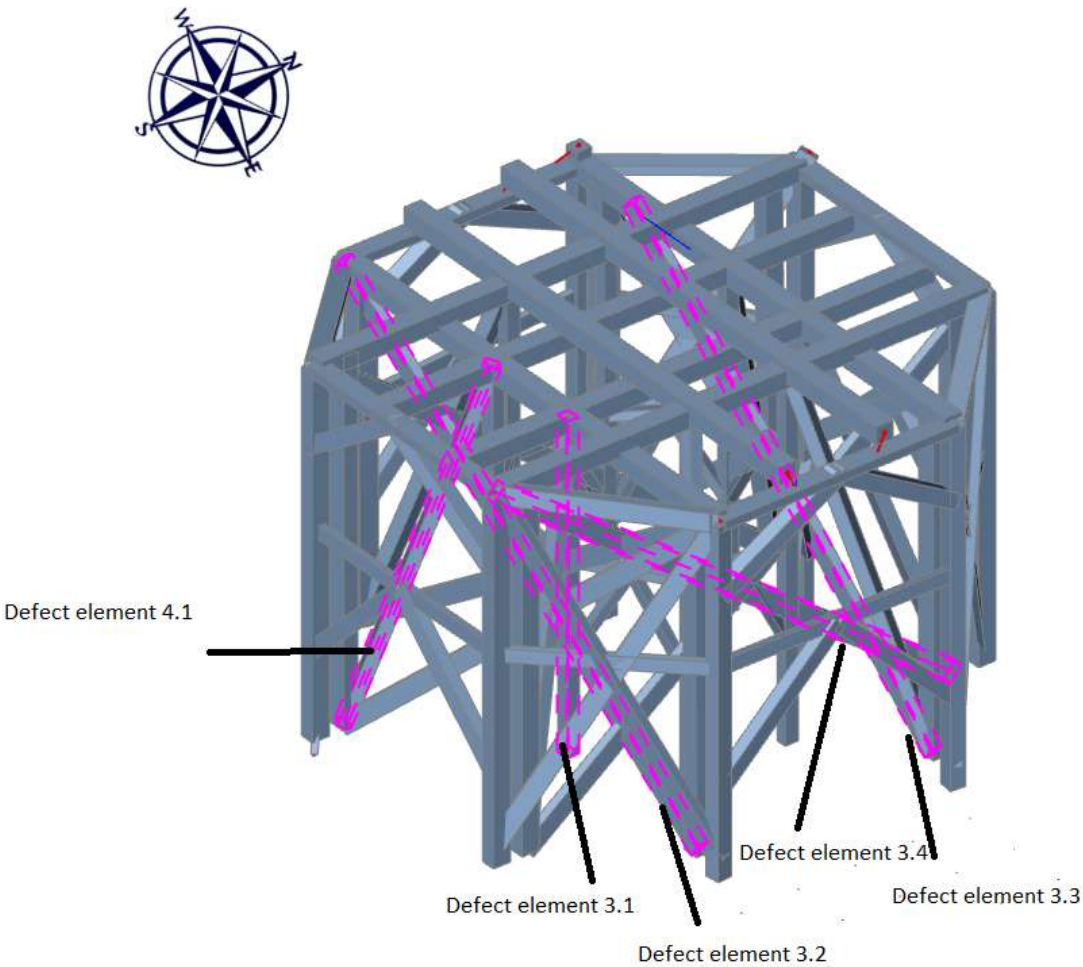

Figure C.9: The defect elements on the third floor.

Figure C.10: The first defect element on floor 3a.

Figure C.11: The second defect element on floor 3a.

Figure C.12: The third defect element on floor 3a.

Figure C.13: The fourth defect element on floor 3a.

Figure C.14: The first defect element floor 3b.

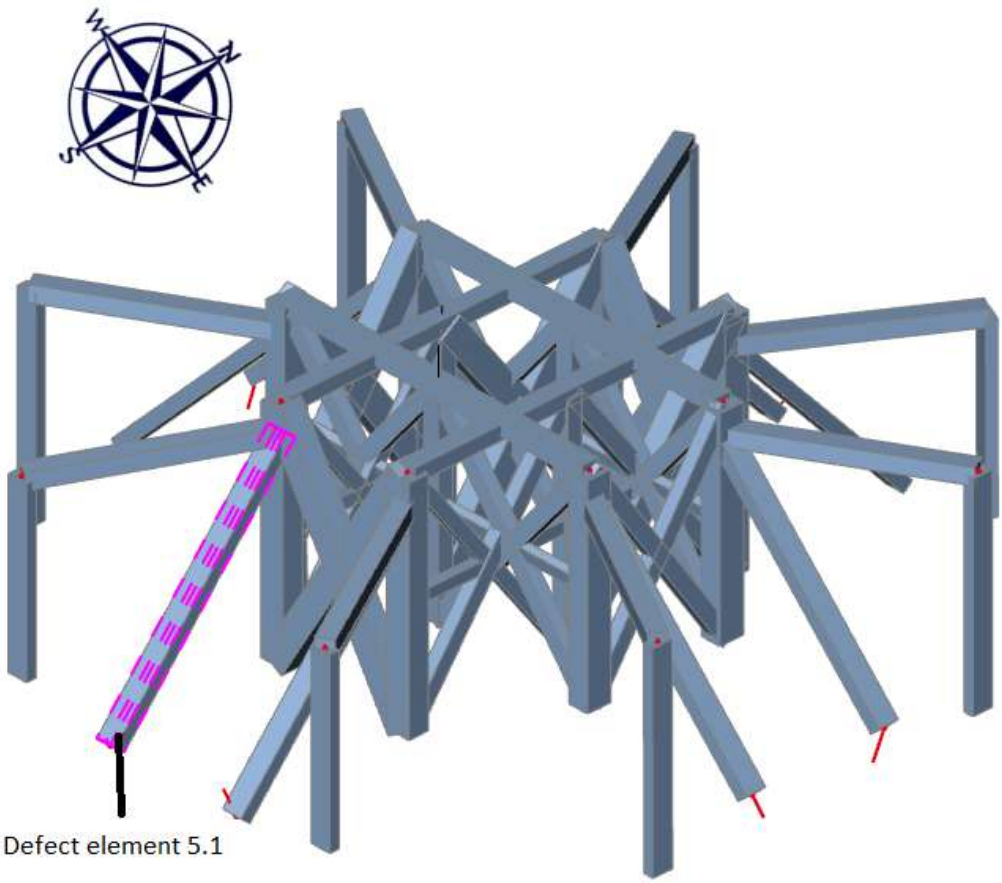

Figure C.15: The defect elements on the fourth floor.

Figure C.16: The first defect element floor 4.

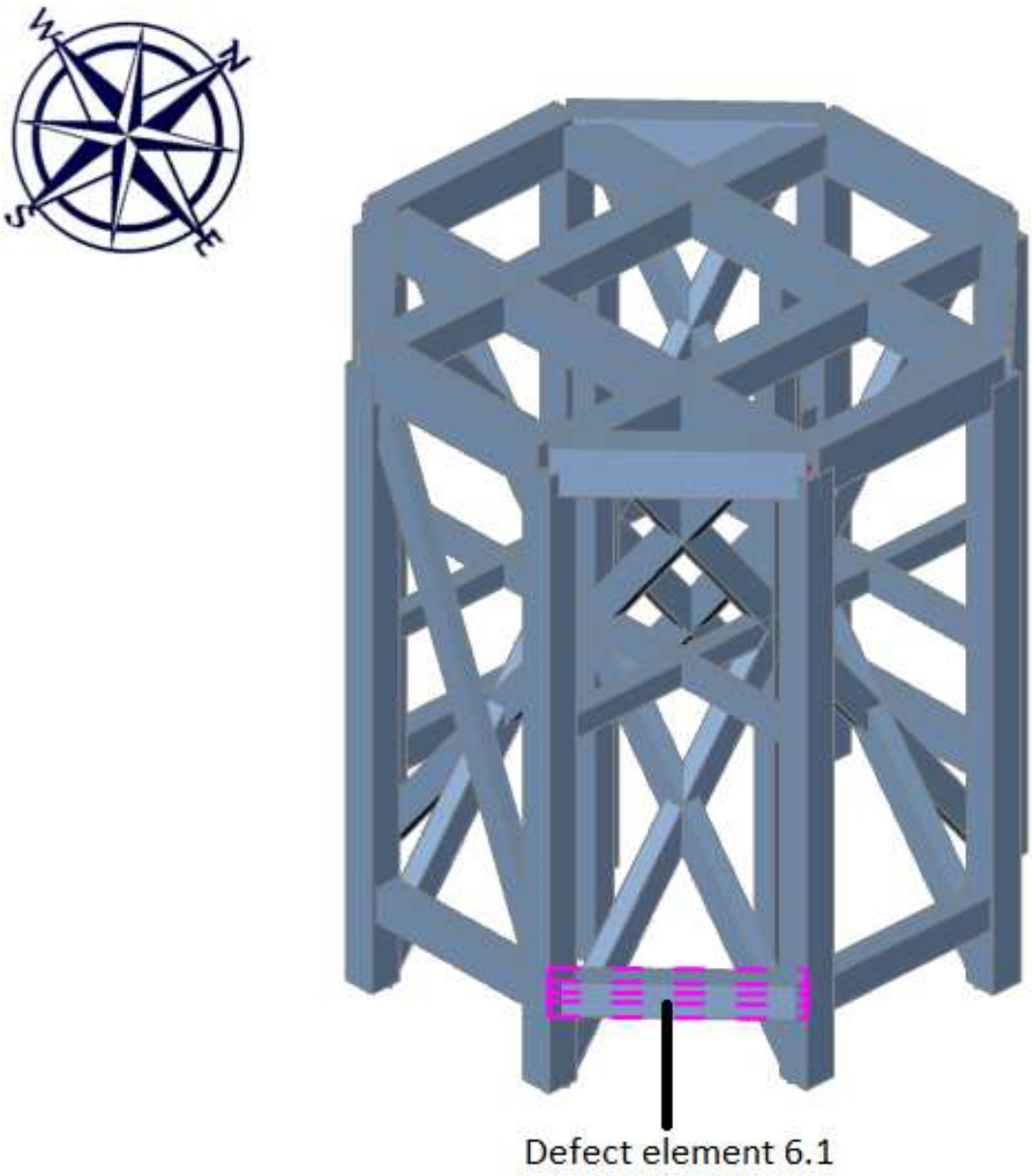

Figure C.17: The defect elements on the first half of the fifth floor.

Figure C.18: The first defect element floor 5a.

D

SCIA Input

SCIAENGINEER
SCIA Engineer 18.1.54

Part	Master Thesis Tu Delft	National code	EC - EN
Author	Pieter	National annex	Standard EN
Date	27. 11. 2018	Licence name	HP Inc.
		Licence number	144500

Project Appendix D: SCIA Input

Student version

1. Project

1.1. Project

Licence name	HP Inc.
Project	Appendix D: SCIA Input
Part	Master Thesis Tu Delft
Description	The Finite element model of the tower of the Grote of St. Bavochurch in Haarlem
Author	Pieter
Date	27. 11. 2018
Structure	General XYZ
No. of nodes :	1472
No. of beams :	651
No. of slabs :	116
No. of solids :	0
No. of used profiles :	57
No. of load cases :	21
No. of used materials :	2
Acceleration of gravity [m/s²]	9.810
National code	EC - EN

1.1.1. Analysis model

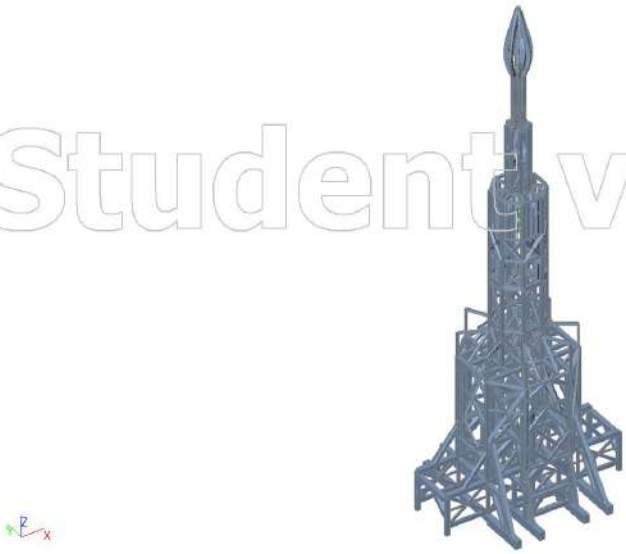

Student version

Student version

Student version

2. Table of contents

1. Project 1
1.1. Project 1
1.1.1. Analysis model 1
2. Table of contents 2
3. General 2
3.1. Materials 2
4. Loads 3
4.1. Load cases 3
4.2. Load groups 3
4.3. Combinations 3
4.4. Nonlinear combinations 5
4.5. Mass groups 6
4.6. Combination of mass groups 6
5. Calculation setup 6
5.1. Mesh setup 6
5.2. Solver setup 6

3. General

3.1. Materials

Timber EC5

Name	Type of timber	μ	E_{mod} [MPa]	$f_{m,k}$ [MPa]	$f_{t,0,k}$ [MPa]	$f_{t,90,k}$ [MPa]	$f_{c,0,k}$ [MPa]	$f_{c,90,k}$ [MPa]	$f_{v,k}$ [MPa]	Colour
	ρ [kg/m³]	α [m/mK]	G_{mod} [MPa]							
D18 (EN 338)	Solid	0	9.5000e+03	18.0	11.0	0.6	18.0	4.8	3.5	
	570.0	0.00	5.9000e+02							
D18 defect	Solid	0	4.7500e+03	9.0	5.5	0.3	9.0	2.4	1.8	
	570.0	0.00	2.9500e+03							

Student version

Student version

SCIAENGINEER

SCIA Engineer 18.1.54

Part	Master Thesis Tu Delft	National code	EC - EN
Author	Pieter	National annex	Standard EN
Date	27. 11. 2018	Licence name	HP Inc.
		Licence number	144500

Project Appendix D: SCIA Input

Student version

4. Loads

4.1. Load cases

Name	Description	Action type	Load group	Direction	Duration	Master load case
	Spec	Load type				
LC1	Self weight	Permanent Self weight	LG1	-Z		
LC2	Imposed floorloads	Permanent Standard	LG1			
LC4	Roelant	Permanent Standard	LG1			
LC5	Carillon	Permanent Standard	LG1			
LC6	Lead cladding	Permanent Standard	LG1			
LC7	Wind Standard	Variable Static	Wind		Short	None
LC8	Wind Standard	Variable Static	Wind		Short	None
LC9	Wind Standard	Variable Static	Wind		Short	None
LC10	Wind Standard	Variable Static	Wind		Short	None
LC11	Wind Standard	Variable Static	Wind		Short	None
LC12	Wind Standard	Variable Static	Wind		Short	None
LC13	Wind Standard	Variable Static	Wind		Short	None
LC14	Wind Standard	Variable Static	Wind		Short	None
LC15	Wind Standard	Variable Static	Wind		Short	None
LC16	Wind Standard	Variable Static	Wind		Short	None
LC17	Wind Standard	Variable Static	Wind		Short	None
LC18	Wind Standard	Variable Static	Wind		Short	None
LC19	Wind Standard	Variable Static	Wind		Short	None
LC20	Wind Standard	Variable Static	Wind		Short	None
LC21	Wind Standard	Variable Static	Wind		Short	None
LC22	Wind Standard	Variable Static	Wind		Short	None

4.2. Load groups

Name	Load	Relation	Type
LG1	Permanent		
Wind	Variable	Exclusive	Wind

4.3. Combinations

Name	Description	Type	Load cases	Coeff. [-]
ULS-Set B (auto)		EN-ULS (STR/GEO) Set B	LC1 - Self weight	1.00
			LC2 - Imposed floorloads	1.00
			LC4 - Roelant	1.00
			LC5 - Carillon	1.00
			LC6 - Lead cladding	1.00
			LC7 - Wind	1.00
			LC8 - Wind	1.00
			LC9 - Wind	1.00

Student version

Student version

Name	Description	Type	Load cases	Coeff. [-]
			LC10 - Wind	1.00
			LC11 - Wind	1.00
			LC12 - Wind	1.00
			LC13 - Wind	1.00
			LC14 - Wind	1.00
			LC15 - Wind	1.00
			LC16 - Wind	1.00
			LC17 - Wind	1.00
			LC18 - Wind	1.00
			LC19 - Wind	1.00
			LC20 - Wind	1.00
			LC21 - Wind	1.00
			LC22 - Wind	1.00
SLS-Char (auto)		EN-SLS Characteristic	LC1 - Self weight	1.00
			LC2 - Imposed floorloads	1.00
			LC4 - Roelant	1.00
			LC5 - Carillon	1.00
			LC6 - Lead cladding	1.00
			LC7 - Wind	1.00
			LC8 - Wind	1.00
			LC9 - Wind	1.00
			LC10 - Wind	1.00
			LC11 - Wind	1.00
			LC12 - Wind	1.00
			LC13 - Wind	1.00
			LC14 - Wind	1.00
			LC15 - Wind	1.00
			LC16 - Wind	1.00
			LC17 - Wind	1.00
			LC18 - Wind	1.00
			LC19 - Wind	1.00
			LC20 - Wind	1.00
			LC21 - Wind	1.00
			LC22 - Wind	1.00
uls wind		EN-SLS Characteristic	LC1 - Self weight	1.20
			LC2 - Imposed floorloads	1.05
			LC4 - Roelant	1.20
			LC5 - Carillon	1.20
			LC6 - Lead cladding	1.20
			LC7 - Wind	1.50
			LC8 - Wind	1.50
			LC9 - Wind	1.50
			LC10 - Wind	1.50
			LC11 - Wind	1.50
			LC12 - Wind	1.50
			LC13 - Wind	1.50
			LC14 - Wind	1.50
			LC15 - Wind	1.50
			LC16 - Wind	1.50
			LC17 - Wind	1.50
			LC18 - Wind	1.50
			LC19 - Wind	1.50
			LC20 - Wind	1.50
			LC21 - Wind	1.50
			LC22 - Wind	1.50
uls imposed		EN-SLS Characteristic	LC1 - Self weight	1.20
			LC2 - Imposed floorloads	1.50
			LC4 - Roelant	1.20
			LC5 - Carillon	1.20
			LC6 - Lead cladding	1.20
			LC7 - Wind	0.90
			LC8 - Wind	0.90
			LC9 - Wind	0.90
			LC10 - Wind	0.90
			LC11 - Wind	0.90
			LC12 - Wind	0.90

Student version

SCIAENGINEER
SCIA Engineer 18.1.54

Part	Master Thesis Tu Delft	National code	EC - EN
Author	Pieter	National annex	Standard EN
Date	27. 11. 2018	Licence name	HP Inc.
		Licence number	144500

Project Appendix D: SCIA Input

Student version

Name	Description	Type	Load cases	Coeff. [-]
			LC13 - Wind	0.90
			LC14 - Wind	0.90
			LC15 - Wind	0.90
			LC16 - Wind	0.90
			LC17 - Wind	0.90
			LC18 - Wind	0.90
			LC19 - Wind	0.90
			LC20 - Wind	0.90
			LC21 - Wind	0.90
			LC22 - Wind	0.90
uls selfweight		EN-SLS Characteristic	LC1 - Self weight	1.35
			LC2 - Imposed floorloads	1.05
			LC4 - Roelant	1.35
			LC5 - Carillon	1.35
			LC6 - Lead cladding	1.35
			LC7 - Wind	0.90
			LC8 - Wind	0.90
			LC9 - Wind	0.90
			LC10 - Wind	0.90
			LC11 - Wind	0.90
			LC12 - Wind	0.90
			LC13 - Wind	0.90
			LC14 - Wind	0.90
			LC15 - Wind	0.90
			LC16 - Wind	0.90
			LC17 - Wind	0.90
			LC18 - Wind	0.90
			LC19 - Wind	0.90
			LC20 - Wind	0.90
			LC21 - Wind	0.90
			LC22 - Wind	0.90
SLS wind		EN-SLS Characteristic	LC1 - Self weight	1.00
			LC2 - Imposed floorloads	0.80
			LC4 - Roelant	1.00
			LC5 - Carillon	1.00
			LC6 - Lead cladding	1.00
			LC7 - Wind	0.20
			LC8 - Wind	0.20
			LC9 - Wind	0.20
			LC10 - Wind	0.20
			LC11 - Wind	0.20
			LC12 - Wind	0.20
			LC13 - Wind	0.20
			LC14 - Wind	0.20
			LC15 - Wind	0.20
			LC16 - Wind	0.20
			LC17 - Wind	0.20
			LC18 - Wind	0.20
			LC19 - Wind	0.20
			LC20 - Wind	0.20
			LC21 - Wind	0.20
			LC22 - Wind	0.20
SLS imposed		EN-SLS Characteristic	LC1 - Self weight	1.00
			LC2 - Imposed floorloads	0.90
			LC4 - Roelant	1.00
			LC5 - Carillon	1.00
			LC6 - Lead cladding	1.00

4.4. Nonlinear combinations

Name	Description	Type	Load cases	Coeff. [-]
NC1	Inclination of 2 m in xy plane	Ultimate	LC1 - Self weight	1.20
			LC2 - Imposed floorloads	1.05
			LC4 - Roelant	1.20
			LC5 - Carillon	1.20

Student version

Student version

Name	Description	Type	Load cases	Coeff. [-]
			LC6 - Lead cladding	1.20
			LC7 - Wind	1.50
			LC8 - Wind	1.50
			LC9 - Wind	1.50
			LC10 - Wind	1.50
			LC11 - Wind	1.50
			LC12 - Wind	1.50
			LC13 - Wind	1.50
			LC14 - Wind	1.50
			LC15 - Wind	1.50
			LC16 - Wind	1.50
			LC17 - Wind	1.50
			LC18 - Wind	1.50
			LC19 - Wind	1.50
			LC20 - Wind	1.50
			LC21 - Wind	1.50
			LC22 - Wind	1.50

4.5. Mass groups

Name	Load case
MG1	LC1 - Self weight

4.6. Combination of mass groups

Name	Mass group	Coeff. [-]
CM1	MG1	1.00
CM1/1 - 1.65		
CM1/2 - 1.69		
CM1/3 - 3.71		
CM1/4 - 3.85		
CM1/5 - 4.40		
CM1/6 - 4.51		
CM1/7 - 5.96		
CM1/8 - 5.99		
CM1/9 - 6.22		
CM1/10 - 7.42		

Student version

5. Calculation setup

5.1. Mesh setup

Name	MeshSetup1
Generation of eccentric elements on members with variable height	✗
Generation of nodes in connections of beam elements	✗
Generation of nodes under concentrated loads on beam elements	✓
Hanging nodes for prestressing	✓
Elastic mesh	✓
Use automatic mesh refinement	✗
Division on haunches and arbitrary members	5
Division for 2D-1D upgrade	50
Average number of tiles of 1d element	1
Average size of 2d element/curved element [mm]	1000.000
Minimal length of beam element [mm]	100.000
Maximal length of beam element [mm]	1000000.000
Average size of cables, tendons, elements on subsoil, nonlinear soil spring [mm]	1000.000
Maximal out of plane angle of a quadrilateral [mrad]	30.0
Predefined mesh ratio	1.5
Minimal distance between definition point and line [m]	0.001
Average size of panel element [mm]	1000.000
Mesh refinement following the beam type	None
Definition of mesh element size for panels	Manual

5.2. Solver setup

Student version

SCIAENGINEER

SCIA Engineer 18.1.54

Part	Master Thesis Tu Delft	National code	EC - EN
Author	Pieter	National annex	Standard EN
Date	27. 11. 2018	Licence name	HP Inc.
		Licence number	144500

Project **Appendix D: SCIA Input**

Student version

Name	SolverSetup1
Neglect shear force deformation (Ay, Az >> A)	X
Initial stress	X
Use IRS (Improved Reduced System) method	X
Number of thicknesses of rib plate	20
Maximum soil interaction iterations	10
Maximum iterations	20
Number of increments	1
Number of buckling modes	2
Number of sections on average member	10
Number of eigenmodes	10
Step for soil/water pressure [mm]	500.000
C1x [MN/m^3]	1.0000e-01
C1y [MN/m^3]	1.0000e-01
C1z [MN/m^3]	1.0000e+01
C2x [MN/m]	5.0000e+00
C2y [MN/m]	5.0000e+00
Coefficient for reinforcement	1
Warning when maximal translation is greater than [mm]	1000.0
Warning when maximal rotation is greater than [mrad]	100.0
Parallelism tolerance for automatic calculation [deg]	10.00
Span length ratio L/beff,max (1 side) for automatic calculation [-]	8.00
Simply supported beam [-]	1.00
Inner span [-]	0.70
End span [-]	0.85
Cantilever [-]	2.00
Solver precision ratio	1
Soil combination	None
Bending theory of plate/shell analysis	Mindlin
Type of solver	Direct
Type of eigen value solver	Lanczos
Type of eigen value solver	Lanczos
Method of calculation	Picard

Student version

Student version